Nitrogen-containing compounds from ammonia co-feed to the Fischer-Tropsch synthesis

Tawanda Sango

Submitted to the University of Cape Town in partial fulfillment of the requirements for the degree Master of Engineering

APRIL 2013

ACKNOWLEDGEMENTS

When I embarked on this journey in my life, I thought to myself: “how difficult can this be?” In retrospect, I look back and I see I couldn’t have done this without all the support I got from friends, family, colleagues, co-workers and more. Now when I look back, it wasn’t the ease nor difficulty of the work. A lot was about keeping your sanity at important times, keeping motivated when the future seemed impossible, having good guidance and mentorship, and everything else fell into place.

There are many people without whom this work would not have been possible. First and foremost I would like to extend my gratitude to Prof Michael Claeys for his invaluable input, patience and support through the last couple of years. I quite enjoyed those meetings where you described everything in a simple, nonchalant way (and I played along- nodding my head in that “I understand everything you are saying” manner, too proud to admit my ignorance, or acknowledge that I didn’t have a single clue on GC columns, let alone install a “simple” GC column, or build one from scratch), or when you sketched a quick picture/equation on a scrap piece of paper or on the white board. Even if it took me a few more weeks to really understand what it was all about (and then actually realize it was easy). Thank you for all your invaluable input and support, keeping the project interesting even when I thought all hope was lost. To Prof van Steen thank you for your insights and input to the project, and thought-provoking questions. Prof Dr Frank Rößner from the University of Oldenburg for the input and assistance I got both in Cape Town and on my tour in Germany.

To everyone in the Catalysis group: Marc, Pete, Youqi, Virginia, Itai, Nico, and to Robert and Dr. Prof. Roessner (Uni Oldenburg), thank you for all your support and help- from demonstrating the ampoule making technique, to explaining how FID’s work, (how to hide -I mean how/why not to hide- evidence of misdemeanors concerning communal lab equipment, calcination and reduction procedures). These are timeless skills handed down from generation to generation of catalysis postgraduate students, with no particular source or reference, just the absolute certainty that each of these methods has been tried and tested and IT WORKS- something that’s very important and oftentimes rare during the course of one’s experimental work. To Helen, Joachim, Bill, Granville,

Egshaan, Debbie, Zedre, Susan, Anastacia for all their very invaluable help and assistance in and out of the lab. To the beer club patrons (2006-2007: when I was so honoured as to be one of the crew entrusted with managing and running the club) - thank you for providing me with a purpose during the long periods when my reactor was down, the lab was out of ampoules, or the calcinations rigs were out of commission. To Kudzai, Ben, Ranga, Fari, Sean – for all the legendary Mzoli's, Pigs', Starlite's.

To c*change, DST-NRF and the Chemical Engineering Department at UCT, thank you for the financial support without which this work wouldn't have been possible.

Finally I would like to thank all my close friends and family for seeing me through. To my mother Tendai, and my siblings Mercy, Samantha, Terence and Shami, I couldn't have done this without your undying support and prayers. Even when it seemed I was at the end of the tunnel, your support kept me going. This thesis is also dedicated to the loving memory of my late father, Samuel Farayi Sango, without whom this journey would never have begun. To everyone I have not mentioned by name -there are countless people, and it would be impossible for me to name every single one- to all of you, I thank you for the special part you played in this journey.

Tawanda
Harare, January 2009

SYNOPSIS

The Fischer-Tropsch (FT) synthesis is a well-researched process for the catalytic conversion of syngas (carbon monoxide and hydrogen) to a wide range of linear hydrocarbon products. As early as the 1930's, the process was being used for industrial production of automotive fuels. A vast amount of research has been carried out on the FT process, including studies on:

- Catalyst type, preparation, particle and pore size, and promotion;
- Reactor configuration and operation;
- Temperature and pressure effects and more.

Iron- and cobalt-based catalysts are the industrially employed catalysts of choice. Different types of reactors are in use, with the choice of reactor depending on factors such as operational temperature and product specification.

The FT synthesis has been used predominantly for production of automotive fuels. This has made the financial benefit from the FT process heavily reliant on crude oil prices. Increasing the financial viability of the process has been achieved by improving production methods, production of alternative products such as waxes, lubricants, as well as valuable chemicals such as olefins and oxygenates. In an attempt to produce additional chemicals in the FT reaction, this work investigates the synthesis of nitrogen-containing compounds via ammonia addition to a low temperature, low pressure, slurry reactor using an unsupported, potassium-promoted, precipitated iron catalyst. The process is subjected to various ammonia contents in the feed. The main goals of the project were to:

- Identify what alternate products could be synthesized from co-feeding ammonia to the system;
- Explore the effect of ammonia partial pressure on the synthesis of these products;
- Determine the effect of ammonia and ammonia partial pressure on the standard FT activity and selectivity;
- Postulate on the mechanism of formation of new products, as well as possible new insights into the current understanding of the FT mechanisms.

The work was conducted using a slurry reactor, operating at a pressure of 5 bar and temperature of 250°C. Synthesis gas was fed at 75 mL(NTP)/min with a H_2:CO ratio of 2:1. The ammonia content in the reactor feed was varied from 0-35 vol% while varying/increasing the total reactor pressure correspondingly.

Previous research, conducted in the 1970s, pointed towards aliphatic, primary, terminal amine formation from the co-feed of ammonia to an FT system. Hence the initial aim of this work was targeted towards amine production, and effects of ammonia partial pressure on activity and selectivity. From the work conducted, not only amines, but also nitriles, amides and formamides were synthesized. FID analysis of the liquid product (C_6-C_{14} cut) obtained under ammonia content in the feed of 5-10 vol%, produced nitrile and amine contents in the product of between 5 and 10% respectively on a carbon weight basis. Both nitrile and amine contents increased with increasing ammonia content in the feed. Whilst not absolutely clear at this stage, the primary mechanism of formation of these compounds is indicative of amine formation via NH_2 species addition at the chain termination stage, coupled with an alkyl chain growth mechanism. Nitrile formation is proposed to occur via the formation and insertion of an intermediate cyano (CN) species. Formation of these compounds via secondary reactions is possibly via:

1. hydrogenation of nitriles to form amines;
2. dehydrogenation of amines to form nitriles;
3. amination of oxygenated species to form amines, amides and formamides – which also accounts for the observed disappearance of alcohols, aldehydes and acids from the product upon ammonia addition to the process.

For both nitriles and amines, both hydroxyl and ethylidene surface species are also hypothesized to take part in the formation of these compounds (regardless of whether primary or secondary formation occurs). Formation of amides and formamides showed a slight increase when ammonia content in the feed was raised above 2 vol%.

In terms of catalyst activity, adding ammonia during the FT synthesis had some negative, but partially reversible effect. Besides formation of nitrogen-containing species, the disappearance of oxygenated products (alcohols, aldehydes and acids) also occurred during addition of ammonia to the system. Chain growth probability, double

bond shift, olefinicity and other features which describe an FT product spectrum remained relatively unchanged with ammonia content.

In summary, ammonia addition to a low temperature, low pressure, iron-catalyzed FT system showed promising results for synthesis of a broad range of (C_2-C_n) nitrogen-containing compounds without significant catalyst degradation. This work showed great promise in adapting the FT process for simultaneous production of valuable nitrogen-containing compounds as well as standard FT products. The benefits and limitations of co-production of nitrogen-containing compounds and standard FT products however have to be researched further to determine whether it is industrially viable to operate in this manner, or whether it is more advantageous to operate a separate system geared for production of nitrogen-compounds at a much higher selectivity to the detriment of olefin and paraffin formation.

TABLE OF CONTENTS

LIST OF FIGURES

LIST OF TABLES

NOMENCLATURE

Abbreviations	Description
AAS	Atomic absorption spectroscopy
ASF	Anderson-Schulz Flory
BET	Brunauer-Emmett-Teller
CFBR	Circulating fluidized bed reactor
FBR	Fluidized bed reactor
FID	Flame ionization detector
FT	Fischer-Tropsch
GC	Gas chromatography
HTFT	High temperature Fischer-Tropsch
LTFT	Low temperature Fischer-Tropsch
MS	Mass spectrometry
Pr_N	Products containing n carbon atoms per molecule
SPR	Slurry phase reactor
NTP	Normal temperature and pressure (273 K, 1.013 bar)
TCD	Thermal conductivity detector
TFBR	Tubular fixed bed reactor

Notation	Description	Unit
$F_{i,TCD}$	Flow rate of component i from TCD analysis	ml/min
$rf_{i,TCD}$	TCD response factor of component i	
A_i	Area of component i from GC chromatogram	
C_i	Concentration of component i	v/v
$n_{i,FID}$	Molar flow rate of component i, obtained from FID analysis	mol/min
$Cf_{i,FID}$	FID response factor of component i relative to cyclohexane	
N_i	Number of carbon atoms in component i	
d_p	Particle diameter	μm

1. INTRODUCTION

The Fischer-Tropsch (FT) Synthesis is defined as the synthesis of hydrocarbon products from the catalysed reaction of hydrogen and carbon monoxide. The process has been used industrially for over 75 years (Schulz 1999 and Steynberg, 2004).

The industrial process consists of three stages (Steynberg 2004):

- firstly coal, natural gas or biomass is converted to produce synthesis gas – a mixture of carbon monoxide and hydrogen;
- in the second stage - referred to as FT synthesis - the synthesis gas is fed into an FT reactor, where it is converted catalytically into a product consisting primarily of aliphatic α-olefins (up to 80% selectivity), n-paraffins and oxygenates.
- in the third and final stage, the FT reactor product is separated into different compound fractions and distributed for use, or processed further to produce fuels, waxes and a range of other important chemicals.

From the review by Schulz (1999), it is evident that the bulk of the research on the FT process in recent years has been on the syngas conversion to FT products with a strong focus on factors concerning the catalyst and fundamental kinetic aspects. The review also outlines a number of developments, of which most have been predominantly focused on optimization of current technology, including work on:

- understanding of the reaction mechanisms and kinetics;
- use and modification of different types of catalysts for improved product selectivity and activity;
- understanding of reactor technology to establish the advantages and limitations of operating using different types of reactors;
- effects of reaction conditions on the process.

Although the primary focus of the FT synthesis is production of liquid automotive fuels, research into the production of alternative chemicals or products exists, including:

- linear olefins, oxygenates and waxes for the chemical industry (Steynberg, 2004);
- amines (Rottig, 1958 and Kölbel & Trapper, 1966) and;

- nitriles (Hummel, 1993).

Research *on ammonia addition to the FT synthesis* is still however very limited. Rottig (1958) and Kölbel & Trapper (1966) describe ammonia addition to an iron catalyzed FT system resulting predominantly in primary, aliphatic amines as well as hydrocarbon products typically obtained in FT synthesis. Historically, there is no prior record of long-chain nitrile, amide or formamide formation from this reaction system. Hummel *et al.* (1993) and Kim & Lane (1992) reported acetonitrile formation from the catalyzed reaction of CO, H_2 and NH_3 over iron and Mo/SiO_2 catalysts respectively, though operating typically at much higher temperatures than standard FT conditions (±400°C), and no formation of longer chain nitriles was observed.

Based on previous work (Kölbel *et al.*, 1966, 1974 and 1984 and Rottig, 1958), the initial aim of this project was to investigate the effect of ammonia partial pressure on amine selectivity, as well as FT activity and product selectivity in a low temperature, iron-catalyzed, slurry-phase Fischer-Tropsch reaction system. After preliminary laboratory test work, the scope was expanded to investigate all of the possible nitrogen-containing compounds as well as the effect of ammonia partial pressure on the selectivity of these compounds from ammonia addition. These experiments were to be conducted in a stirred slurry reactor in order to allow for extracting true kinetic information on the role of ammonia in a gradientless reactor system. Activity and selectivity of the FT system was to be monitored to determine any promotional or detrimental effects. Depending on the success of small scale studies, this process can potentially be adapted for larger scale production, leading to a novel way of producing certain classes of chemical compounds, which can be used both as final products, as well as intermediates for downstream production processes.

Research problem/goal

The initial objective of this work was to investigate the effect of ammonia partial pressure on amine selectivity, FT activity and FT selectivity. These were discovered after the scoping run of the system. The problem statement was then broadened to include identification and characterization of all nitrogen-containing compounds in the objectives, and effect of ammonia partial pressure on their formation rates and selectivities.

Furthermore, it was the purpose of this research to suggest possible mechanisms for formation of these products as well as possibly shed new light on current proposed mechanisms for the FT synthesis.

2. LITERATURE REVIEW

2.1. Fischer-Tropsch synthesis: a short history

Franz Fischer and Hans Tropsch worked on the production of hydrocarbons from gasified coal at the Kaiser Wilhelm Institute for Coal Research in Mülheim, Germany. Their work started producing results in the 1920s, and as early as 1935, Ruhrchemie commissioned the first industrial Fischer-Tropsch unit. Early FT processing mainly focused on the production of automotive fuels, lubricating oils and other petroleum products (Steynberg 2004).

The industrial process consists of three stages (Steynberg 2004):

1. Production of syngas – a mixture of carbon monoxide and hydrogen – from coal, natural gas or biomass::

   From coal:

   $$C + H_2O \rightarrow CO + H_2 \quad (2.1)$$

   From natural gas:

   $$CH_4 + H_2O \rightarrow CO + 3H_2 \quad (2.2)$$

2. In the second stage, the syngas is fed into an FT reactor (typically with a H_2:CO ratio of 1:1 to 2:1), where it is converted catalytically into a product consisting primarily of linear aliphatic α-olefins (up to 80% selectivity), n-paraffins and oxygenates (mainly primary alcohols and aldehydes and to a lesser extent acids and methyl-ketones). The main reactions that occur in the FT synthesis are as follows:

   Paraffin formation:

   $$nCO + (2n+1)H_2 \rightarrow C_nH_{2n+2} + nH_2O \quad (2.3)$$

   Olefin formation:

   $$nCO + 2nH_2 \rightarrow C_nH_{2n} + nH_2O \quad (2.4)$$

   Alcohol formation:

$$nCO + 2nH_2 \rightarrow C_nH_{2n+1}OH + (n-1)H_2O \quad (2.5)$$

Aldehyde formation:

$$nCO + (2n-1)H_2 \rightarrow C_nH_{2n}O + (n-1)H_2O \quad (2.6)$$

Use of an iron catalyst results in the water-gas shift reaction occurring as a side reaction:

$$CO + H_2O \leftrightarrow CO_2 + H_2 \quad (2.7)$$

Selectivity towards a required product class is maximized by modifying reaction conditions. The parameters that are variable include reaction temperature and pressure, type of reactor, catalyst type, catalyst particle size, catalyst promoters, space velocity, and H_2:CO ratio in the feed.

3. In the third and final stage, the mixed hydrocarbon product from the FT reactor is separated into different compound classes and distributed for use or processed further to produce fuels, waxes and a range of other important chemicals.

From the study of available literature, recent research on the FT process has been predominantly focused on optimisation of current technology, including work on:

- understanding of the reaction mechanisms and kinetics;
- understanding the interactions on the catalyst surface;
- modification of catalysts for improved product selectivity and activity;
- understanding of reactor technology to establish the advantages and limitations of operating using different types of reactors and reaction conditions.

2.2. Economic aspects of the FT process

Historically, the FT synthesis has been used predominantly for producing automotive fuels. Since the price of fuels is strongly reliant on world crude oil prices, the economic viability of the FT process is also strongly influenced by the world crude oil prices and supply. Calculated minimum crude oil prices required to sustain an FT plant have been estimated to be between US$10-30/barrel, with most estimates closer to US$20/barrel (Gradassi, 1998; Jager, 1998; Vosloo, 2001; Dry, 2004a and Steynberg 2004). As seen

from Figure 2.1, for most of the last 90 years, crude oil was less than US$20/barrel. This has resulted, until recently, in limited interest in and industrial use of the FT synthesis.

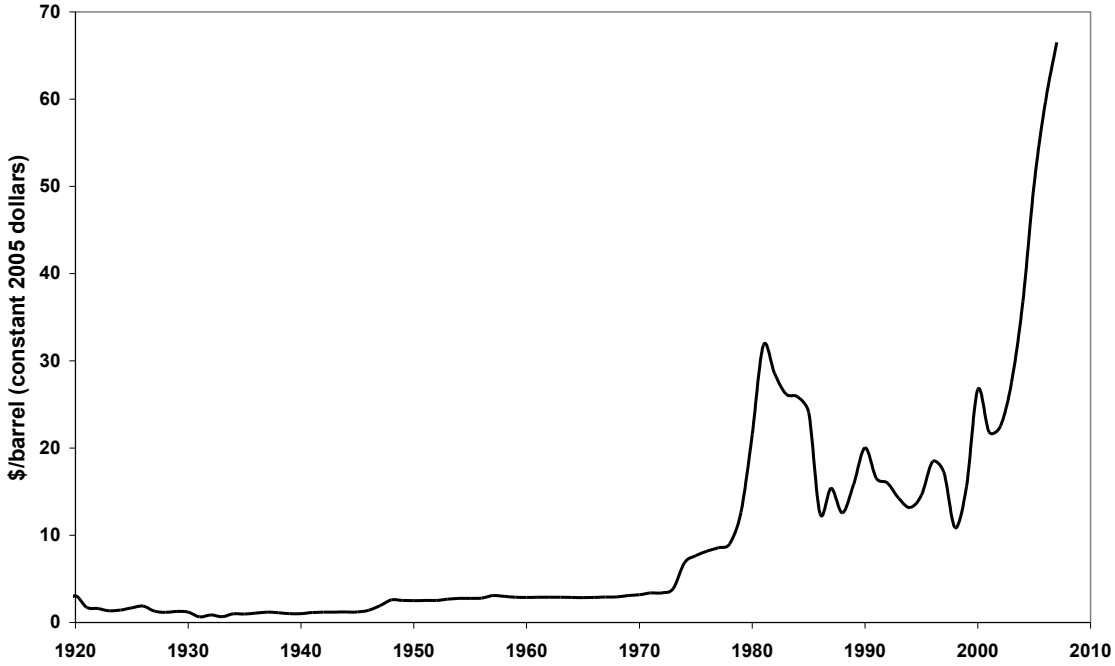

Figure 2.1: Average annual crude oil price (US$ per barrel)
(Data obtained from http://tonto.eia.doe.gov/dnav/pet/hist/f000000__3a.htm)

However, Sasol in South Africa has been operating FT synthesis industrially over the last 60-70 years, with their operation and technology being predominantly based on coal, though recent developments (e.g. Qatar) include use of natural gas (Dry, 2002).

With the cost of production of FT fuels not being economically viable for competition with the crude oil derivatives, ways of reducing the cost of production as well as production of alternative products have been researched. These include (Dry 1996):

- selling valuable products such as linear alpha olefins, oxygenates and waxes;
- maximizing ethylene production, followed by the oligomerization of ethylene to even-numbered alpha olefins;
- manufacturing synthetic lubricating oils or linear primary alcohols from the higher alpha olefins;
- manufacture of polypropylene and acrylonitrile from propylene.

Research into co-feeding other compounds to the process so as to produce other valuable, variable chain length, linear products has also been done. Ammonia has been added to the feed, resulting in the normal FT spectrum as well as primary aliphatic amines (Rottig, 1958; Kölbel and Trapper, 1966; Brown & Maselli, 1973, Knifton *et al.*, 1993). The stoichiometric equation for amine production is shown below:

$$nCO + 2nH_2 + NH_3 \rightarrow C_nH_{2n+1}NH_2 + nH_2O \quad (2.8)$$

In summary, FTS has been limited until recent years by little or no opportunity for profitable operation. The two main ways of mitigating the cost disadvantage of FT synthesis versus crude oil alternatives are the synthesis of alternative (non-fuel products) or the optimization of current technology so as to decrease the cost of production.

2.3. Fischer-Tropsch operation modes

The industrial modes of operation are classified in general into either:

- high temperature Fischer-Tropsch (HTFT); or
- low temperature Fischer-Tropsch (LTFT).

The choice depends on the product requirement. LTFT is used in general for the production of diesel and high molecular weight linear hydrocarbons, whereas HTFT targets gasoline and light olefins (Dry, 2004a and Steynberg, 2004).

In general, FTS is operated at around 20 to 30 bar. This is mainly due to the high-pressure requirement of the upstream gasification process and in order to increase productivity. From stoichiometry of this polymerisation reaction, kinetics and Le Chatelier's principle, high pressure enhances the rate of product formation and the equilibrium conversions.

2.3.1. Low temperature Fischer-Tropsch operation (LTFT)

The low temperature FT process is used to produce long chain, liquid phase products including high molecular weight waxes. The operational temperatures range between 220-240°C. Fixed bed and slurry phase reactors are used and both iron and cobalt are used as active catalyst components (Steynberg, 2004; Dry, 2004c).

2.3.2. High temperature Fischer-Tropsch operation (HTFT)

The high temperature process is used to produce a molecular lower weight, more olefinic product. This process operates between 320-350°C. Fluidized bed reactors are used for this application, with iron being the only catalyst of choice (Steynberg, 2004; Dry, 2004c).

2.3.3. Fischer-Tropsch reactors

There are four types of commercially operated FT reactors:

- fluidized bed reactor (FBR);
- circulating fluidized bed reactor (CFBR);
- tubular fixed bed reactor (TFBR);
- slurry phase reactor (SPR).

Each of these reactors has its own advantages and disadvantages. The earlier reactors used were the TFBR for the low temperature operation and the CFBR for high temperature operation. More recent are the FBR which employs a fixed, i.e. non-circulating fluidized bed, for high temperature and the SPR for low temperature operation.

For this project, a stirred slurry phase reactor was used. The advantages of using this reactor type include no bulk temperature, pressure or concentration gradients in the slurry allowing for kinetic studies varying single reaction parameters, in this case the partial pressure of ammonia.

2.3.4. Catalysts

The four main metals active for the Fischer-Tropsch reaction are iron, cobalt, nickel and ruthenium. Despite having the highest activity, ruthenium has a very limited world reserve and supply, and is much more expensive than the others. Nickel also has high FT activity, but tends towards high methane selectivity. Catalyst loss in the form of volatile carbonyls makes it even more unfavorable (Schulz, 1999 & Dry, 2004b). This leaves iron and cobalt as the two industrial catalysts of choice. Cobalt has a higher FT activity than iron. However, iron is cheaper and more abundant. Furthermore, iron has low methane selectivity, even at higher temperatures (Schulz, 1999).

The active metals for the catalysts can be used either in supported or unsupported form. Owing to cost considerations, cobalt is usually immobilized onto a support for maximized dispersion whereas iron is commonly used in bulk, unsupported form (Dry, 2004b). Alkali promotion on iron catalysts is essential so as to enhance catalyst activity and selectivity. Potassium promotion has been proven to increase catalyst activity, olefin selectivity and chain growth probability leading to a longer chain product, with copper promotion increasing the catalyst reducibility (Miller and Moskovits, 1988; O'Brien *et al.*, 1997; Dry, 2004b).

The catalysts are reduced to the metallic state prior to reaction, usually using hydrogen. There are a different number of suggested active phases (mostly carbides) for the iron based catalyst (Anderson, 1984; Schulz, 1999). These typically only form during the FT synthesis.

2.3.5. Fischer-Tropsch reaction mechanism

The FT reaction can be classified as a surface polymerization. Although there is still on-going discussion on the exact mechanism, all of the proposed pathways consist of three steps (Claeys and van Steen, 2004):

1. chain initiation;
2. chain propagation via sequential addition of a monomer; and
3. chain termination.

The surface polymerization is illustrated in Figure 2.2. Carbon monoxide and hydrogen are fed into the reactor. Hydrogen chemisorption occurs dissociatively onto the catalyst surface as mono-atomic hydrogen with CO is adsorbed as the molecule initially. Chain initiator and C_1-monomer species are formed on the surface, and then followed by the surface polymerization to form hydrocarbons of various chain lengths.

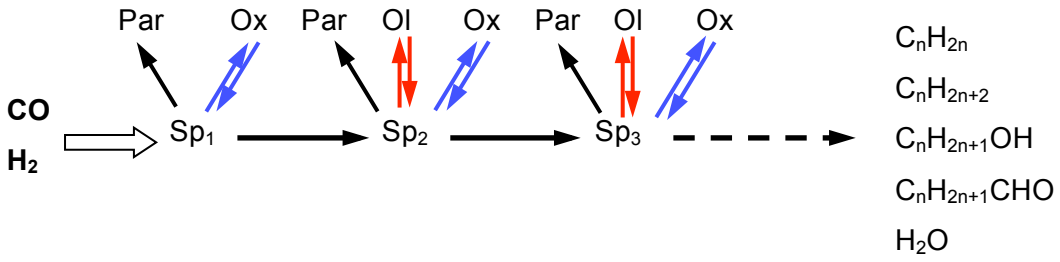

Figure 2.2: Simplified reaction mechanism on the catalyst surface
(Par=paraffins, Ol=olefins, Ox=oxygenates, Sp_n=surface species with n carbon molecules)

The specific reaction mechanism on the surface is still a subject of debate, with a number of different mechanisms postulated over the years. The following sections summarize four of the main chain growth mechanisms that have been proposed in literature. The summary is based on the review by Claeys and van Steen (2004) and is illustrated in Figure 2.3 and followed by brief explanations in sections 2.3.5.1-4.

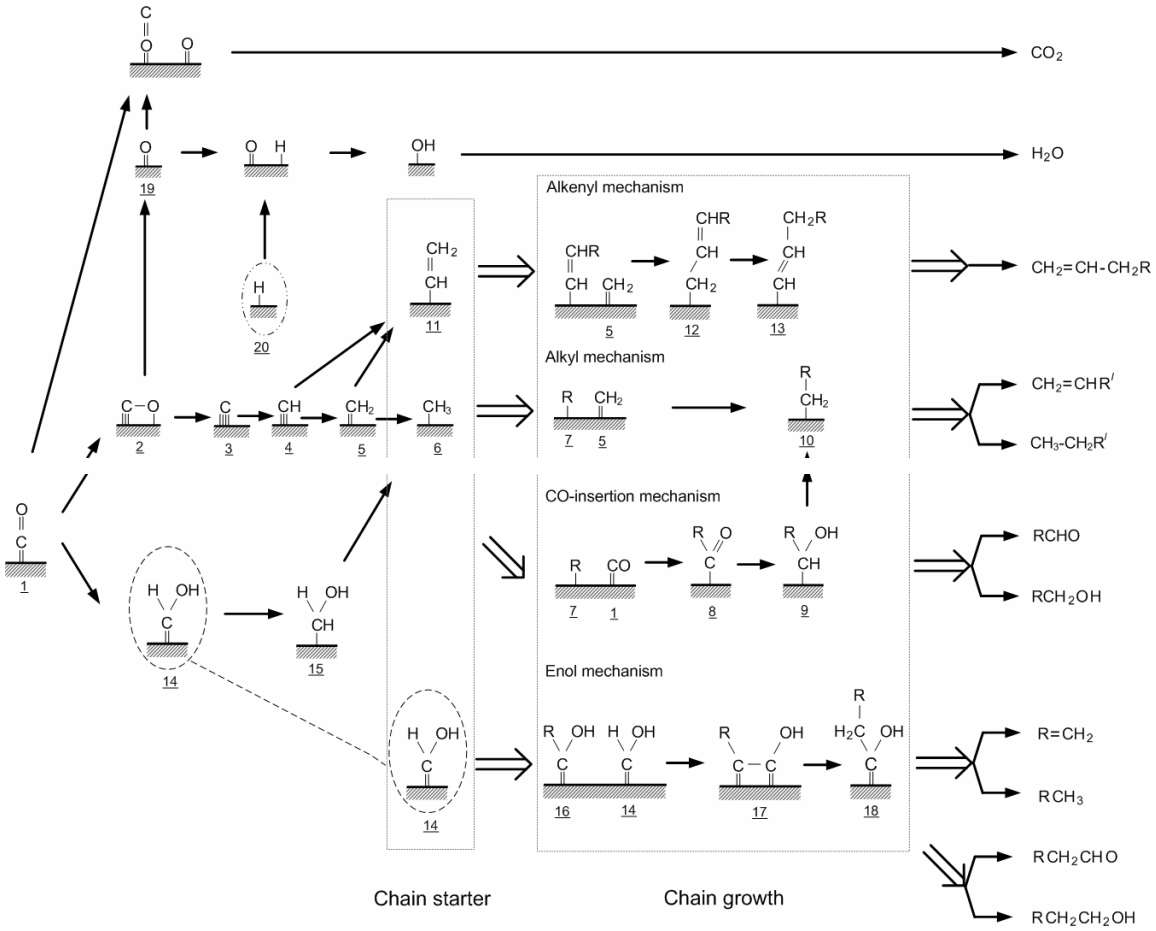

Figure 2.3: Overview of Fischer-Tropsch reaction pathways (adopted from Mabaso (2005))

2.3.5.1 Alkyl mechanism

This is the currently most widely accepted mechanism. The chain initiator is the surface CH_3 (6) species, with the methylene (5) surface species acting as the monomer for chain propagation. CO is adsorbed dissociatively onto the catalyst surface (1-3), subsequently reacting with adsorbed hydrogen to produce water and on the catalyst surface, CH (4), CH_2 (5) and CH_3 (6) species. The CH_3 initiator (6) undergoes a subsequent series of the CH_2 (5) monomer additions in the chain propagation steps forming surface alkyl (10) species. Chain termination occurs by β-hydrogen elimination for α-olefin production or by hydrogen addition at the terminal C atom resulting in paraffin production.

The main drawback of the alkyl mechanism is the failure to explain primary oxygenate formation. A possible explanation was proposed by Johnston and Joyner (1993), where

a surface alkylidene species is formed on the surface and reacts with a surface hydroxyl to produce the oxygenated species (9). The surface hydroxyl is proposed to come from reaction of a surface O (19) species with adsorbed hydrogen (20).

2.3.5.2 Alkenyl mechanism

In the alkenyl mechanism, the proposed chain initiator is the vinyl (11) surface species formed from the coupling of the CH (4) and CH_2 (5) surface species. Chain propagation involves the addition of a methylene (5) surface species to the surface alkenyl species, resulting in a surface allyl (12) species. This undergoes allyl-vinyl isomerization to form an alkenyl (13) species. Hydrogen addition to the alkenyl species results in α-olefin formation. Primary paraffin formation is however not explained from this mechanism.

2.3.5.3 Enol mechanism

The enol mechanism describes a reaction route with the enol (14) surface species acting as both the chain initiator and monomer. The enol species is formed from the reaction of chemisorbed CO (1) species with adsorbed hydrogen (20). Chain growth occurs through a condensation reaction, with two surface enol (14, 16) species to form a new species (17), accompanied by elimination of water. Hydrogen addition to this species (17) results in a new enolic species (18). Desorption of the enolic species yields oxygenates and α-olefins, with n-paraffins being formed by the hydrogenation of olefins in a secondary reaction step.

2.3.5.4 CO insertion mechanism

The surface methyl, CH_3 (6), species is thought to be the chain initiator for this mechanistic route. Chain propagation occurs through the addition of chemisorbed CO (1) species to a surface alkyl species to form species (8). Hydrogenation of this species will result in formation of species (9), which forms a surface alkyl (10) after a further hydrogenation step accompanied by water elimination. Thereafter, α-olefin and paraffin formation occurs via similar chain termination steps to the alkyl mechanism. Oxygenate formation can occur via desorption of species (8) and (9).

2.4. Current synthesis methods for nitrogen-containing organic compounds

Based on a study of similar research done on ammonia addition to the FT process, the main class of nitrogen-containing compounds expected from this work were primary, aliphatic, terminal amines. Previous work on the addition of ammonia to the FT reaction resulted in a product containing amines as the predominant new class of compounds (Kölbel & Trapper, 1966; and Rottig, 1958). In the current work (this project), amines were synthesized, but in addition, nitriles, and some amides and formamides were also detected in the product spectrum. This section describes the methods for production of amines and nitriles under both FT and non or pseudo-FT reaction conditions.

2.4.1. Current amine production routes

Amines are described by Turcotte & Hayes (2001) in the Kirk-Othmer Encyclopaedia as derivatives of ammonia and hydrocarbons. There are three different types: primary, secondary and tertiary amines resulting from mono-, di-, or tri-substitution respectively of an alkyl group for a hydrogen atom on an ammonia molecule.

Primary amines: Secondary amines Tertiary amines

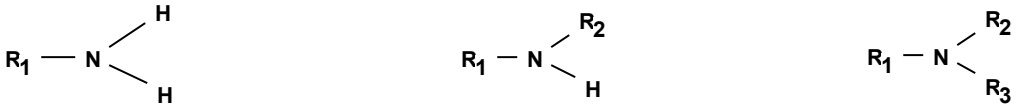

Alkylamines have a wide variety of applications including use as surfactants, for synthesis of dyes, emulsifying agents, pesticides, and pharmaceuticals. Using current amine production methods, it is virtually impossible to produce primary amines exclusively, and for that matter, secondary or tertiary amines. The product spectrum consists of a non-selective mixture of primary, secondary and tertiary amines. Selectivity to any of these can however still be influenced by controlling factors such as ammonia feed ratio and overall feed conversion.

Aliphatic amines are classed into lower amines (C_2-C_4) and higher (fatty) amines (C_8-C_{22}). In terms of production, lower amines have a wider range of feedstock, including alcohols, aldehydes, ketones, olefins, nitriles and alkyl halides (Turcotte & Hayes, 2001). Fatty amines are produced in lower volumes partially due to a lower availability of feedstock, consisting mainly of fatty alcohols and nitriles, both of which are produced from fatty oil feedstock. The four routes for producing aliphatic, lower amines (Turcotte & Hayes, 2001) as well as the two routes for producing fatty amines (Visek, 2001) as described in Kirk-Othmer are summarized in the following sections.

2.4.1.1 Amination of alcohols over a dehydrating agent (Turcotte & Hayes, 2001)

The alcohol and ammonia are passed either over a solid acid catalyst (e.g. metal oxides, zeolites) or supported metal catalysts (e.g. cobalt, nickel, chromium). The acid-catalyzed synthesis operates at temperatures of 300-500°C and pressures of 8-36 bar, with the metal-catalyzed processes operating at 130-250°C and 8-22 bar. Metal-catalyzed synthesis is favoured due to higher yields, lower operating temperatures and lower extent of side reactions. The resulting product consists of a non-selective mixture of primary, secondary and tertiary amines. Sewell (1996) also investigated the amination of ethanol over cobalt, nickel and copper under similar reaction conditions and obtained a mixture of primary, secondary and tertiary amines.

Primary amines are formed from reaction of ammonia and alcohols, with secondary amines formed from reaction of primary amines with an alcohol in a secondary reaction step and tertiary amines formed from reaction of secondary amines with alcohol. These steps are shown in equations 2.9-2.11.

$$ROH + NH_3 \rightarrow RNH_2 + H_2O \quad (2.9)$$

$$ROH + RNH_2 \rightarrow R_2NH + H_2O \quad (2.10)$$

$$ROH + R_2NH \rightarrow R_3N + H_2O \quad (2.11)$$

Secondary and tertiary amines are also formed from the reactions of primary and secondary amines:

$$2\ RNH_2 \rightarrow R_2NH + NH_3 \quad (2.12)$$

$$RNH_2 + R_2NH \rightarrow R_3N + NH_3 \quad (2.13)$$

Rausch *et al.* (2008) also investigated the hydroamination of alcohols (specifically, ethanol) over a cobalt catalyst, resulting in a mixture of primary, secondary and tertiary amines in the product as well as acetonitrile, diethylimine and C_1-C_3 paraffins and olefins:

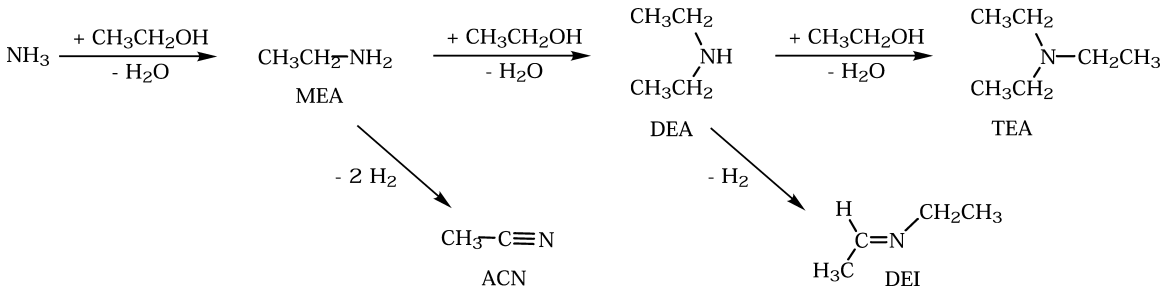

Figure 2.4: Overview of ethanol hydro-amination (adopted from **Rausch *et al.*, 2008**)

2.4.1.2 Amination of oxygenates over a hydrogenation catalyst

Ammonia, hydrogen and aldehydes or ketones are reacted over a hydrogenation catalyst (e.g. nickel, cobalt, platinum) to produce amines. Typical conditions are 50-180°C, and pressures of 4.5-36 bar. Replacement of ammonia with primary or secondary amines, results in the formation of higher degree amines (Turcotte & Hayes, 2001). Selectivity control is better achieved using this process compared to alcohol amination as reforming reactions are much less thermodynamically favoured compared to the reductive alkylation at the lower temperatures employed.

2.4.1.3 Nitrile reduction (Turcotte & Hayes, 2001)

Nitriles can be reduced with hydrogen using hydrogenation catalysts to produce amines. Temperatures of 50-150°C, and pressures of 4.5-74 bar are employed. Reforming reactions of product amines to higher amines can be suppressed by addition of ammonia to the feed, thereby confining the product composition to consist predominantly of primary amines.

2.4.1.4 Olefin amination (Turcotte & Hayes, 2001)

More recently, alkylamines have been synthesized from the zeolite-catalyzed reaction of ammonia and an olefin. Operating conditions are 200-350°C, and pressures of up to 300 bar.

2.4.1.5 Hydrogenation of fatty nitriles (Visek, 2001)

This is a 2-stage process, with the first stage involving synthesis of nitriles. Fatty acids or esters are reacted with ammonia to form the corresponding nitrile, which is then hydrogenated to form the fatty amine. The nitriles are formed at temperatures >250°C over zinc or bauxite catalysts. The nitriles are then hydrogenated at 50-200°C over e.g. aluminium-nickel Raney alloy, Raney cobalt, cobalt and copper pellets. Selectivity to primary amines is enhanced by using ammonia to suppress secondary amine formation For secondary and tertiary amine syntheses, high selectivities can be achieved in the absence of ammonia and when the nitrile reduction is carried out in a semi-batch process at low pressure and elevated temperatures with a hydrogen feed and ammonia (from reforming reactions) removal.

2.4.1.6 Amination of fatty alcohols (Visek, 2001)

Fatty alcohols can be reacted with ammonia to form the corresponding amines. Fatty acids or esters are reduced to the corresponding alcohols. The fatty alcohols are then reacted at 50-340°C and high pressure (ca. 35 bar). The feeding of hydrogen and ammonia to the system as well as the reaction pressure controls selectivity to primary, secondary and tertiary amines.

In general, these methods use oxygenated hydrocarbons and are aimed at the production of low molecular weight amines. The main production routes result in a mixture of primary, secondary and tertiary amines in the product, with exclusive selectivity to a single type of amine (primary, secondary or tertiary) not easily achievable.

2.4.2. Nitrile production

From a review on organonitriles (McKinney and DeVito, 1998) nitriles are used broadly as solvents, and chemical feedstock for production of pharmaceuticals and pesticides. The reactivity of the cyano-bond makes nitriles important reagents that can be used to produce a wide variety of compounds including amines, amides, carboxylic acids, esters, synthetic polymers and other compounds. Of all the nitriles, acrylonitrile (CH_2CHCN) has the largest commercial production capacity by volume, with acetonitrile (CH_3CN) being produced as a by-product. Acrylonitrile is polymerised to produce plastics and synthetic fibres with acetonitrile having important use as a solvent, surfactant and for pharmaceutical production.

There is a wide range of preparation methods for nitriles. McKinney and DeVito (1998) listed the following as the most common, commercially practiced preparation methods:

- ammoxidation of hydrocarbons - mainly olefins - with ammonia and oxygen (see section 2.4.2.2;
- metathesis of organohalides - (reaction of organic halides with metallic cyanides (e.g. KCN, NaCN));
- dehydration of amides, which was the first commercial preparation method, but is not widely practiced today;
- addition of hydrogen cyanide to unsaturated organic compounds such as aldehydes, ketones and olefins.

In addition processes including the amination of hydrocarbons and reaction of acids with ammonia have been reported (see section 2.4.2.1 and 2.4.2.2).

2.4.2.1 From hydrocarbons and ammonia

A number of researchers have investigated the production of nitriles from the ammoxidation of hydrocarbons. The processes described below consist of a feed containing an alkane, ammonia and air/oxygen. The first stage in this case would be dehydrogenation of the alkane to the olefin and then ammoxidation of the olefin to the corresponding nitrile. Khoobiar *et al.* (1986 and 1988) for example discuss in particular the preparation of acrylonitrile from propane, steam, oxygen and ammonia in a 2-stage process. The dehydrogenation is carried out over a Group VIII noble metal catalyst at

400-700°Cand 0.1-5 bar and the ammoxidation at 375-550°C between 0.1-10 bar. Ramachandran *et al.* (1989) describe an improvement in the process for the production of nitriles (acetonitrile in particular) from alkanes/alkenes, air and ammonia. Industrially, the preparation of nitriles (e.g. acrylonitrile) from reacting olefins and ammonia is well known. However, the corresponding paraffins are usually cheaper than the olefins as a feedstock, and hence the interest in use of paraffins.

Dixon and Burgoyne (1986) studied the reaction of ammonia with olefins over various heterogeneous transition metal catalysts (Fe, Co and Ni). The reactions were conducted in a fixed bed reactor between 125-300°C, and 20bar with a GHSV of 200 hr^{-1}. The feed comprised of a 6:1 molar ratio of ammonia:olefin. The starting olefins tested were ethylene and propylene. The major product type collected was the nitrile of chain length one above the starting olefin, which was attributed to formation of adsorbed cyanide species on the surface, which would subsequently attach to the olefin.

2.4.2.2 From acids and ammonia

A number of U.S. patents (Nicodemus & Wulff, 1939; Hull, 1956; and Hagemeyer & Holmes, 1976) all describe processes and improvements in the processes for the production of nitriles from the catalyzed reaction of acids and ammonia at temperatures ranging from 220°C to 600°C. The most common catalysts employed are dehydrating catalysts. These include bauxite, aluminium oxide, phosphoric acid, butyl phosphate, thoria and silica gel. Although these processes are not necessarily feasible under FT synthesis conditions, they may be relevant due to the fact that the production of carboxylic acids, which are a side product in FT synthesis, is suppressed when ammonia is added to the process described in this thesis, and nitriles are among the new products formed. Consequently, a possible explanation may be that the carboxylic acids formed in the experiments conducted in this work could undergo a secondary reaction to form nitriles.

2.5. Ammonia addition to the Fischer-Tropsch synthesis

There is limited documentation on the addition of ammonia to the FT process. Most of the recorded work details the addition of ammonia to fixed bed processes, with amines being the predominant novel species formed (Kölbel & Trapper, 1966; Kölbel & Ralek, 1984; Kliger *et al*., 1986; Rottig, 1958; Brown & Maselli, 1973).

2.5.1. Amine formation

Rottig, (1958), in a patent document, describes the addition of ammonia or methylamine to the FT process. In his work, a potassium-promoted, precipitated-iron catalyst was used with an Fe:K_2O ratio of 100:8 (g/g). The end results included a high content of oxygenates in the product, and formation of nitrogen-containing compounds. The process was carried out with 0.5-2 vol% ammonia in the feed with a H_2:CO ratio varying from 0.5:1 to 6:1. The feed gas was passed over the catalyst at a rate of 10-1000 l_{gas}/l_{cat}·h. Reactor pressure and temperature were 1-100 bar and 190-210°C respectively. The combined $CO+H_2$ conversion ranged from 50-70%, with total oxygenate content in the product ranging from 30-40 wt%, of which the main constituent was aliphatic alcohols. The total content of nitrogen-containing compounds ranged from 10-20 wt%, with primary, aliphatic amines making up the bulk.

Kölbel and Trapper (1966) and Kölbel and Ralek (1984) described the co-feeding of ammonia to a fixed bed reactor containing a potassium promoted, precipitated-iron catalyst. The process was carried out under Kölbel-Engelhardt (KE) synthesis conditions, where steam was substituted for hydrogen, thereby exploiting the water-gas shift properties of the catalyst. The synthesis was carried out at 11bar and temperatures ranging between 219-235°C. The reactor feed consisted of 52.6% CO, 20.6% H_2O, 0.9% NH_3 and 23.7% Ar. CO and NH_3 conversions under these conditions were reported to be 80% and 31-35% respectively. The results showed formation of predominantly primary, unbranched, terminal alkylamines, accounting for up to 25 wt% of the total hydrocarbon product. Use of a slurry-reactor was reported to be unfavorable, and led to a lower ammonia conversion (Kölbel & Ralek 1984). They concluded from the results that the

formation of amines must follow a reaction mechanism that results in C-chain termination and elimination of water with the addition of chemisorbed ammonia.

In further investigations that complements their study on mechanism of ammonia/amine addition, Kölbel *et al*. (1974) investigated the co-feeding of methylamine and dimethylamine to the FT process, and reported the formation of terminal n-monomethyl-alkylamines (R-NH-CH_3) and N,N-dimethyl-n-alkylamines (R-N-$(CH_3)_2$ respectively. These results supported the findings from the initial work, that the amine/ammonia is added at the chain-termination stage. Furthermore, this indirectly proves that amines can readsorb and react further. However, their research showed a change in the degree of the amine alkylation, i.e. from primary to secondary or secondary to tertiary amines respectively with possibly little or no participation in chain growth of the readsorbed species.

Brown & Maselli (1973) published a patent describing the reaction of hydrogen, carbon monoxide and ammonia over a Group VIII metal, supplemented by smaller amounts of Group III and Group IA or IIA metals. The reactions were carried out between 160-220°C, and 50-200 bar. A typical feed comprised of NH_3:CO:H_2 of 0.03-0.5: 0.8-1.2: 1.0-3.0. n-Alkylamines of chain lengths 3-22 were reported, with amine selectivity in the product of 20-40 wt%.

Kliger *et al*. (1986) researched the effect of ammonia/amine addition on the aliphatic alcohol content in the product. From their findings, they concluded that aliphatic alcohols are not affected by the amines/ammonia, and that formation of alkylamines probably occurs through hydroamination of surface species in a primary synthesis step.

Knifton *et al*. (1993) worked on the homogeneous preparation of primary amines using cobalt catalysts, with phosphine ligands and under other ether/acetamide solvent systems. In their process, the feed comprised of olefin(s), syngas and ammonia and the reaction was carried out between 34-136bar and 150-250°C. The major products formed were primary, aliphatic amines. From a feed containing a C_n olefin substrate, the resultant amines were of a single carbon number greater (C_{n+1}), or two or three carbons

longer than twice or thrice the length of the starting olefin substrate (C_{2n+2}, C_{3n+3}). The main by-products formed were the corresponding alcohols.

2.5.2. Nitrile formation

Most work on nitrile preparation from a mixture of CO, H_2 and NH_3 focuses on the production of acetonitrile (see also section 2.4.2). In a number of U.S. Patents (Olivé & Olivé, 1979); Gambelli & Auvil, 1981; and Auvil & Penquite, 1981) the high temperature (350-600°C) reaction of CO, H_2 and NH_3 over transition metal catalysts is described. The metals tested include molybdenum and iron. Feed ratios of $CO:H_2:NH_3$ range from 1:0.5-1:1 up to 1:10:0.5-4.5. Product selectivities towards acetonitrile of up to 80 (wt)% have been reported (Auvil & Penquite, 1981). Hummel *et al*. (1993) also describe a method for producing acetonitrile over iron catalysts using CO, H_2 and NH_3 as feedstock. The reaction was done in a fixed-bed reactor at 425-450°C and atmospheric pressure.

Kim and Lane (1992) reacted CO, H_2 and NH_3 over Mo/SiO_2. CO conversion ranged from 29-64%, and selectivity to acetonitrile ranged from 37-96 (wt)% (excluding CO_2). They reported a significantly different carbon number distribution from the corresponding CO/H_2 feed in the absence of ammonia.

2.6. Reaction thermodynamics

The four main compound classes produced from the FT process are olefins, paraffins, alcohols and aldehydes. A thermodynamic study was done to determine:

- the relative stability of the different compound classes;
- relative stability of different chain lengths within the same compound families;
- from the above 2 points – the possibility of secondary reactions as system tends towards thermodynamic equilibrium;
- the temperature dependency of the reactions;
- insight into thermodynamic vs kinetic influences.

Furthermore, this data is compared with the corresponding data pertaining to amine and nitrile formation. C_1-C_{10} data is used where available. In the case of nitriles, only C_1-C_6

data was available. The thermodynamic constants for these calculations were obtained from Daubert (1999).

Figure 2.5 and 2.6 show the relation between carbon number and the normalised Gibbs free energy of formation at 500 K. The calculations were based on using CO, H_2 and NH_3 as the starting materials, and the Gibbs energy was normalised to the energy per mole of carbon monoxide reacted.

The following conclusions arise:

- The Gibbs free energy of formation for methane is much lower than that for any other compound in all classes, hence methane should be the only product in an ideal system.
- Alkanes are the most thermodynamically favourable product across all chain lengths (C_1-C_{10}), followed by alkenes, amines, alcohols, nitriles and aldehydes respectively.
- Methane is also the only C_1 compound with a negative Gibbs free energy of formation, hence the only thermodynamically favourable C_1 compound.
- All compounds from C_2 above have negative values for the free energy change. Hence they can all be formed from the reaction of carbon monoxide, hydrogen and ammonia, with their relative concentrations in an ideal state at equilibrium dependent on their relative Gibbs free energies of formation. Otherwise stated, this means amines can react to form alkanes and alkenes and the oxygenates can react to form amines, alkenes and alkanes etc due to their relative Gibbs free energies.
- With the exception of the alkanes, all the compounds have increasing thermodynamic stability with increasing carbon number.
- At higher chain lengths, the differences in the relative stability both between the compound classes, as well as between increasing chain lengths are much smaller.

In general, thermodynamic equilibria are not obtained in the product of Fischer-Tropsch synthesis, as kinetic factors play a much bigger role. This is clearly seen, for example, in the fact that olefin selectivities can be in excess of 80 mol% in a carbon number

hydrocarbon fraction in an FT process, and methane selectivities are generally much lower than 10-20 C%, whereas thermodynamics would predict more than 99 C% methane in the product (Anderson, 1984).

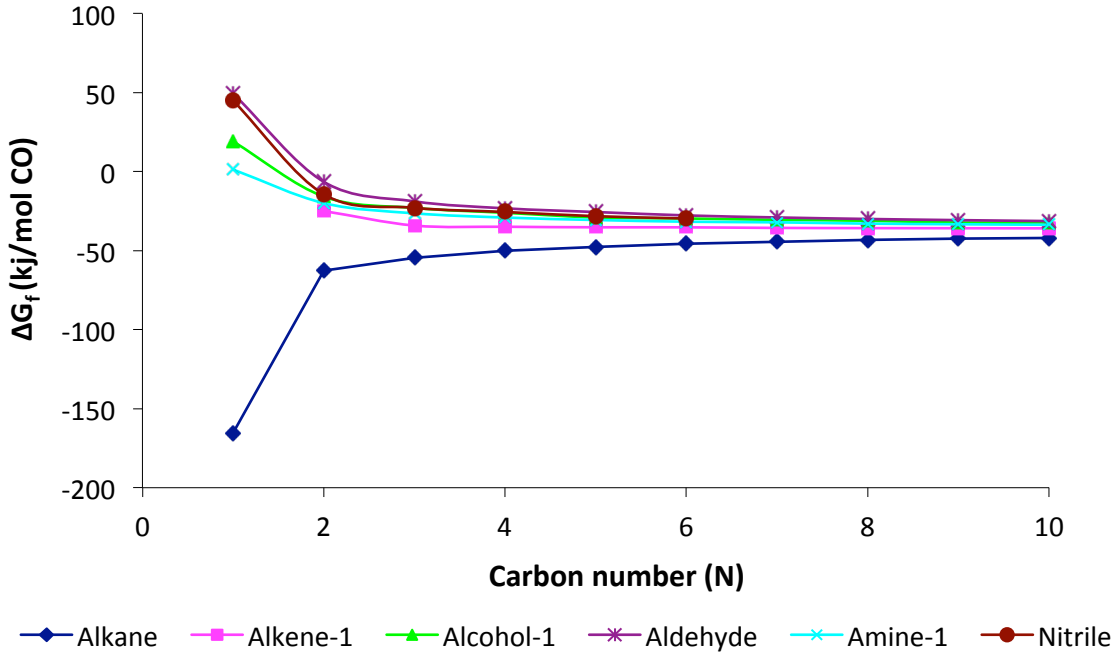

Figure 2.5: Gibbs free energy of formation of different linear products (range: C_1-C_{10}) as function of carbon number at 500K (per mole of carbon monoxide reacted)

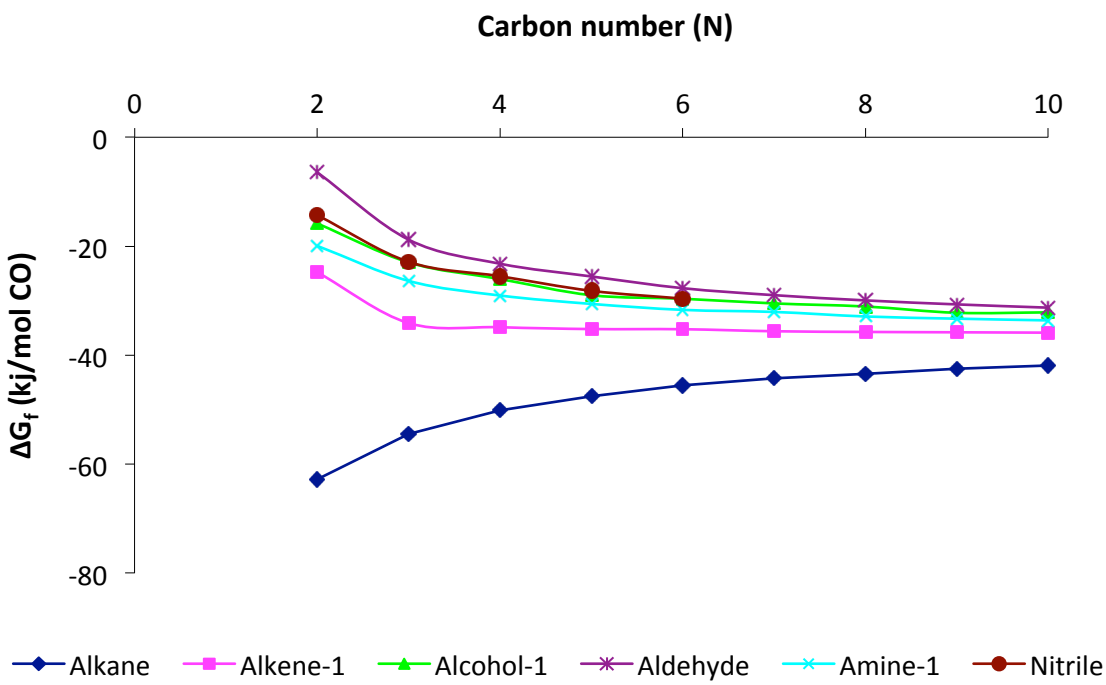

Figure 2.6: Gibbs free energy of formation of different linear products (range: C_2-C_{10}) as function of carbon number at 500K (per mole of carbon monoxide reacted)

Figure 2.7 shows the temperature dependency of the Gibbs free energy of formation for the linear C_{10} products. All the reactions are exothermic, hence increasing temperature will shift the reaction towards the left, i.e. decrease conversion. However, operating at low temperatures is not feasible as the rate of formation of the compounds is suppressed. Ultimately, the operating temperature is chosen based on achieving a reasonable rate of conversion of CO and H_2 whilst limiting the formation of undesirable products (especially methane, favoured by higher temperatures).

At low temperatures, the difference between the amine-1 and olefin-1 Gibbs free energies of formation is small, with the alcohol slightly higher than both. However, as temperature increases, the olefin becomes more favorable and the difference between the amine and the oxygenate becomes much smaller.

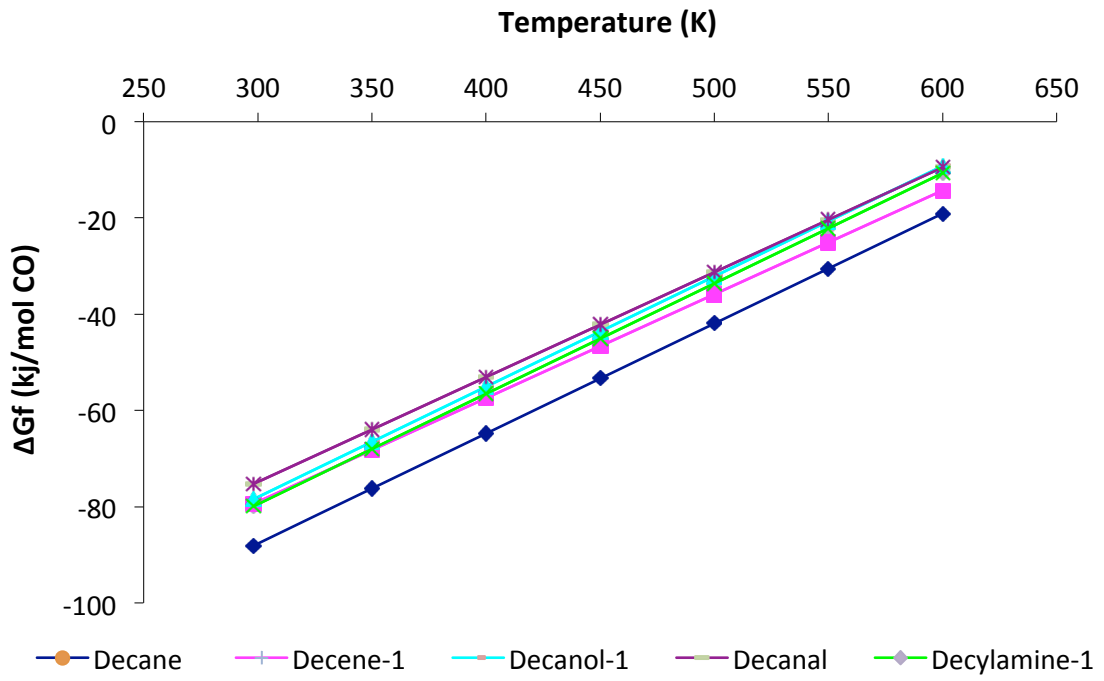

Figure 2.7: Temperature dependency of Gibbs energies of formation of different linear products in the C_{10} fraction

In summary, from figures 2.5-2.7, the following are predictable from a thermodynamic perspective under our system conditions:

- production of amines from oxygenates and nitriles;
- nitrile formation from aldehydes and (to a lesser extent) alcohols;
- amine and nitrile reaction to form paraffins, olefins and some oxygenates.

The thermodynamic study gives an indication of the relative stability of the different compounds under FT synthesis conditions. However, a thermodynamic analysis does not take into account reaction pathways. The employment of a catalyst will affect the reaction pathways and kinetics. Ideally, a catalyst is employed such that it provides a reaction pathway favoring the desired product(s). This means that the system can operate away from equilibrium, with the product composition shifted towards less thermodynamically stable but more desired compounds. In general, the FT reaction is not operated under thermodynamic constraints, but controlled via kinetic limitations. Depending on the product requirement, a catalyst is tailored to maximize production of certain compounds classes. Ultimately, this means production of nitrogen-containing

compounds can be enhanced in the process by studying the kinetics of formation of these compounds. The process parameters can also be modified to further enhance synthesis of selected product classes. Parameters that can be changed include feed ratios, partial pressures, space velocities/residence time, reaction temperature, catalyst composition and other factors.

3. SCOPE OF THIS WORK AND RESEARCH QUESTIONS

Based on the results from previous research, the initial objectives of this study were focused on amine formation from the modification of the Fischer-Tropsch reaction. Preliminary work done at the Centre for Catalysis Research during the course of this study resulted in a product spectrum containing the 'normal' FT products (paraffins, olefins, oxygenates) and primary, aliphatic amines. Unlike previous studies, however, nitriles, amides and formamides were also detected in the product spectrum. This resulted in the widening of the scope of this study to include identification and quantification of all nitrogen-containing species.

The primary goal of this project was therefore to identify the range of nitrogen-containing compounds that could be synthesized from the co-feeding of ammonia during Fischer-Tropsch synthesis, followed by the determination of the effect of ammonia partial pressure on the activity and product distribution. Parallel GC-MS and GC-FID analyses would be used to respectively identify and quantify the nitrogen-containing compounds in the product stream. An iron based, potassium promoted catalyst was tested in a low temperature (maximum 250°C), low pressure, slurry phase process. A set of basic FT operation conditions was selected and held constant through the whole project, as the ammonia partial pressure in the feed is increased systematically. The total pressure of the system was adjusted to the corresponding ammonia partial pressure to maintain constant partial pressures of the synthesis gas components throughout the study. The slurry reactor provided an ideal reactor system for this study as one reaction parameter (in this case ammonia partial pressure) could be varied while all other parameters/partial pressures were kept constant.

The following were then the main research questions that this work was seeking to shed light on:

1. Is the production of amines from co-feeding ammonia to a slurry phase, low temperature FT system feasible and comparable to previous work?
2. What other nitrogen-containing compounds can be synthesized from this system?
3. What are the effects of ammonia partial pressure on:

- Catalyst (FT) activity?
- Product selectivity?

4. Is there any evidence of secondary reaction of any of the compounds in the product spectrum, e.g. readsorption of oxygenates to form nitrogen-containing compounds or readsorption of nitrogen-containing compounds to form more stable compounds?
5. Can the mechanism of formation of any new compounds be determined, and can the results give clues to confirm or disprove previous theories on FT mechanisms of product formation?

4. EXPERIMENTAL METHODOLOGY

4.1. Catalyst preparation

A potassium-promoted, precipitated iron catalyst was used for this study. To minimize discrepancies, sufficient catalyst for the duration of the study was synthesized at the beginning of the study in a single preparation. An amount of 30g of catalyst was synthesized on an iron-weight basis and Figure 4.1 shows the overview of the catalyst preparation steps, with the details of each preparation stage described thereafter. The catalyst was prepared/treated in bulk until the potassium-promotion stage. Thereafter, reduction was carried out separately for each individual test.

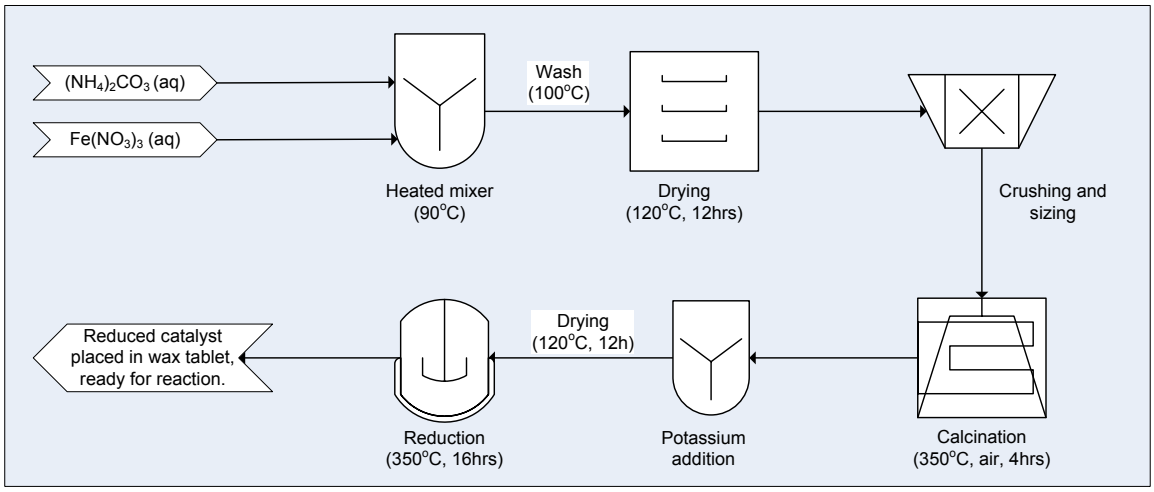

Figure 4.1: Summary of catalyst preparation stages and conditions.

4.1.1. Catalyst precipitation

Hydrated iron nitrate ($Fe(NO_3)_3 \cdot 9H_2O$, 99%, Sigma-Aldrich Inc.) and ammonium carbonate ($(NH_4)_2CO_3$, 30% as NH_3, Fluka) were used to prepare a 1M aqueous iron nitrate solution and a 20 wt% ammonia solution respectively. The iron nitrate solution was heated to 90°C and the ammonium solution to 60 °C (lower temperature to avoid ammonium carbonate decomposition/ammonia loss) in a fume hood. The ammonium solution was added to the iron nitrate solution until a pH of 7 was achieved. The mixture was agitated using an overhead stirrer (Heidolph RZR 2020, 45-2000 rpm) during the

ammonia addition, and was stirred at 1000 rpm for a further 15 minutes after pH 7 was attained. The supernatant solution was filtered off and the precipitate washed, nitrate free, with 4 litres of boiling de-ionised water.

4.1.2. Catalyst drying, crushing, calcining, and promotion

The precipitate was dried overnight in an oven at 120°C. After drying, the precipitate was crushed to a powder, d_p < 125 µm. The crushed precipitate was calcined under air flow (120ml/min/g) at 350°C (heating rate of 10°C) for 4 hours in order to form iron oxide, Fe_2O_3. The calcined catalyst was potassium-promoted via incipient impregnation using a 1 molar aqueous solution of potassium nitrate (KNO_3, 99%, Kimix) in a rotary evaporator (Büchi R-205). This was targeted at producing a catalyst with an Fe:K ratio of 100:2 (g/g). This was followed by drying overnight at 120°C and calcining under air flow (120ml/min/g) at 350°C (heating rate of 10°C) for a further 4 hours.

4.1.3. Catalyst characterization

The promoted, calcined catalyst was analyzed using atomic absorption spectroscopy (AAS) to determine potassium loading and the Brunauer-Emmet Teller (BET) method for determination of the surface area of the catalyst. AAS analysis of the resultant precipitated, calcined and promoted catalyst showed a ratio of Fe:K of 100:1.52 (g/g), with an iron content of 69.2 wt% and a BET area of 30 $m^2/g_{catalyst}$.

4.1.4. Catalyst reduction

The catalyst was activated externally under hydrogen flow in a fluidised bed reactor, using a temperature programmed reduction procedure. The temperature was ramped at 1°C/min from ambient to 100°C, and held at this temperature for 1 hour; and then ramped at 1°C/min to 350°C, where it was held for the 16 hours reduction time under a hydrogen flow of 4000 ml(NTP)/g_{Fe}·hr.

To produce the 2g of the reduced catalyst (basis: metallic iron, assuming complete reduction) required for the slurry reactor, 3.2g of the promoted, calcined catalyst was

loaded. After reduction, flow was switched from hydrogen to argon to create an inert atmosphere. As the reduced catalysts is allowed to cool, 5g wax (Sasol grade wax, “H1”, carbon number >30) was melted in a covered beaker. Argon flow was fed into the beaker for 20 minutes to displace air/oxygen. The reduced catalyst was then transferred into the beaker, and the wax-catalyst mixture allowed to cool and solidify. The resultant catalyst tablet keeps the reduced catalyst from reoxidation, and is stored until the start of each run, when it is added to the slurry reactor, containing 270 g molten wax (purged of air with argon).

4.2. Fischer-Tropsch synthesis

4.2.1. Experimental setup

A slurry phase reactor was used for the Fischer-Tropsch study. The reactor vessel (Parr Instruments 452HC03, stainless steel, volume: 600ml) was equipped with an external heating jacket and a magnetic stirrer-drive (Parr instruments A1120HC), which operated at 300 rpm for the purposes of this study.

The externally reduced catalyst was suspended in 270g of a Sasol grade wax (“H1”, carbon number >30), filling up the reactor vessel to ca. 60% of the total volume. The feed gases were supplied from pressurized cylinders (Air Products: H_2 5.0, CO 5.0, Ar 5.0, N_2 5.0). The ammonia/hydrogen mixtures were sourced from Air Liquide. The gas flows were controlled using Brooks 5850 series mass flow controllers. The mixed feed gas was bubbled into the slurry and reactor product was removed in the gaseous phase together with the formed liquid phase using a filter device (Figure 4.2). A porous frit was suspended in the slurry, and the liquid product filtered through this device into the gas outlet line via a T-piece. The other end of the T-piece was open ended, and suspended above the slurry mixture providing an exit pathway for the gaseous product.

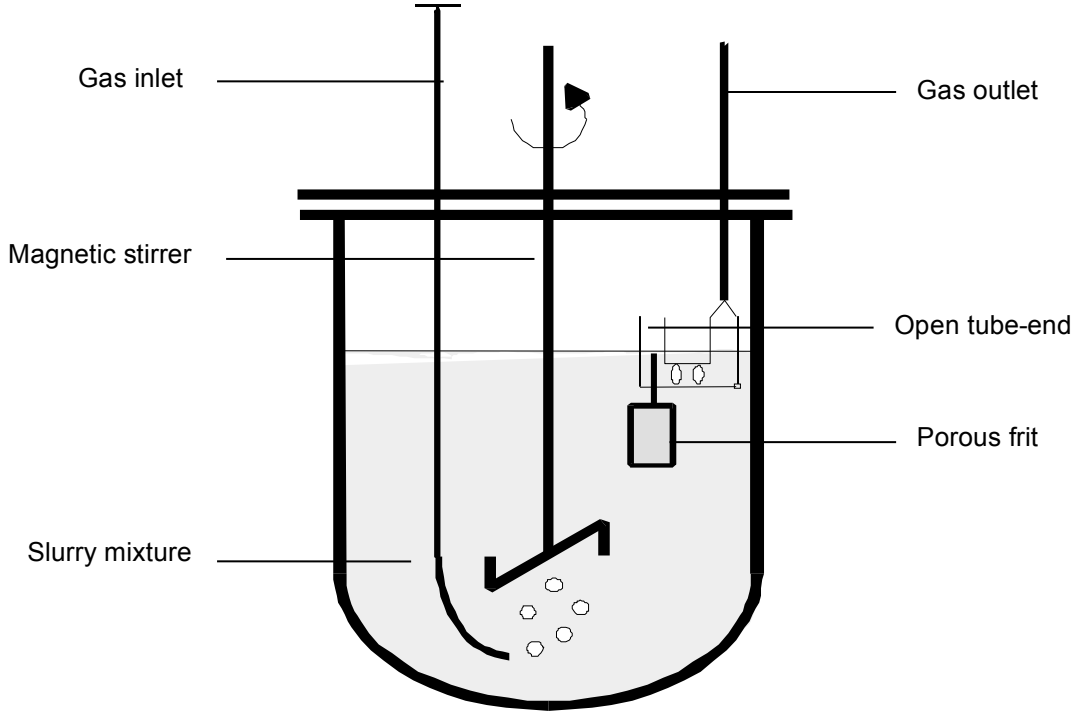

Figure 4.2: Schematic representation of the slurry reactor

A schematic of the full experimental setup is shown in Figure 4.3. A bypass to the reactor was also available to enable feed gas composition to be determined using the online GC-TCD. Reactor pressure was controlled using an argon stream, fed to the hot gaseous product downstream of the reactor before a flow restricting needle valve. The flow through the needle valve was set to 150-200 ml/min (NTP). A pressure regulator was used to maintain the argon line pressure. A reference gas mixture containing nitrogen and cyclohexane (0.15% cyclohexane) was fed into the product stream downstream of the flow restricting needle valve. The gases were used as internal standards for chromatographic analyses.

The lines downstream of the reactor were lagged using glass wool and were electrically heated to 180°C. The wax trap was kept at 180°C, and was targeted at removal of heavy wax components from the product stream. Gas, liquid and solid samples were collected from the system. A gas sampling point was located downstream of the wax trap, and glass ampoules where used to collect this product. The ampoule sampling point was followed by two cold traps, one at room temperature and the second one at ca. 4°C. The samples and conditions were as follows:

1. Glass ampoules for collection of a sample representative of the total gaseous product (180°C, 1 bar), including reference gas (cyclohexane in nitrogen carrier gas).
2. A cold trap for collection of condensed liquid (containing both oil and water) at room temperature (ca. 22-24°C, 1 bar).
3. A second cold trap placed in ice water for collection of any heavier liquid fractions and a solid product that was formed in the ammonia-containing syntheses (ca. 4°C, 1 bar).

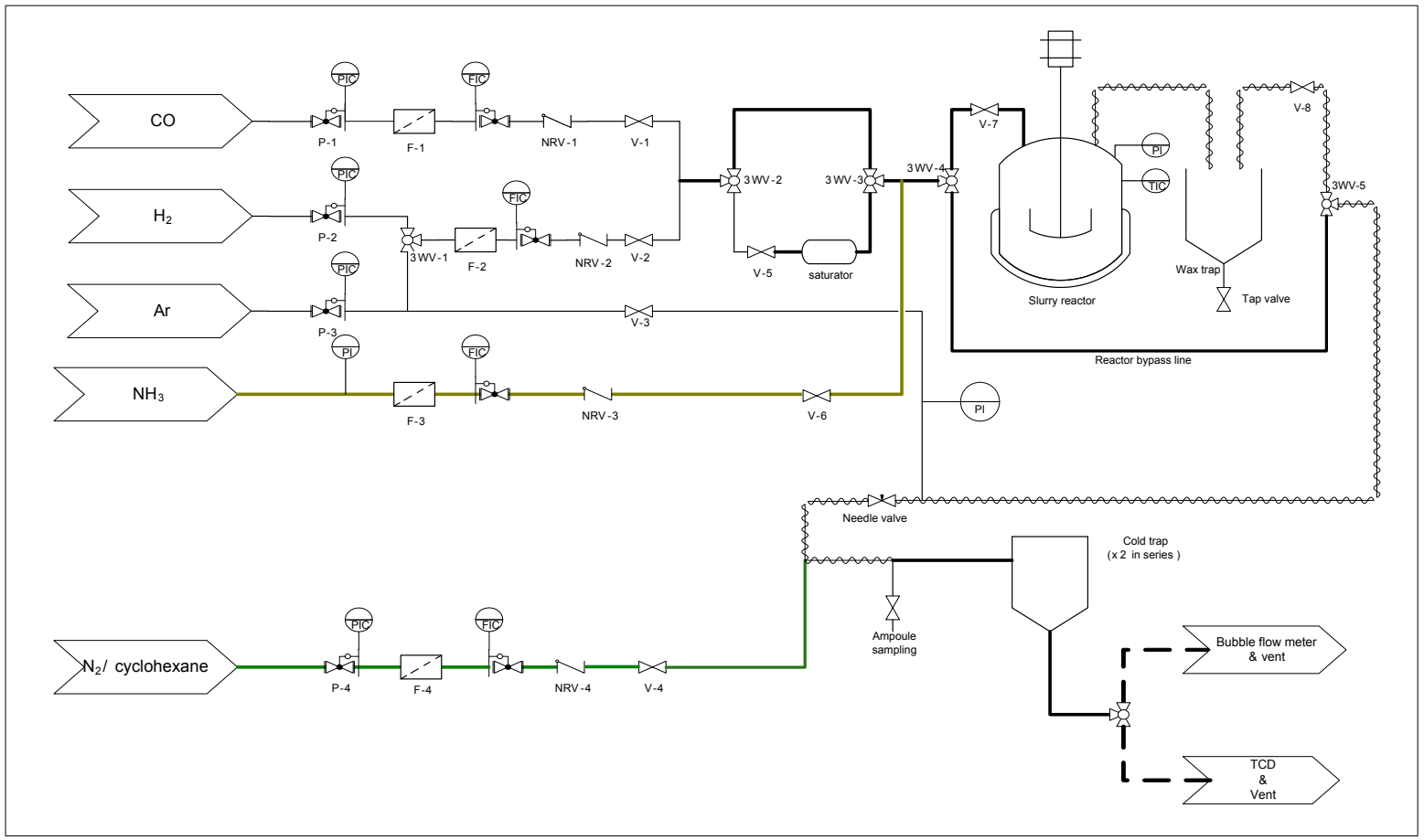

Figure 4.3: Schematic representation of the experimental setup for FT testing using a slurry reactor

Key: PIC: Pressure indicator controller; P1-4: pressure regulators; F1-4: Filters; FIC: Flow indicator controllers, NRV1-4: Non-return valves; V1-8: On-off valves; TIC: temperature indicator controller; 3WV1-5: three-way valves

4.2.2. Sampling procedure

This section describes the different types of samples that were collected for offline analysis, and the methods used for their collection.

4.2.2.1. Collection of gas/vapour samples using the ampoule technique

Gas samples were collected using evacuated, preheated glass ampoules as illustrated in Figure 4.4. The ampoule samples were collected after running each condition for 48hrs time-on-stream (the last 3 experiments where shortened due to buildup of a white solid in the product lines).

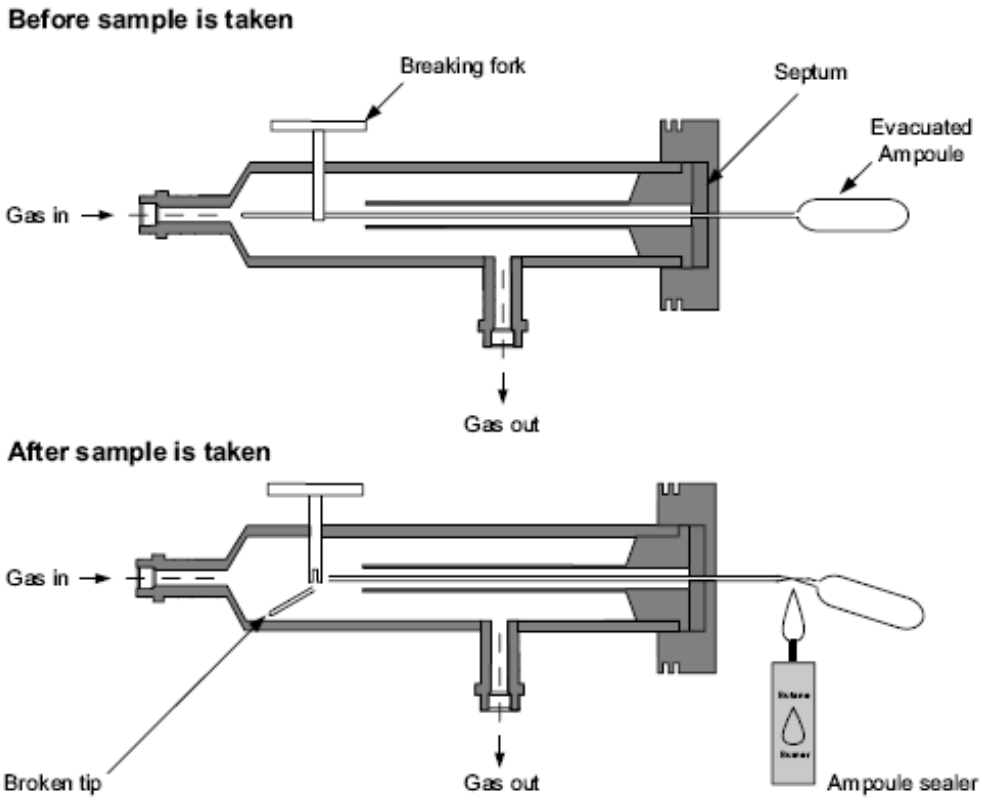

Figure 4.4: Ampoule sampling device and setup

The ampoules consist of a capillary end, and a bulbous end. The capillary end is inserted into the heated product line of the Fischer-Tropsch unit via a gas-sampling device. The capillary is inserted via a septum, and the tip is subsequently broken, allowing gas product to be sucked into the previously evacuated ampoule. The ampoule

is then partially withdrawn from the gas sampling device, and sealed off close to the bulbous end using a butane flame. This sample then contains all of the products which are present as gases or vapors at reaction temperature.

4.2.2.2. Collection of liquid and solid phase product

The procedure for collecting the liquid and solid samples was relatively simple. Samples were collected over the last 12 hour period for each condition in the two cold traps. A 3-way valve was used to temporarily redirect the reactor effluent to the vent whilst the cold traps were emptied and the 2nd cold trap replenished with ice water. The 3-way valve was then used to redirect flow through the cold traps. After 12 hours, the flow was redirected again, and the cold traps decanted.

4.2.3. Base case conditions

Before ammonia addition to the process was carried out, a base set of FT conditions was decided on. The conditions are tabulated in Table 4.1.

Table 4.1: Base case FT synthesis conditions for the study

Catalyst	Precipitated iron
Potassium loading (Fe:K, g/g)	100:2
Catalyst loading in reactor (reduced iron, g)	2.0
H_2:CO ratio (mol/mol)	2:1
Syngas Feed (H_2+CO) (ml/min(NTP))	75
Reactor temperature ($^{\circ}$C)	250
Reactor (syngas) pressure (bar)	5

4.2.4. Variation of ammonia partial pressure

The primary purpose of this study was to establish the change in the FT product spectrum upon addition of ammonia to the system. This was closely coupled with the investigation of the effect of varying the ammonia content on the system. The low vapor pressure of ammonia at room temperature necessitated using pre-mixed

ammonia/hydrogen gases to allow operation of the system at pressures higher than or close to that of the ammonia vapor pressure at room temperature. As seen from Figure 4.5, the ammonia vapor pressure is ca. 8 bar at room temperature (20°C).

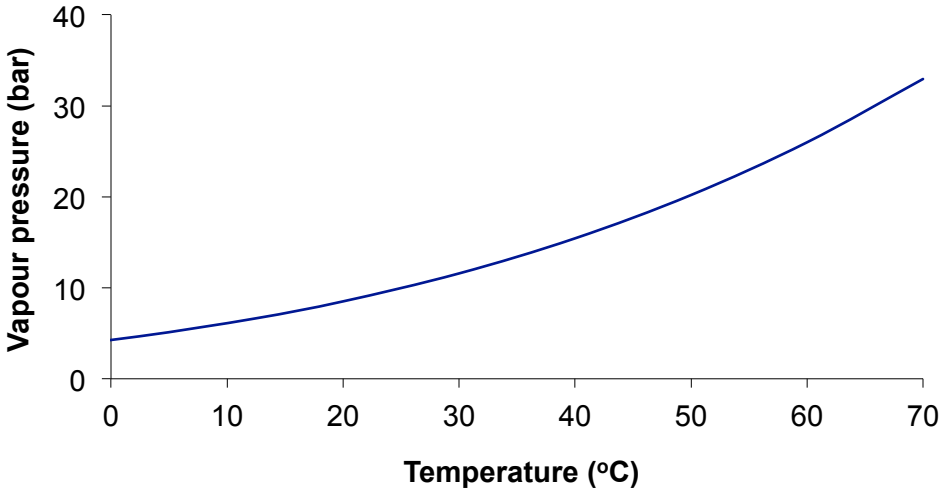

Figure 4.5: Vapor pressure curve for pure ammonia
(Thermodynamic data obtained from Daubert, 1999).

The partial pressure of ammonia in the mixture has to be kept well below its ambient vapor pressure to avoid any condensation. Therefore ammonia-hydrogen mixtures were used with the partial pressure of ammonia always being kept well below 8 bar. Two different mixtures were used - for low and high ammonia feed contents into the Fischer-Tropsch system respectively. For low ammonia content in the system, an ammonia:hydrogen ratio of 1:4 (vol/vol) was used, with a total pressure of the mixture of 25 bar. For higher ammonia content, the mixture was 1:1.7 (vol/vol), with a total pressure of 13 bar.

Based on a similar study by Kölbel & Trapper (1966) a low level of ammonia (2 vol% in the feed gas) was used as a starting point. The ammonia content in the feed was then increased sequentially up to 35 vol%. The reactor pressure was increased in tandem to account for ammonia partial pressure so as to keep the syngas ($CO+H_2$) partial pressure in the reactor feed constant at 5 bar. With the exception of the 20 vol%, 35 vol% and 10 vol% rerun, each condition was run for 48 hours The 20 vol%, 35 vol% and the 10 vol% reruns were shortened to 24 hours due to clogging up of the system by a solid product.

Base case conditions without ammonia in the feed were revisited after the run with 10 vol% ammonia in the feed to ascertain catalyst deactivation effects. The rerun at 0 vol% ammonia was used to check for any significant variations or reversible deactivation as compared to both the original run at 0 vol% and the ammonia-containing runs. Furthermore, at the end of the series (after the run under 35 vol% ammonia in the feed), it was decided to run the system at 10 vol% ammonia to check for any significant changes in activity relative to the original run under 10 vol% ammonia, and also for any shifts in activity relative to the other runs. Both of these reruns were done purely to observe activity in terms of CO conversion to FT product. The feed conditions for the different levels of ammonia co-feed are summarized in Table 4.2.

Table 4.2: Summary of ammonia feed conditions, and modified reactor pressures.

Ammonia content in feed (vol%)	Syngas flow rate (H_2+CO) (ml/min(NTP))	Ammonia flow rate (ml/min(NTP))	Reactor pressure (bar)
0	75	0.0	5.0
2	75	1.5	5.1
5	75	4.0	5.3
10	75	8.3	5.6
0[a]	75	0.0	5.0
20	75	18.8	6.3
35	75	40.4	7.7
10[b]	75	8.3	5.6

a-0 vol% rerun; b-10 vol% rerun.

4.3. Product analysis

4.3.1. TCD analysis (online)

An online Varian 3600 GC equipped with a 4-filament thermal conductivity detector connected to an HP 3390A peak integrator was used to determine syngas (H_2 and CO), carbon dioxide and methane exit flow rates from the reactor. The column parameters are summarized in Table 4.3.

Table 4.3: Conditions for online chromatographic analysis using TCD detection

Detector	4-filament thermal conductivity detector (TCD)
Column type	Packed, stainless steel, 3 m x 2.1 mm (ID)
Stationary phase	Carbosieve II, 100-120 mesh (Supelco)
Carrier gas	Argon
Flow rate (column and reference)	30 ml(NTP)/min
Column temperature (°C) (isothermal)	150
Detector temperature (°C)	180
Filament temperature (°C)	200

Nitrogen was used as the reference gas for the determination of inorganic gas (CO, H_2, CO_2) and methane flow rates from the TCD analysis. The nitrogen was fed in at 25 ml(NTP)/min downstream of the reactor (see figure 4.3). The flow rates of each of the individual gases ($F_{i,TCD}$) were then computed from the TCD peak areas (A_i), and calibration factors of each component relative to nitrogen ($rf_{i,TCD}$) using equation 4.1:

$$F_{i,TCD} = 25 \times rf_{i,TCD} \times \frac{A_i}{A_{N_2}} \quad (4.1)$$

Detector (TCD) response factors for the respective gases relative to nitrogen were determined via analysis of a gas mixture with a known and certified composition (Afrox, 41.1% H_2, 9.7% CH_4, 19.6% CO, 9.8% CO_2, 9.7% N_2, balance-argon). Equation 4.2 below was used to obtain the TCD response factor for each component ($rf_{i,TCD}$) relative to that of nitrogen:

$$rf_{i,TCD} = \frac{C_i}{C_{N_2}} \times \frac{A_{N_2}}{A_i} \quad (4.2)$$

where A_{N_2} and A_i are the peak areas obtained for nitrogen and component i respectively, and C_{N_2} and C_i are the molar concentrations of nitrogen and component i in the standard mixture respectively. Typical response factors obtained for the TCD were:

$$rf_{CO,TCD} = 1.0750,\ rf_{H_2,TCD} = 0.1022,\ rf_{CH_4,TCD} = 0.3464,\ rf_{CO_2,TCD} = 1.1564$$

(sample calculations given in appendix B).

An analysis of ammonia was not possible with this set-up and ammonia conversion could not be determined in this study. However, a nitrogen balance was done on the

reactor product and compared to the incoming ammonia to determine ammonia consumption to a certain extent.

4.3.2. FID and GC-MS analysis (offline)

Identification and quantification of organic products was conducted via offline gas chromatography using parallel GC-MS and FID analyses. An HP6890 GC (Agilent Technologies) equipped with 2 parallel OV-1-type capillary columns connected to an FID and MSD (Agilent Technologies 5973N) was used. The details of the columns and detectors are given in Table 4.4. Samples collected in the ampoules and in the liquid cold trap were analyzed. Once injected into the GC via a split/splitless injector (split ratios: 1:10 to 1:100 depending on the sample), each sample was split equally into two streams, with each split eluted through one of the two parallel, fused silica capillary columns. The two columns provided separate feeds to the MS and the FID respectively. Different methods were employed for the gas and liquid analyses (Table 4.5 and Table 4.6 respectively later in the chapter).

Table 4.4: Conditions for offline chromatographic analysis using MS/FID detection

	Column 1 (MSD)	Column 2 (FID)
Detector	MS	FID
Column	Fused silica capillary column, Restek 661049	Fused silica capillary column, Restek 661049
Stationary phase	0.5 μm dimethyl polysiloxane	0.5 μm dimethyl polysiloxane
Carrier gas	Helium	Helium
Column length (m)	60	60
Nominal diameter (μm)	250	250
Nominal thickness (μm)	0.5	0.5
Operation mode	Constant pressure	Constant pressure
Detector	MS	FID
Detector temperature (°C)	230	250

Based on the experimental setup, analysis of the ampoule samples was expected to give the most thorough representation of the product. Due to the fact that ampoule samples are collected from the unabridged stream exiting the reactor (see figure 4.2), it is expected that all components which are volatile at reaction conditions (i.e. C_1 to approx. C_{20}) would be collected in the ampoules. Any heavy waxes produced in the reactor with high boiling points as well as any of the Sasol wax used for the slurry escaping from the reactor would be expected to deposit in the hot trap which was kept at 180°C. Based on the setup, and absence of any runoff from the hot trap, the flow calculation for compounds in the product was predominantly based on ampoule analysis.

The response of the FID is carbon specific. This means that the observed area is proportional to the effective number of carbon atoms detected. For most of the organic product, the detector "sees" all the carbon atoms in the molecule. However, for some molecules, the detector gives a response less than the number of carbon atoms present, e.g. oxygenated components such as alcohol, aldehydes, acids etc. Theoretical incremental response factors (Appendix C as described by Kaiser, 1969) were used for determining the corrected area:

- the response of all carbon atoms not connected to an oxygen atom is 1,
- a carbon atom connected to an oxygen atom via a single bond giving a response of 0.55 and,
- a carbon atom double-bonded to an oxygen atom giving a response of 0.

Cyclohexane, which is not a product of FT synthesis, was used as the internal standard for FID analyses. Feeding a known amount of cyclohexane (via the reference gas line) allows for the calculation of the flow of all carbon-containing compounds detected in the ampoules. The cyclohexane (in a N_2/cyclohexane mixture, 0.15 vol% cyclohexane) was fed into the product line downstream of the reactor. The molar flow rate of cyclohexane in the reference gas line was then used to determine the flow rates of the different organic components in the product using relative (theoretical) response factors between the different compounds and cyclohexane as described by Kaiser (1969).

Molar flow rates of each component (denoted by i) from ampoule analysis were then computed using equation 4.3:

$$F_{i,FID} = \frac{A_i}{A_{ref}} \times \frac{rf_i}{rf_{ref}} \times \frac{N_{ref}}{N_i} \times F_{ref} \quad (4.3)$$

(where $F_{i,FID}$ and F_{ref} are the molar flow rates of component i and the reference compound –cyclohexane, calculated from the reference gas composition and flow rate- respectively; rf_i and rf_{ref} are the FID response factors of component I and cyclohexane respectively: A_i and A_{ref} are the peak areas obtained for component i and cyclohexane respectively; and $N_{C,i}$ and $N_{C,ref}$ are the respective number of carbon atoms in a molecule of component i and cyclohexane respectively).

The FID response factor for each component is obtained using equation 4.4 below:

$$rf_i = \frac{N_{C_i,actusl}}{N_{C_i,FID}} \quad (4.4)$$

(where $N_{c,actual}$ and $N_{c,FID}$ effective number of actual carbon atoms per molecule and effective number of atoms detected per molecule by the FID respectively).

The response factors where determined and used as described by Kaiser (1969) and typical response factors are shown in appendix C. Response factors for nitrogen-containing compounds were obtained from C_8 standards, with the corresponding olefin as a reference compound. Based on the results, the C_8 nitrile gave a response of 8 carbons per molecule (i.e. rf=$\frac{8}{8}$), with the C_8 amine giving a response of 7 carbons per molecule (i.e. rf=$\frac{8}{7}$). By adopting the same theory as used by Kaiser, all nitriles were assumed to give a response equivalent to the number of carbon atoms in the molecule and amines were assumed to give a response of 1 less than the carbon number of the compounds respectively, and these are included in appendix C.

Absence or disappearance of certain classes of compounds occurred in the analysis of the ampoule samples and this has been reported before (Cairns, 2008). These included acids, amines and amides, which were later detected in the liquid phase analysis. The reasons for this phenomenon are not wholly understood, but could be due (but not limited) to any of the following:

- the compounds adhere to the glass surface of the ampoules;
- the compounds adhere to the surface of the metallic transfer line on the GC-MS/FID from the ampoule breaker to the column.

The liquid samples from the cold trap were hence used to identify and quantify some of the compounds. The liquid product formed two distinct layers as expected - a water-rich (water) bottom layer and an oil-rich (oil) top layer. The total amount of liquid collected was however not consistent, with the volume collected dropping significantly with increasing ammonia content in the feed. From visual inspection, the split shifted to being water rich with increasing ammonia content. The volumes collected where small (mostly less than < 1 ml), yet fully sufficient for qualitative and quantitative chromatographic analysis except for the experiments where a very high ammonia concentration was used (20 and 35 vol%); here no sufficient amount of liquid could be collected so that only analysis of ampoule samples was possible.

The formation rates of the compounds observed in the liquid analysis, but absent from the ampoule analysis were estimated by performing a mass balance over the two analyses. Using a common component observed in both analyses as a reference, the formation rates of all other components in the liquid phase were calculated. The formation rate of the tie component was determined from ampoule analysis. The common component was then assumed to condense completely in the cold trap. Hence the formation rate of this component was easily determined by performing a mass balance over the 2 liquid fractions (oil and water) and the ampoule results. In this case, the C_{15} alpha-olefin (n-pentadecene-(1)) formed in the reactor was used as the common component and was divided into the oil (predominantly) and water layers in the cold trap. Hence the rate of condensation of this component into the 2 layers in the cold trap is equal to the flow rate / formation rate of the n-pentadecene-(1) obtained from ampoule analysis:

$$F_{\mathrm{n-pentadecene-(1),amp}} = F_{\mathrm{n-pentadecene-(1),oil}} + F_{\mathrm{n-pentadecene-(1),aq}} \qquad (4.5)$$

where $F_{C12\text{-}CN,amp}$ is the molar flow rate of n-dodecane-nitrile obtained from the ampoule FID analysis, $F_{C12\text{-}CN\text{-}ol,oil}$ and $F_{C12\text{-}CN,aq}$ are the molar flow rates of n-dodecane-nitrile into the oil and aqueous layers respectively in the cold trap. The formation/condensation rates of all other compounds into the two liquid fractions were then computed from the respective oil and water FID analyses using the C_{12} nitrile as the reference/common

compound (eq 4.6), and using the theoretical response factor approach developed by Kaiser.

$$F_{i-liq,FID} = F_{C_{12-CN}-liq} \times rf_{i-l,FID} \times \frac{A_{i-liq,FID}}{A_{C_{12-CN}-liq,FID}} \quad (4.6)$$

where $F_{i\text{-}liq,FID}$ and $F_{C12\text{-}CN\text{-}liq}$ are the molar formation rates of component i and the C_{15} olefin-1 in each liquid layer (either oil or water) respectively i, $rf_{i\text{-}lid,FID}$ is the relative response factor of compound i relative to the C_{12} nitrile and $A_{i\text{-}liq}$ is the area of each component from the FID analysis. (Note, pentadecene-1 was initially used as the reference compound for the gas-liquid mass balance. However, this was later changed to the C_{12} nitrile as it was also obtained cleanly in all phases, but more importantly, n-pentadecene-1 losses were possible from the cold trap analyses -i.e. not all of it condensed- and hence save for the ammonia-free run, the C_{12} nitrile was found to be more suitable).

4.3.2.1 Ampoule analysis conditions

The glass ampoules are introduced to the GC column using an ampoule breaking device (heated to 220°C). The ampoule breaking device is connected to the column via a 6 port valve. Figure 4.6 shows the configuration of the system, with the ampoule breaking device and associated piping represented by the sample loop. The device has a continuous flow of helium through it with the valve normally set to position A. The carrier/mobile phase for the column is also helium. At the start of a GC run, the ampoule is broken (within the sample loop) and the valve switched to position B for 30 seconds, allowing the sample to be fed to the column. After 30 seconds, the valve is returned to the default setting.

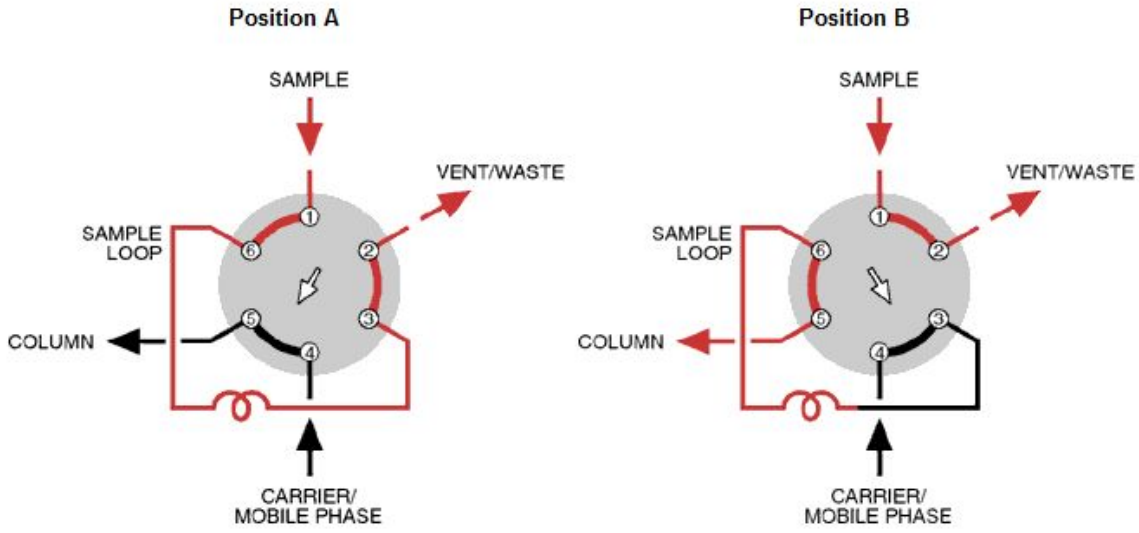

Figure 4.6: Schematic of gas sample (ampoule) injection onto the GC-MS/FID

Table 4.5 below details the temperature programme used for the analysis of the gas/vapor phase reactor product.

Table 4.5: Temperature programme used for GC-MS/FID analysis of ampoule samples (the column head pressure was kept constant at 2.0 bar throughout analysis):

Oven operation:	Initial temperature: -60 °C	
Ramp (°C/min)	Final temperature (°C)	Hold time (min)
-	-60	5
15	-35	1
10	-5	2.5
2.5	25	0
5	280	30

A typical chromatogram obtained from FID analysis of the ampoule samples taken during an experiment without ammonia addition is depicted in Figure 4.7, with the major hydrocarbon peaks (linear olefins-1 and paraffins) indicated.

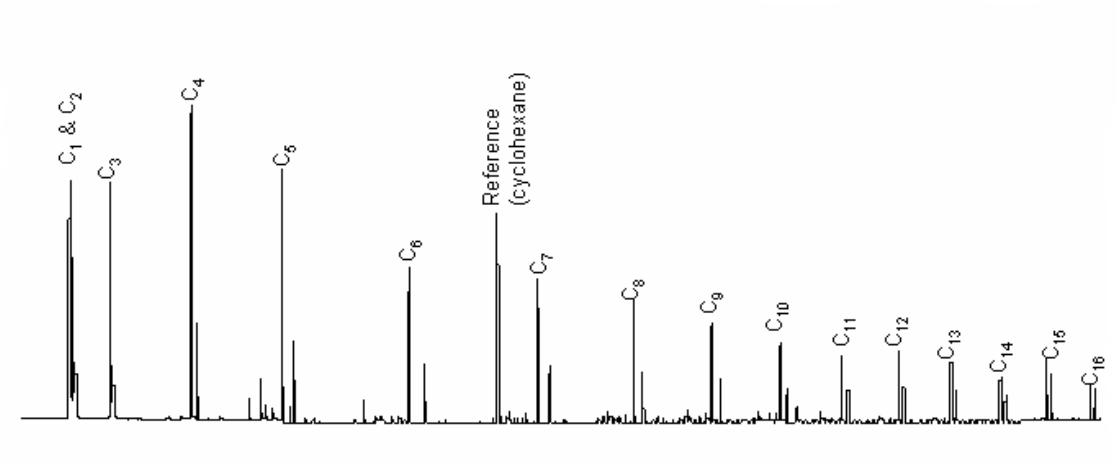

Figure 4.7: A typical FID chromatogram obtained from an ampoule sample taken during base case FT synthesis without ammonia addition showing the location of the major hydrocarbon peaks.

Figure 4. 8 and Figure 4.9 go on to identify the typical locations of the main products relative to the location of the major product peaks.

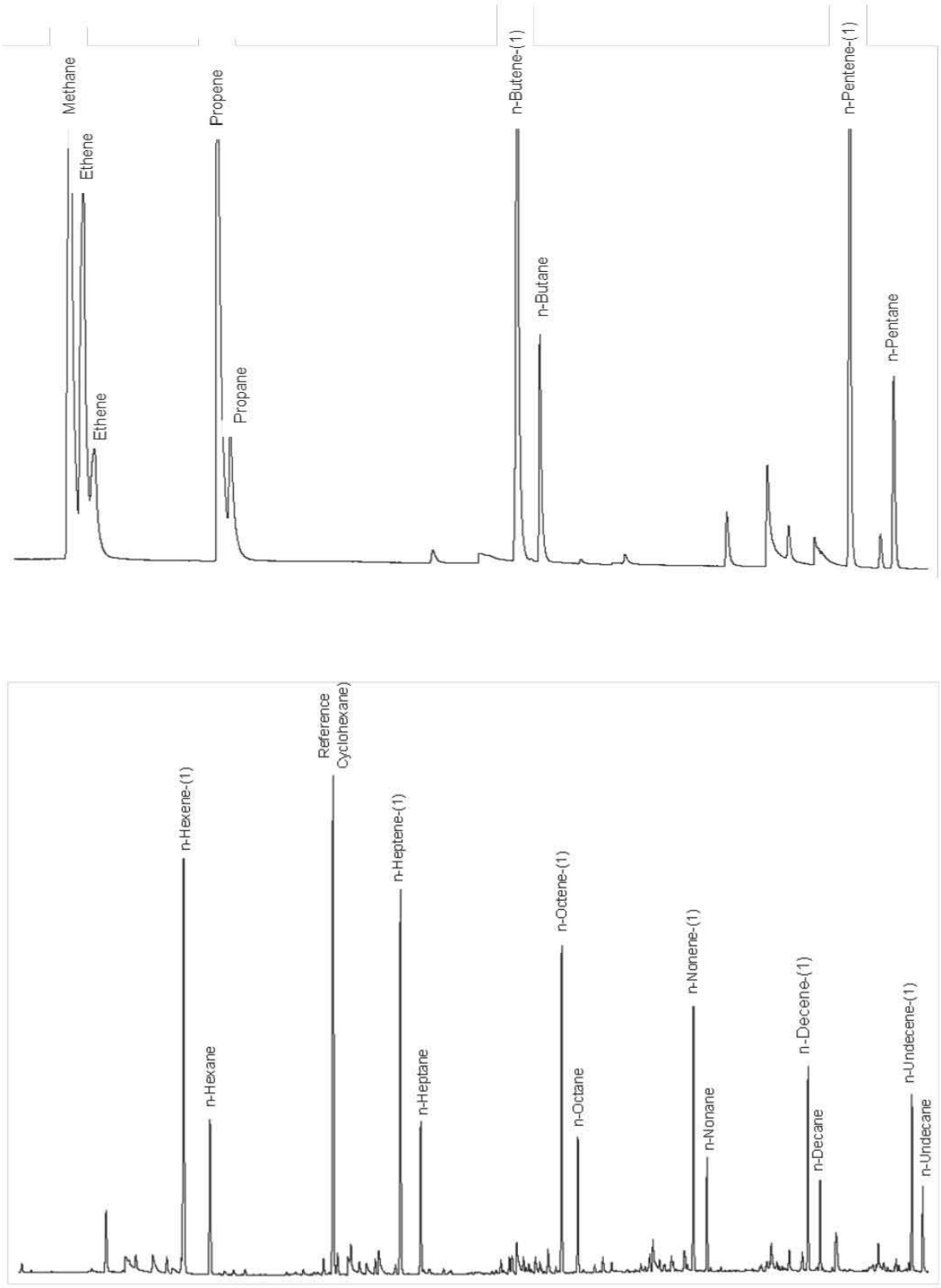

Figure 4. 8: Identification and location of the major linear 1-olefin and paraffin products.

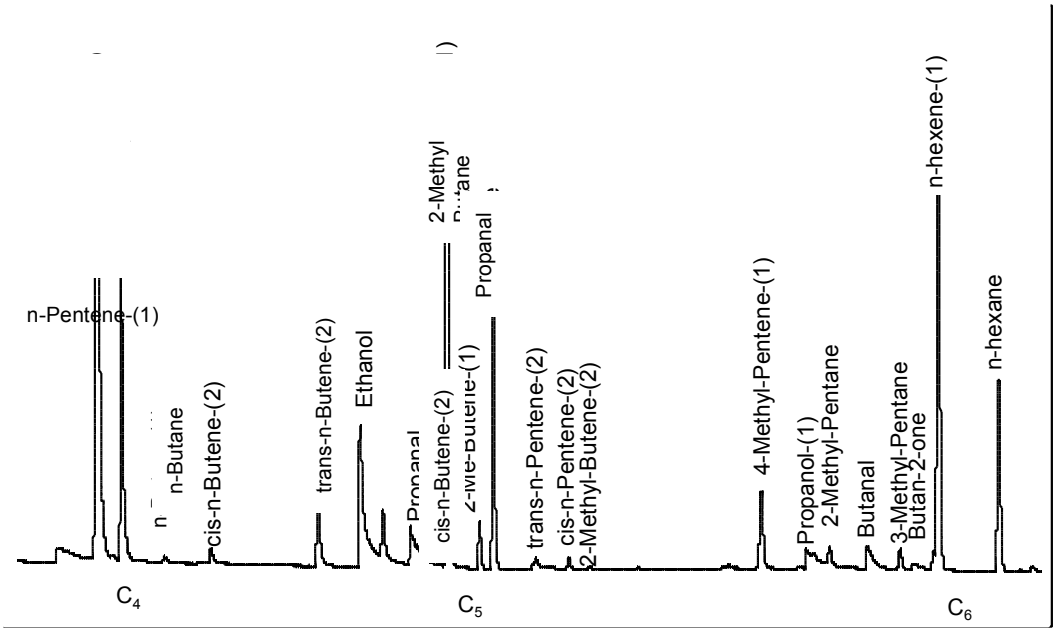

Figure 4.9: Cross-section of products obtained in each carbon number fraction.

4.3.2.2 Liquid phase analyses

GC-MS/FID analyses of liquid product samples (oil and water phases) were carried out for both a comparison with the results from ampoule samples as well as identification and quantification of the "missing" compounds from the ampoule analyses (acids, amides, amines). The drawbacks in the gas phase analyses were noted in the previous section, and as such, the liquid phase analysis was used to fill in the gaps. Table 4.6 lists the column conditions used for liquid phase analyses. Identification was done using the MS signal while quantification was done from the corresponding FID signal.

Table 4.6: Temperature programme used for GC-MS/FID analysis of liquid samples

Ramp (°C/min)	Final temperature (°C)	Hold time (min)
-	40	2
2.5	100	5
5	280	13

The column head pressure was kept constant at 1.8 bar throughout analysis; and the volume of sample injected was 1 μL. Both the water and oil samples were analyzed using this method.

Figures 4.10-4.13 show the typical chromatograms obtained from FID analyses of liquid samples collected during FT synthesis without ammonia addition (oil and water samples), with Figure 4.10 and Figure 4.12 representing the full chromatogram, and Figure 4.11 and Figure 4.13 indicating the relative locations of the different compound classes detected. As to be expected it can clearly be seen that oxygenates, being polar compounds, are preferably found in the water phase.

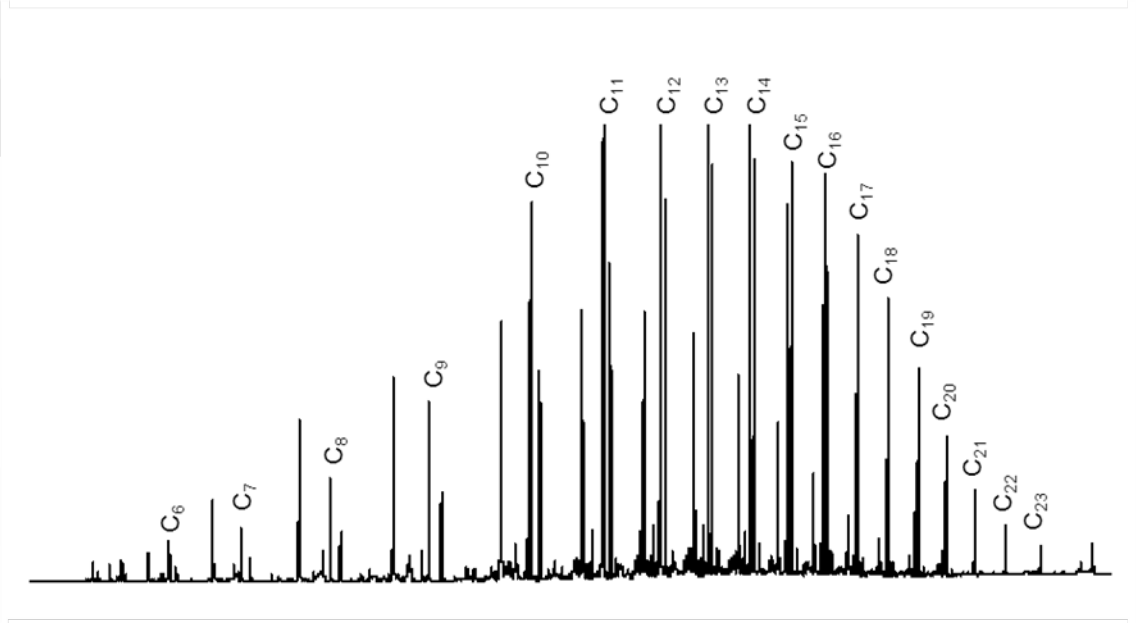

Figure 4.10: A typical FID chromatogram obtained from a liquid sample (oil sample) taken during base case FT synthesis without ammonia addition with the major hydrocarbon peaks labelled.

(Labeled peaks -C_7-C_{23}- show the location of the main linear hydrocarbon product (olefins-1 and paraffins) for each carbon number fraction)

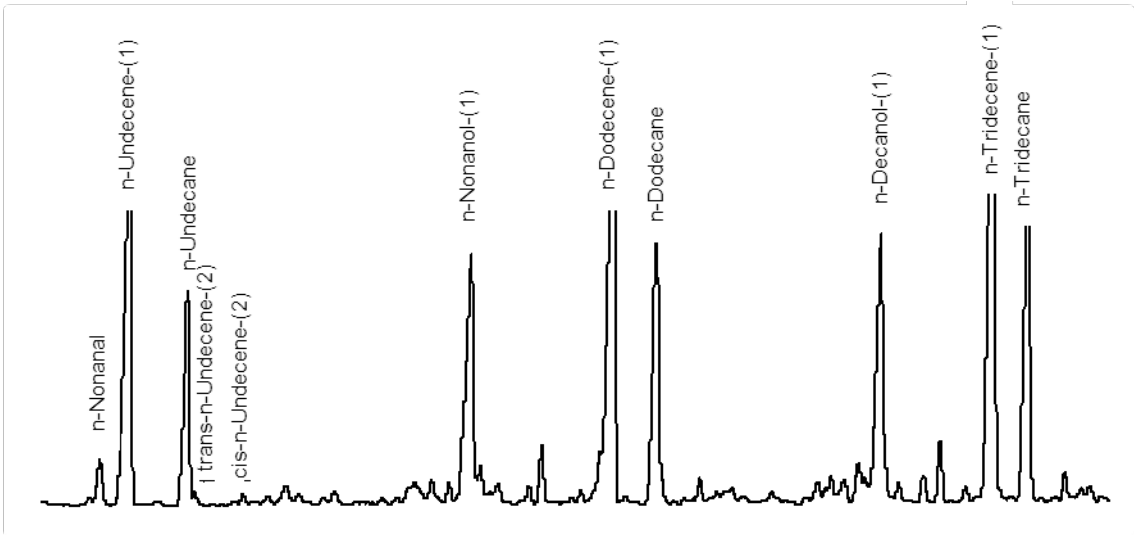

Figure 4.11 Expanded view of Figure 4.10 indicating typical relative locations of the different compound classes (oil sample).

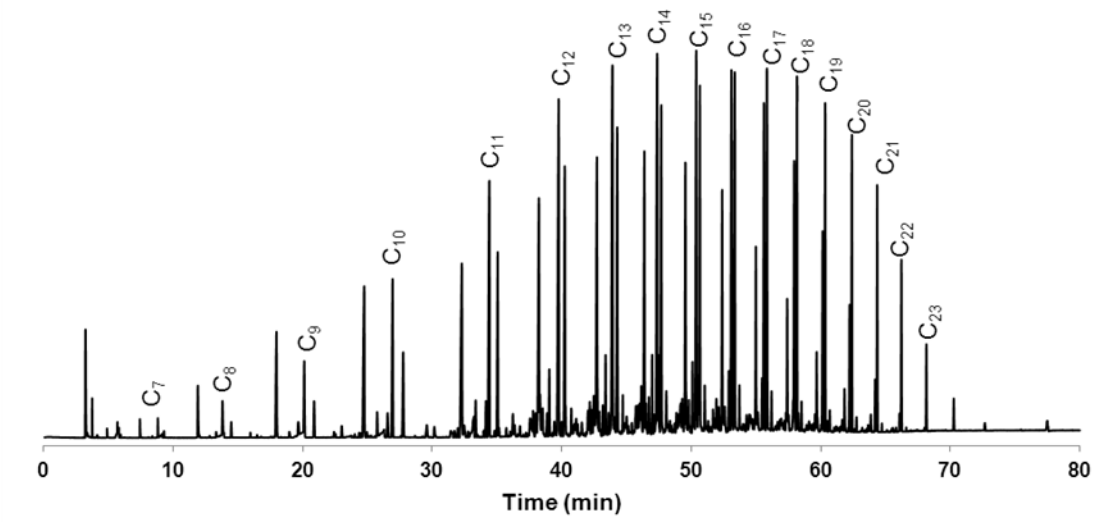

Figure 4.12: A typical FID chromatogram obtained from a liquid sample (water sample) taken during base case FT synthesis without ammonia addition with the major hydrocarbon peaks labelled.

(Labeled peaks -C_7-C_{23}- show the location of the main linear hydrocarbon product (olefins-1 and paraffins) for each carbon number fraction)

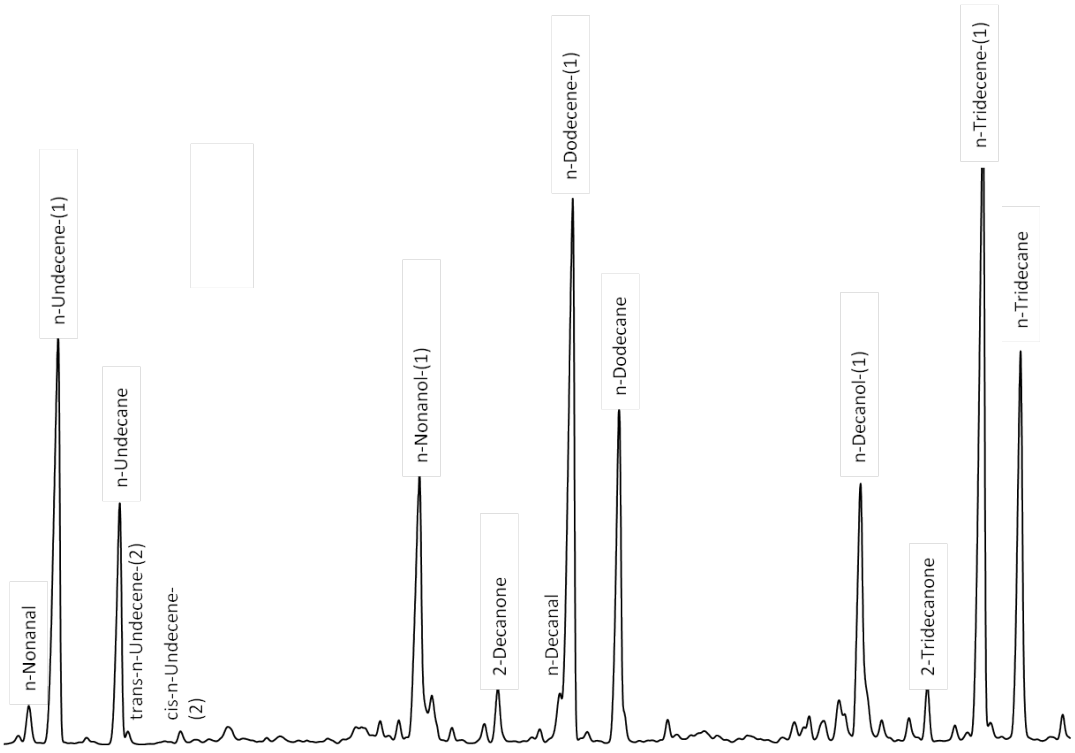

Figure 4.13: Expanded view of Figure 4.12 indicating typical relative locations of the different compound classes (water sample).

4.3.3. GC-MS analysis principles

A mass spectrometer (MS) is used to identify molecules based on the fragments that can be obtained from the dissociation profile of each molecule. Each molecule entering the MS detector is bombarded by high-energy electrons, breaking it up into a number of positively charged ions with associated molecular weight to charge (m/z) ratios. Each molecule can only be broken up into a finite number of fragments. Thereby, all molecules will have unique associated ionic spectra (histograms) with a finite number of fragments with m/z ratios, and associated frequency/concentration of these fragments. Given this, the MS will produce a histogram from an unknown molecule, and compare this with a database containing histograms of known compounds and match the unknown sample with the closest possible match. In this study, the GC-MS is equipped with an NIST database (NIST/EPA/NIH Mass Spectral Library Version 2.0) containing MS spectra obtained from over 100 000 different compounds. Examples of MS histograms of some molecules relevant to this study are shown in figures 4.14 to 4.22.

Figure 4.14 - 4.16 show the MS histograms (i.e. relative abundance versus mass/charge ratio, m/z) of three alkanes – methane, ethane and hexane - from which the following is observed:

- Molecules in the same compound class (e.g. linear paraffins) theoretically contain all the peaks observed in all molecules in the same class, but of lower molecular mass. For example, the n-hexane histogram should contain all the ions with m/z ratios as those observed for methane and ethane (propane, butane and pentane), with the exception of the molecular ion.
- However, the frequencies/concentrations of the ions in the different components will differ. This is partially due to bond strength. The stability of different positions on the carbon skeleton has a significant influence – e.g. breaking of a terminal bond requires much more energy than that for breaking a C_2 or a C_3 position on a long chain molecule, or breaking up a C-H bond. This results, for example, in the frequency of C_1 (and C_{N-1}) ions being much lower for ethane and hexane than that for methane.

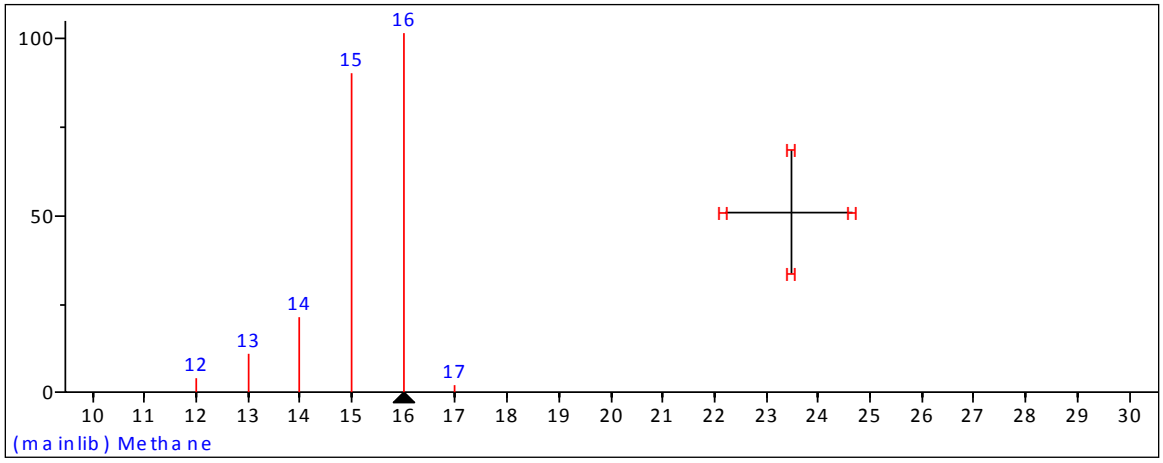

Figure 4.14: MS histogram of methane (from NIST database).

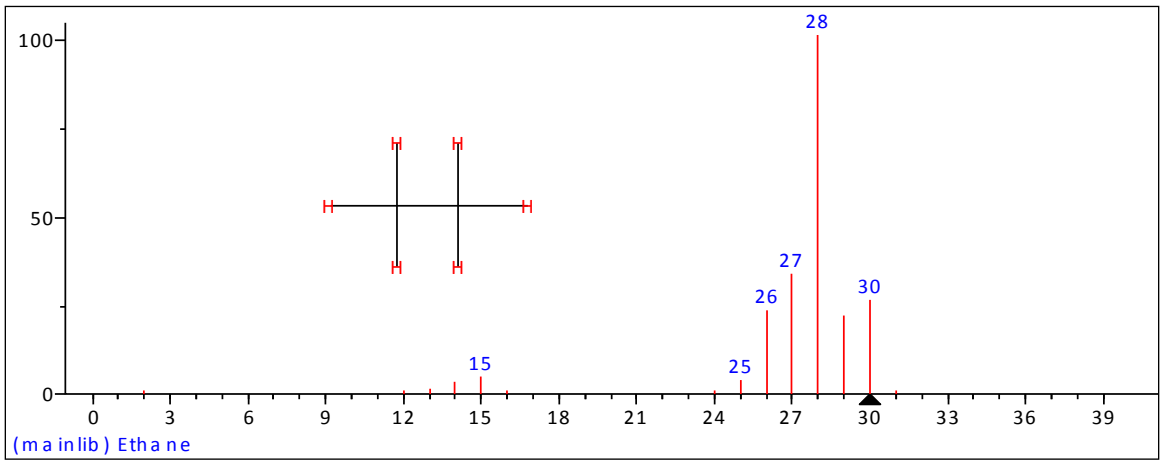

Figure 4.15: MS histogram of ethane (from NIST database).

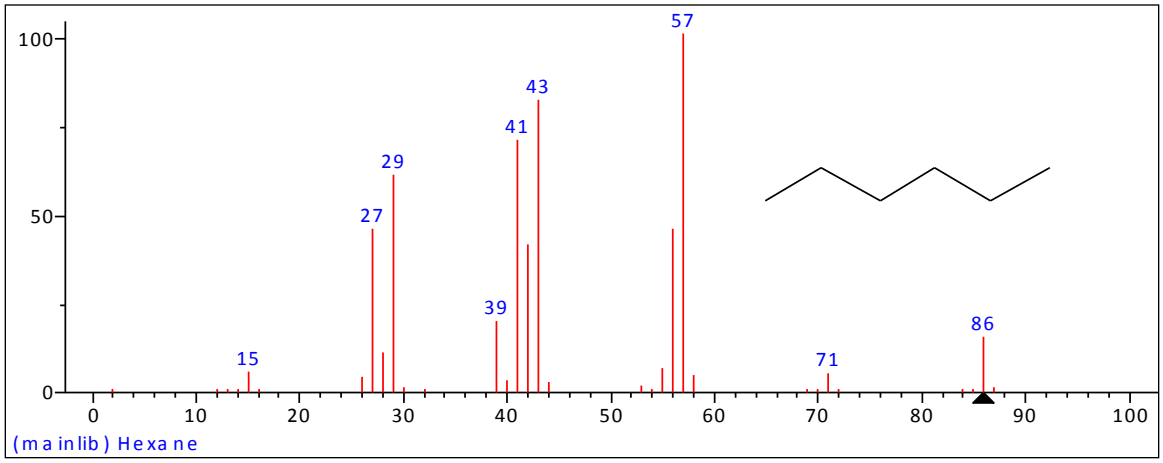

Figure 4.16: MS histogram of hexane (from NIST database).

Figure 4.16 - 4.22 show the histograms associated with a number of linear C_6 compounds with different functionality, from which the following observations are made:

- For compounds with similar carbon skeletal structure, the spectra of the different compounds contain many similarities, especially in terms of the fragment "groups" produced. Because of their similar backbone, they will have a significant number of common fragments. Some shifting or "broadening" of the "groups" can occur due to the number and nature of different functional groups.
- The different functional groups affect the stability of the compounds differently, resulting in significant differences in relative abundance of the different ions.
- Most importantly the compounds of the different classes can have fragments which are unique or relatively unique to a class (for example: m/z=31 for

1-alcohols, m/z=60 for carboxylic acids, m/z=58 for methyl-ketones, m/z=30 for primary amines, and m/z=82 for nitriles) which can help to identify those components in complex mixtures (see also below)

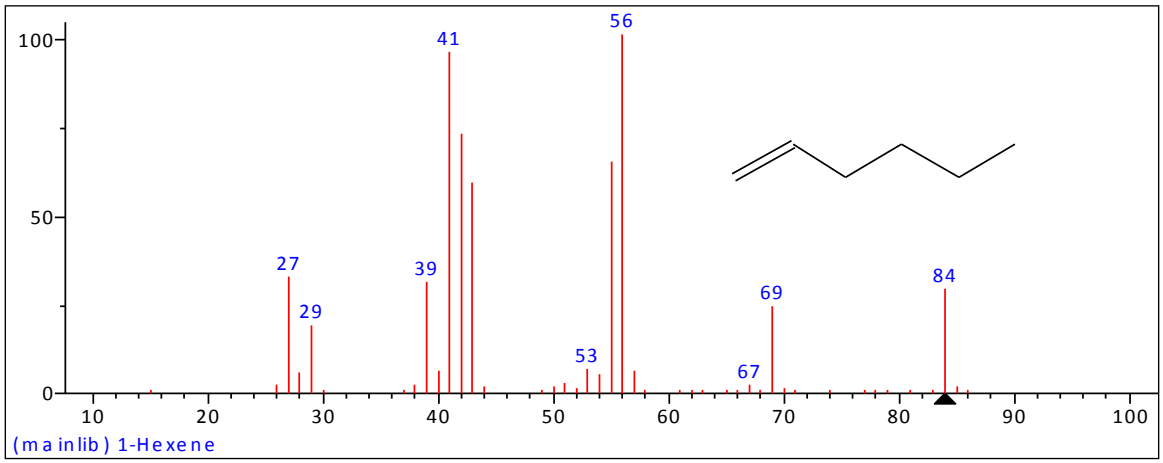

Figure 4.17: MS histogram of n-hexene-1 (from NIST database).

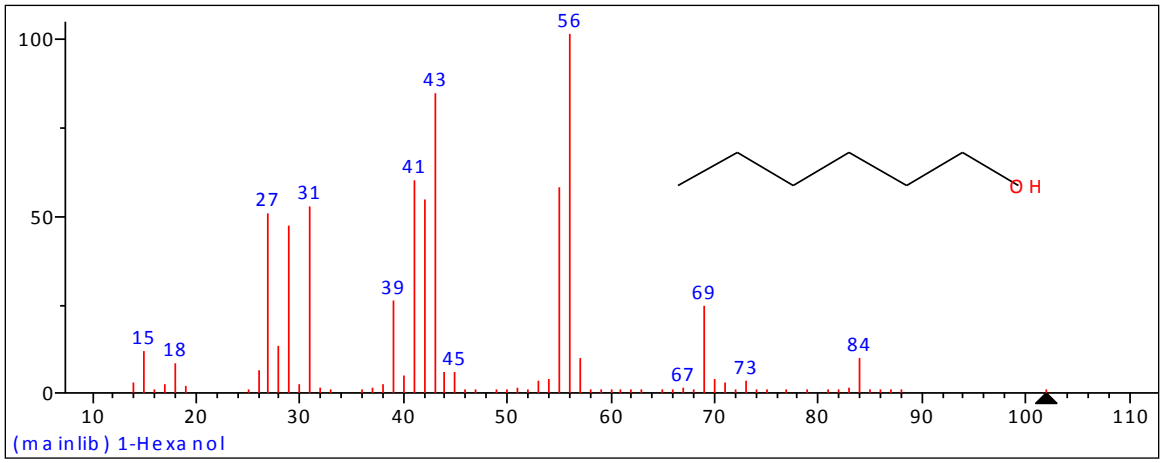

Figure 4.18: MS histogram of n-hexanol-1 (from NIST database).

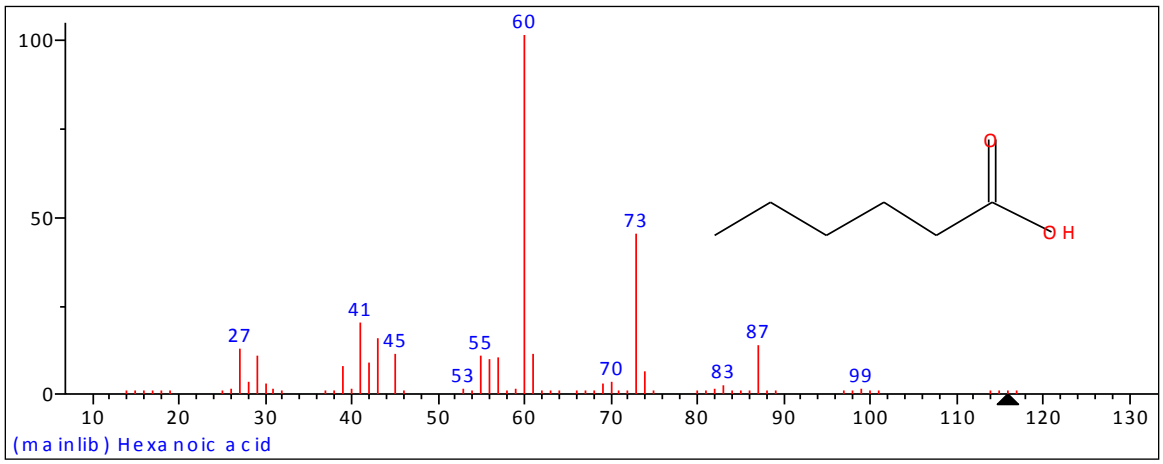

Figure 4.19: MS histogram of n-hexanoic acid (from NIST database).

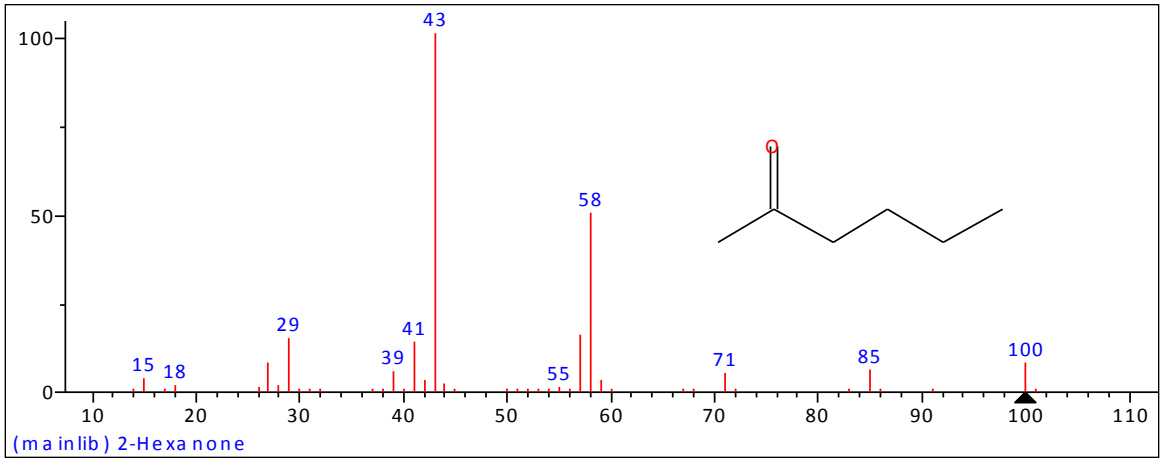

Figure 4.20: MS histogram of n-hexan-2-one (from NIST database).

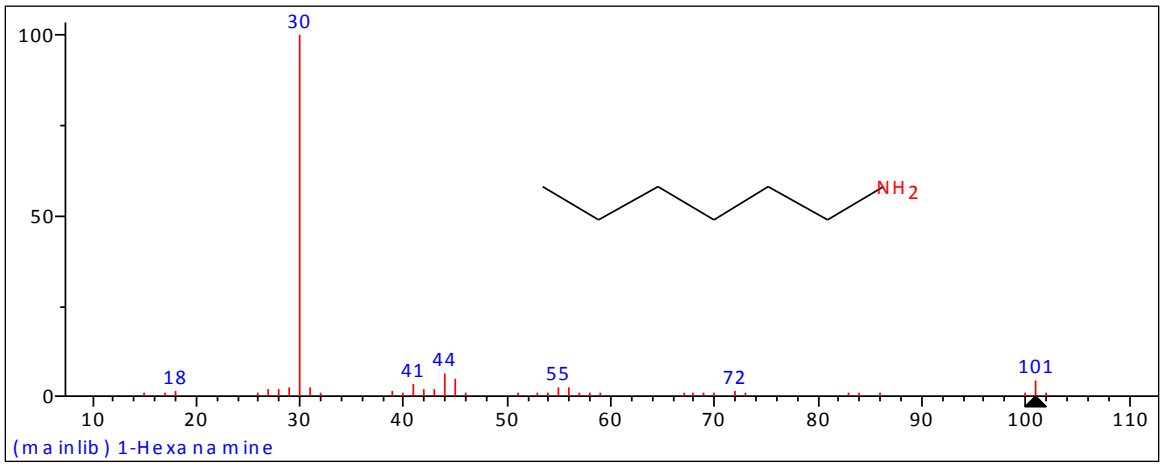

Figure 4.21: MS histogram of n-hexanamine (from NIST database).

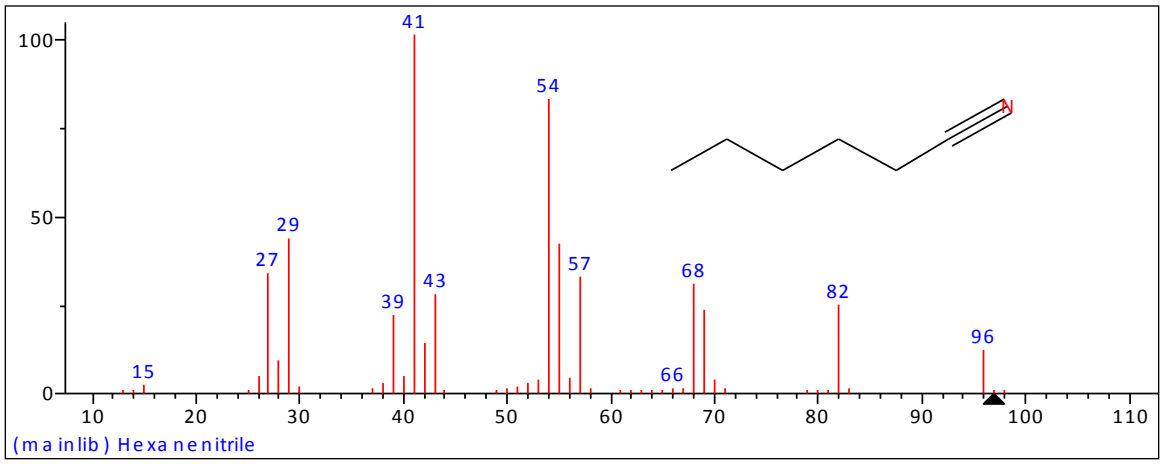

Figure 4.22: MS histogram of n-hexanenitrile (from NIST database).

The MS ultimately gives a total ion chromatogram, i.e. a chromatogram constructed from all ion histograms taken at high frequency and their intensity. Figure 4.23 illustrates an example of such a chromatogram for a sample of the water product phase obtained from an ammonia-free FT process. The fragments from each eluted component are essentially grouped together to give a single data point (peak) on this chromatogram. Individual fragments can be "extracted" from such a chromatogram by utilising a tool that extracts ions of specific m/z ratio. This is useful for a number of reasons:

- Where 2 or more components have the same retention time in the column, ions specific to each of the components can be used to identify the components.
- Extracting specific, unique peaks results in a "neater" chromatogram, which can be used for e.g. for quantification if the MS has been calibrated using standards.

The effectiveness of this method is clearly seen when Figure 4.23 is compared with Figure 4.24. Figure 4.23 shows the total ion chromatogram, with figure 4.24 showing ions of m/z of 31 and 60 (indicative of 1-alcohols and carboxylic acids respectively) extracted from the same chromatogram. From Figure 4.24, it is much easier to identify and confirm the locations of all the 1-alcohols and acids from this sample. This method was used to identify peak positions in the chromatograms. The quantification, however, was ultimately done from the chromatograms obtained on the parallel FID channel of the GC setup as an FID generally gives a linear and more accurate response whereas often non-linear component responses are obtained on MS detectors. (Seeing the large number of peaks of interest a calibration of the MS would hence require a wide range of

standards for calibration of the individual components, which would be costly and would require a significant amount of time to calibrate for the individual samples).

.

The identification of the nitrogen-containing compounds was done in this manner, and is described in detail in the results section (chapter 5).

.

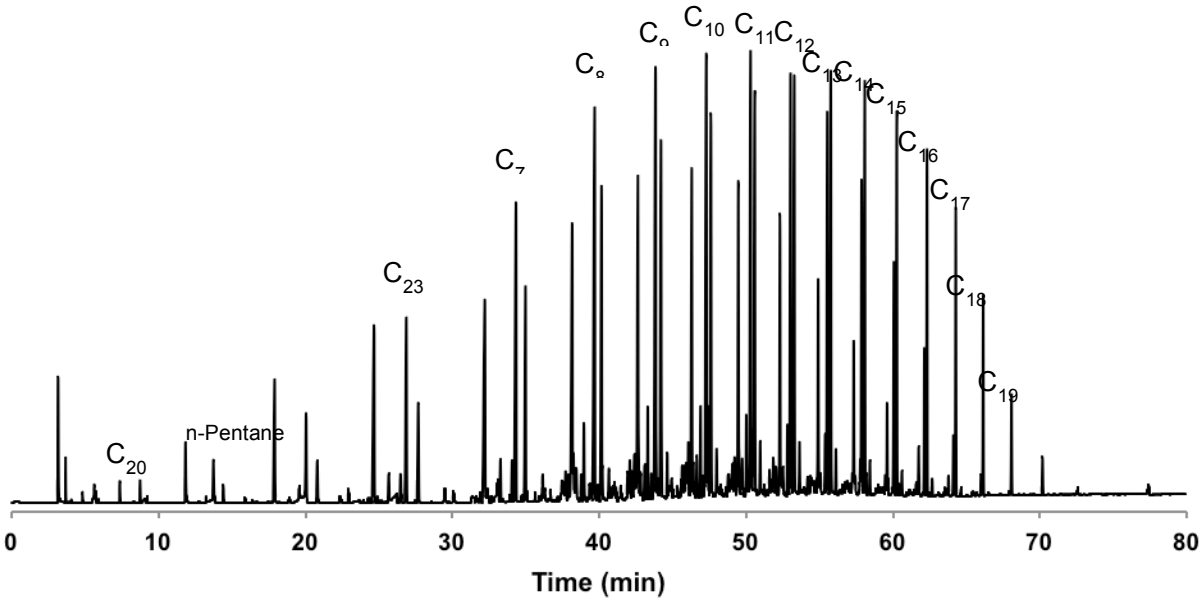

Figure 4.23: A typical GC-MS total ion chromatogram obtained from a water sample collected during base case FT synthesis without ammonia addition, with the major hydrocarbon peaks labelled.

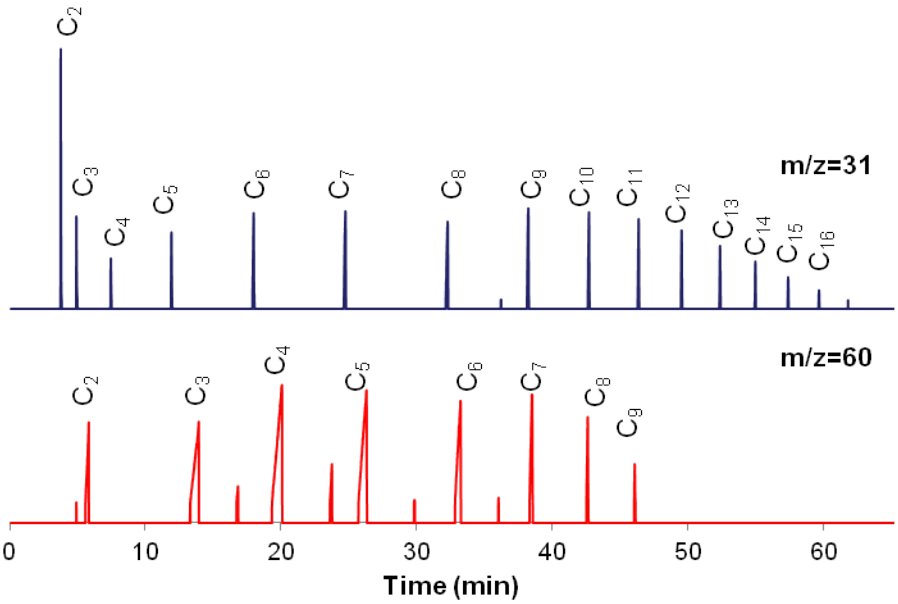

Figure 4.24: Ion chromatograms, m/z=31 and m/z=60 indicative for 1-alcohols and carboxylic acids respectively, extracted from total ion chromatogram shown in figure 4.23.

In summary, when a sample containing unknown compounds is injected into the GC-MS, the compounds in the sample are exposed to high-energy electrons, which fragment and ionize the parent compounds into a number of ions, which can then be matched up with known standards from a database and used to identify the different components with high accuracy.

5. RESULTS

The results in sections 5.1 to 5.3 below are presented primarily to highlight the effect of ammonia feed concentration on the FT activity and the composition of the FT-typical products, hydrocarbons and oxygenates, whereas in section 5.4 the formation of nitrogen containing products will be discussed. The system was run with no ammonia initially, then the ammonia content in the feed was increased stepwise to 35 vol% (Table 4.2). After the 35 vol% condition, the ammonia feed content was reduced to 10 vol% ("10 vol%(i)"). In addition, after the initial test with 10 vol% NH_3 in the feed the base case condition was revisited ("0 (i) vol%"). These conditions were repeated to study the reversibility of effects of ammonia addition on catalyst activity, methane and CO_2 formation and results are included in the corresponding sections below.

5.1. Catalyst activity, CO_2 formation and ammonia conversion

Carbon monoxide and hydrogen conversions were obtained using the online chromatograph equipped with the TCD. The conversions were calculated using equation 5.1 below:

$$X_i = \frac{F_{i,in} - F_{i,out}}{F_{i,in}} \% \quad (5.1)$$

where $F_{i,in}$ is the inlet flow rate of compound i (carbon monoxide or hydrogen in this case) and $F_{i,out}$ is the outlet flow rate of component i as measured via the TCD analysis of the inlet and exit gases. This however does not take into account the WGS activity of the catalyst. Equation 5.2 below shows the corrected equation for CO conversion to Fischer-Tropsch products only:

$$X_{CO,FT} = \frac{F_{CO,in} - F_{CO,out} - F_{CO_2,out}}{F_{CO,in}} \% \quad (5.2)$$

Figure 5.1 shows the results for overall CO conversion, CO conversion to FT products, and the trend with increasing ammonia content in the feed, including the two repeat conditions.

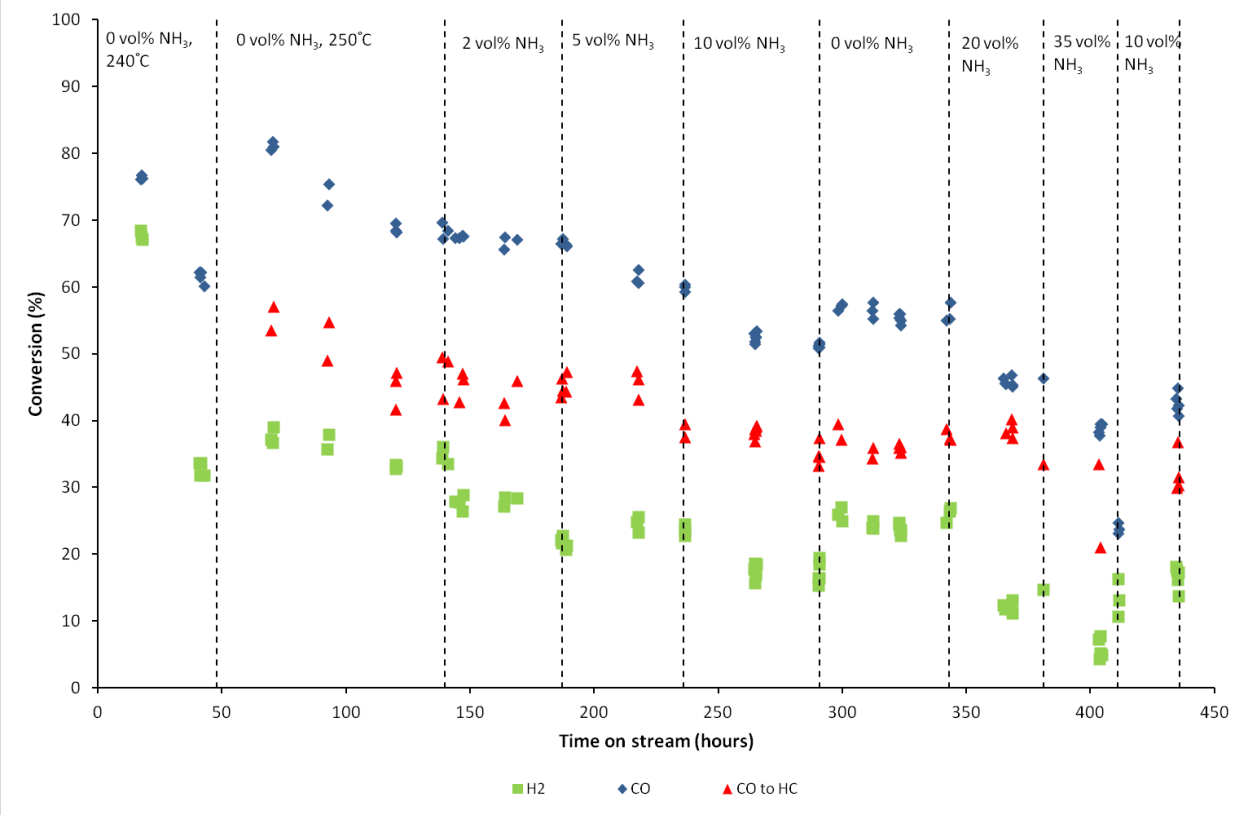

Figure 5.1: Overall CO conversion, CO conversion to organic FT-products and hydrogen conversion as a function of ammonia content in the feed (note: results of repeat experiments "0 vol%(i)" and "10 vol%(i)" are also included and indicated next to the condition after which they were run)

A gradual drop of conversions is observed with increasing ammonia content in the feed. Lowering the ammonia concentration to 0 or 10 vol%, respectively, in the two repeat experiments led to a slight recovery of conversions compared to the corresponding previous conditions, 10 and 35 vol%. This is indicative of ammonia inhibiting the conversion of synthesis gas over the iron catalyst used in this study. However, the repeat experiments did not lead to a complete recovery of activity, which may be due to catalyst deactivation. To what extent the deactivation behavior is due to ammonia would need to be shown in experiments without ammonia addition over the same duration as the series of conditions used in this study, i.e. 2 to 3 weeks. It is however remarkable that the presence of ammonia, which is generally regarded as strong poison in the

Fischer-Tropsch synthesis – at least with cobalt-based catalysts - has only a relatively weak effect on the catalyst activity.

A closer inspection of the data shown in Figure 5.1 reveals a decrease of total CO and hydrogen conversion while the conversion of CO to FT products appears to level off between 10 to 35 vol%, which may indicate suppressed water-gas-shift activity at these conditions.

CO_2 selectivity is defined as the yield of CO_2 as a fraction of the amount of CO converted in the reactor. The CO_2 selectivity is calculated based on TCD analysis and is given by equation 5.3:

$$S_{CO_2,TCD} = \frac{F_{CO_2,out}}{F_{CO,in} - F_{CO,out}}\% \quad (5.3)$$

The CO_2 selectivities observed during the experiments are shown in Figure 5.2. The CO_2 selectivity is fairly constant at low ammonia contents in the feed. There is indeed a pronounced decrease at high levels of ammonia in the feed suggesting suppressed CO_2 formation via the water gas shift reaction. However, at the experimental conditions of high ammonia feed concentration the formation of a white solid was detected. This was later confirmed to most probably be ammonium carbonate (see section 5.4.5). It is likely that this was formed in a reaction involving ammonia, CO_2 and water:

$$2\,NH_3 + CO_2 + H_2O \rightarrow (NH_4)_2CO_3 \quad (5.4)$$

Looking at Figure 5.1, we observe that the overall CO conversion decreases but conversion to FT products is relatively constant at the higher ammonia contents in the feed. Comparing this with the CO_2 selectivity, as suggested earlier, a decrease in the extent of the WGS reaction may explain this.

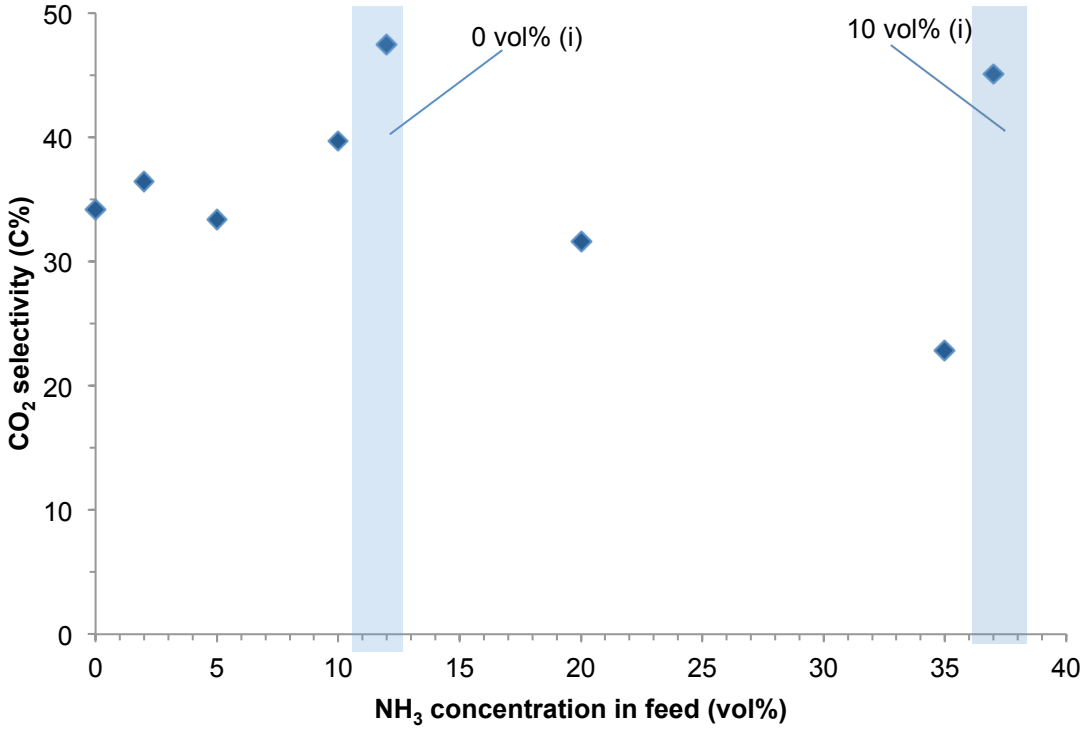

Figure 5.2: CO_2 selectivity from TCD analysis (note: results of repeat experiments "0 vol%(i)" and "10 vol%(i)" are also included and indicated next to the condition after which they were run)

However, because the amount of solid obtained from our system could not be quantified (section 5.4.5) a bias will be present in the WGS and other calculations. Assuming ammonium carbonate is formed from CO_2, ammonia and water as explained later, the following would be the expected effect:

- Consumption of CO_2 would lead to an apparent drop in the extent of the WGS;
- Looking at equation 5.2, this would in turn lead to a higher calculated CO conversion to hydrocarbons, than the actual.
- Figure 5.3 indicates that formation rates for the gaseous hydrocarbons from

ampoule analysis (i.e. C_1-C_{20}[1], including nitrogen-containing compounds) does not vary much over the range of our experiments. Hence we can attribute the drop in overall conversion due to a decrease in WGS activity of the catalyst.

What is conclusive from these results is that the overall CO conversion decreases with ammonia content, leading to the deduction that presence of ammonia does indeed suppress catalyst activity. The decrease in activity seems strongly linked not to a drop in FT activity of the catalyst, but rather to a drop in WGS activity and/or an increase in the consecutive formation of ammonium carbonate.

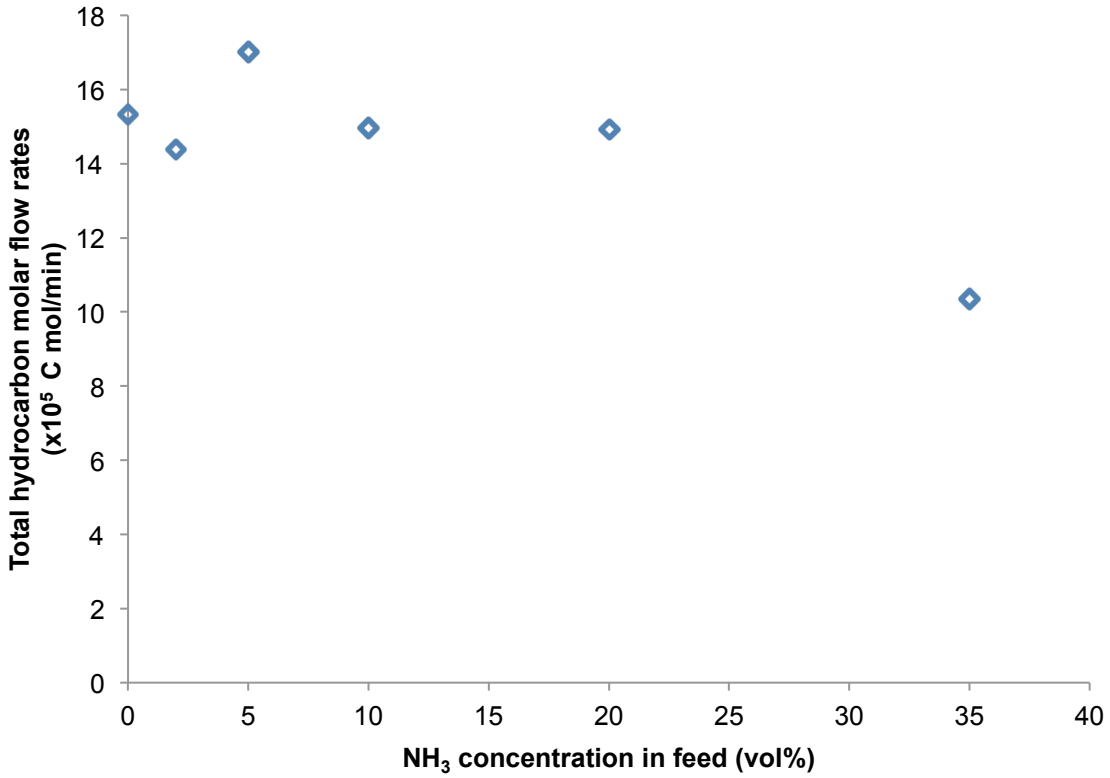

Figure 5.3: Variation of the combined C_1-C_{100} product carbon molar flow rates with increasing ammonia content in the feed

[1] These formation rates were calculated using the organic reference component in the FID, cyclohexane, which was added to the reactor product stream

A carbon balance was conducted to determine to what extent ammonium carbonate was formed:

$$F_{CO,in} = F_{CO,out} + F_{CO_2,out} + F_{C-org,out} + \Delta F_C \quad (5.5)$$

with $F_{C\text{-}org,out}$: molar flow of organic products (C_1-C_{100}) on a carbon basis; note that only C_1-C_{20} was measured directly using FID analysis of ampoule samples, C_{21}-C_{100} was determined via extrapolation of formation rates assuming ideal Anderson-Schulz-Flory kinetics and constant chain growth probabilities as listed later in section 5.3.1. ΔF_C: includes all carbon unaccounted, i.e. mainly carbon present in the white solid believed to be ammonium carbonate

The percentage of carbon unaccounted for is listed in Table 5.1 but contrary to what we expect, it can be seen that at higher ammonia contents in the feed decreased amounts of ammonium carbonate were found, with the ΔC only increasing at ammonia contents >10 vol%). It should be noted though that ΔC does not only represent the formation of ammonium carbonate, but it also gives an indication of the mass balance. In the experiment without ammonia co-feeding for example, where no ammonium carbonate formation can occur, 28% of the carbon is unaccounted for.

Table 5.1: Carbon balance, ΔC (wt %), corresponding to white solid formed during ammonia co-feeding.

	vol% NH_3 in feed					
	0	**2**	**5**	**10**	**20**	**35**
ΔC (wt %)	**28.3**	**27.6**	**22.4**	**15.0**	**17.7**	**20.4**

Both the total CO and H_2 conversions decrease by about 40% and 60% respectively when the NH_3 content is increased from 0 to 35% (Figure 5.1). Although a decrease in the WGS reaction would support an apparent increase in hydrogen conversion, we observe a decrease in H_2 conversion with increasing ammonia content for our system. Factors that can be attributed to this behavior include:

- Increased olefin content (Table 5.9);
- Competition for bonding sites with ammonia – incorporated NH_3 essentially acts as a substitute for H_2, leading to a lower H_2 conversion/incorporation.

- Formation of nitriles further reduces the positions available for hydrogen on the molecular skeletons.
- Mechanism of ammonia incorporation results in hydrogen formation.

Removal of ammonia from, or decreasing ammonia content in the system results in recovery of some of the loss in activity observed on ammonia addition. This draws the conclusion that some of the loss in activity of the catalyst is due to the presence of ammonia (e.g. competition for active sites on the catalyst) and is reversible. As a final note, the catalyst employed was quite robust and remained active over 500 hours on stream and under quite extreme ammonia conditions (35%).

Although ammonia conversion could not be directly obtained from this setup, an indication of the ammonia consumption was determined by doing a mass balance. Ammonia consumption was determined to be predominantly towards amine, nitrile, amide and formamide formation as will be discussed later. There were indications of further nitrogen containing compounds such as ethyl amides, but these gave much weaker responses on the FID and were hence assumed to be negligible. Note, a considerable amount of ammonia consumption was however attributed to formation of ammonium carbonate, as will be discussed later. Table 5.2 gives the combined ammonia conversion to amines, nitriles, amides and formamides. Also included in the table are the amounts of ammonia consumed.

Table 5.2: Ammonia conversion and ammonia usage to amines, nitriles, amides and formamides under the varied ammonia feed conditions.

	vol% NH_3 in feed		
	2	**5**	**10**
Conversion (mol %)	**0.85**	**2.5**	**1.3**
NH_3 usage (x10^7 mol/min)	**5.3**	**40.4**	**44.5**

5.2. Methane selectivity

Methane selectivities were obtained directly from the online TCD ($S_{CH4,TCD}$). The methane selectivity was also calculated using methane formation rates as determined via the GC-FID analysis together with results obtained from the TCD analysis ($S_{CH4,FID/TCD}$), and this was compared to the value obtained from TCD analysis. The methane selectivity is defined as the amount of methane formed relative to the amount of CO converted to FT product and equations 5.6 and 5.7 were used to calculate the selectivities based on TCD and FID flow data (equations 4.1 and 4.3) respectively:

$$S_{CH_4,TCD} = \frac{F_{CH_4,TCD}}{F_{CO,in} - F_{CO,out} - F_{CO_2,out}}\% \quad (5.6)$$

$$S_{CH_4,FID/TCD} = \frac{F_{CH_4,FID}}{F_{CO,in} - F_{CO,out} - F_{CO_2,out}}\% \quad (5.7)$$

(with methane flow from FID analysis obtained using equation 4.3 in chapter 4 and the rest of the outlet flows obtained from TCD analysis-equation 4.1).

However, as indicated earlier (section 5.1), there is some uncertainty in the formation rates of Fischer-Tropsch products from TCD analysis due to the additional formation ammonium carbonate. For this reason a third method for the calculation of the methane selectivity (in C%) was used. This was determined from FID analysis, and formation rate of organic products, C_1-C_{100} (on a carbon basis). The corresponding methane selectivity, $S_{CH4,FID}$, is:

:

$$S_{CH_4,FID} = F_{CH_4} / \sum F_{C_1 - C_{100}} \quad (5.8)$$

The following assumptions were made;

- The product C_{21}-C_{100} is predominantly paraffinic, based on both thermodynamic data and FID analysis (product spectrum shift towards paraffin product);
- The ASF chain growth probability was used to extend and calculate the product content to the C_{21}-C_{100} product range.

$$\log\left(\frac{W_n}{n}\right) = n \log \alpha + C \quad (5.9)$$

where W_n is the fraction of chain length n in the total product on a carbon basis. The slope (log α) and the intercept (C) are determined from fitting FID data for C_9-C_{13} product range, and therefore all product mass fractions can be determined for all carbon chain lengths, n.

Figure 5.4 shows the methane selectivities obtained using these three methods.

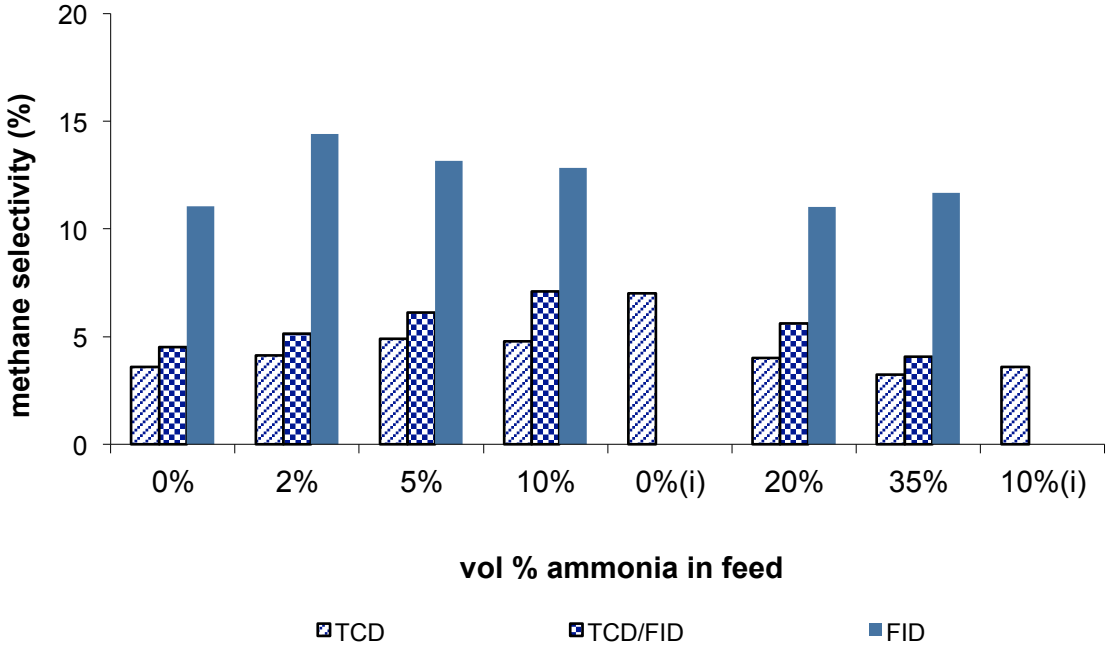

Figure 5.4: Methane selectivity (note: results of repeat experiments "0 vol%(i)" and "10 vol%(i)" are also included and indicated next to the condition after which they were run)

Selectivity to methane is low as expected under our operating conditions. The methane selectivity peaks at 4.8 C% (TCD), and 7.1 C% (FID/TCD) at an ammonia volumetric feed content of 10 vol% with the FID results indicating another maxima with a selectivity of 14.2% at ammonia vol concentration of 2%. This points towards two opposing effects. Lower synthesis gas conversion favours increased methane selectivities (Claeys and van Steen, 2004), which may explain the increase of methane selectivities obtained at low levels of ammonia addition. The decrease of methane selectivity at high levels of ammonia in the feed stream may be a direct result of ammonia present which may inhibit the desorption of surface alkyl species to form methane, favouring chain initiation/growth instead:

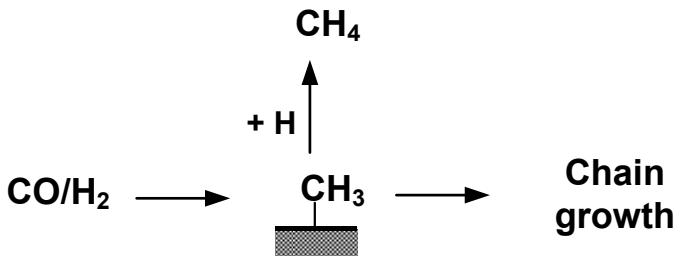

Figure 5.5: Mechanism for the formation of methane from the $-CH_3$ surface species on the catalyst surface versus chain growth.

When the system is changed from 10 vol% to the 0 vol% rerun, or from 35 vol% to 10 vol% rerun respectively, CH_4 selectivity shows a marked increase. This is a direct confirmation that ammonia indeed suppresses the formation of methane.

5.3. Fischer-Tropsch selectivity

This section looks at the standard gauges for FT selectivity (i.e. hydrocarbons and oxygenates) and the effect of ammonia contents on these. The factors checked include among others, chain growth probability (ASF), olefinicity, oxygenate content and extent of branching.

Table 5.3-5.7 show a summary of how the FT product distributions vary with increasing ammonia content in the feed. These results are obtained from FID analysis of the gas and liquid products and are based predominantly on linear compounds. The product fractions are normalized on a carbon basis to the C_1-C_{20} product consisting of paraffins, olefins, alcohols, aldehydes, acids, nitriles, amines, amides and formamides. The nitrogen-containing compounds are discussed in subsequent sections.

Looking at these tables, the paraffin and olefin contents are fairly constant for 0-10 vol% ammonia in the feed. For 20 and 35 vol% ammonia, no liquid was obtained in the cold traps, hence calculations for these were limited to C_1-C_{20}, and uncorrected for amides, amines etc. which could only be analyzed from the liquid phase. Significant changes can be seen in the contents of oxygenates, i.e. alcohols, aldehydes and acids, which decrease significantly upon addition of ammonia, often to undetectable amounts. It

should be noted that the normalized distributions are somewhat biased as the increase or decrease of one class of components impacts on the amount of the other products. A better way of looking at the data is to consider relative contents within corresponding carbon number fractions, which allows for easier mechanistic data interpretation (see sections 5.3.1-5.3.6).

Table 5.3: Selectivity to paraffins as a percentage of the total linear C_1-C_{20} products.

	n-paraffin content in linear product (C %)					
vol% NH_3 in feed	**0**	**2**	**5**	**10**	**20**	**35**
C_1	12.1	13.5	13.4	13.3	12.4	11.8
C_2-C_5	9.8	9.2	8.7	8.2	7.7	11.4
C_6-C_{12}	7.3	6.4	6.6	6.5	6.2	4.0
C_{13}-C_{20}	4.2	3.6	3.3	3.4	2.6	1.6
C_1-C_{20}	**33.3**	**32.7**	**31.9**	**31.4**	**28.9**	**28.9**

Table 5.4: Selectivity to olefins as a percentage of the total linear C_1-C_{20} products.

	Linear olefin content in linear product (C %)					
vol% NH_3 in feed	**0**	**2**	**5**	**10**	**20**	**35**
C_2-C_5	33.1	34.6	33.9	32.0	39.4	47.0
C_6-C_{12}	18.0	16.8	17.6	17.4	22.5	15.3
C_{13}-C_{20}	4.0	4.2	4.9	5.5	4.3	2.2
C_1-C_{20}	**55.1**	**55.6**	**56.4**	**54.9**	**66.2**	**64.5**

Table 5.5: Primary alcohol selectivity as a percentage of the total linear C_1-C_{20} products.

	1-alcohol content in linear product (C %)					
vol% NH_3 in feed	**0**	**2**	**5**	**10**	**20**	**35**
C_2-C_5	4.4	0.4	0.4	1.1	0.8	1.3
C_6-C_{12}	1.5	0.8	0.8	0.5	0.1	0.7
C_{13}-C_{20}	0.7	0.2	-	0.3		
C_2-C_{20}	**6.5**	**1.4**	**1.2**	**1.9**	**0.9**	**1.9**

Table 5.6: Aldehyde selectivity as a percentage of the total linear C_1-C_{20} products.

	Aldehyde content in linear product (C %)			
vol% NH_3 in feed	**0**	**2**	**5**	**10**
C_2-C_5	2.7	0.7		
C_6-C_{12}	2.3	0.4	0.2	0.1
C_1-C_{20}	**5.0**	**1.2**	**0.2**	**0.1**

Table 5.7: Carboxylic acid selectivity as a percentage of the total linear C_1-C_{20} products.

	Carboxylic acid content in linear product (C %)			
vol% NH_3 in feed	**0**	**2**	**5**	**10**
C_2-C_5	0.12	-	-	-
C_6-C_{12}	0.14			
C_1-C_{20}	**0.26**			

5.3.1. Chain growth probability

The probability of a surface species to grow (via addition of a C_1 monomer) as opposed to desorbing is described as the chain growth probability, α. From the schematic shown in Figure 5.6 below, we can see that a surface species (Sp_N) of carbon number n on the catalyst surface can either desorb to form any of a number of product species

(paraffin/olefin/alcohol etc.) of carbon number n, or react with a monomer species to form a new surface species with n+1 carbon atoms (Sp_{N+1}). The chain growth probability is a statistical tool that hence defines the probability of a surface species to stay on the catalyst surface and grow further versus desorption from the catalyst surface as a final product species.

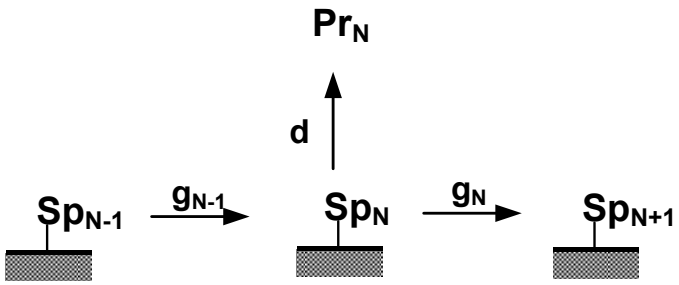

Figure 5.6: Chain growth kinetics vs. desorption/chain termination on the catalyst surface.

If the chain growth probability is independent of carbon number, then its value - α - can be derived from the ideal Anderson-Schulz-Flory kinetics:

$$\log\left(\frac{W_n}{n}\right) = n \log \alpha + C \qquad (5.9)$$

where W_n is the mass fraction of the product species with carbon number n and α is the chain growth probability.

Anderson-Schulz Flory distributions were plotted for the linear hydrocarbons (paraffins+olefins) for each of the different ammonia feed conditions. The plots are shown in Figure 5.7 and the calculations are shown in table D.1 in appendix D. At least 2 carbon number ranges show a linear relationship between the log of the normalized weight distribution, (W_n/n), and carbon number (n). These ranges are C_3–C_7, and C_9-C_{13}. The respective chain growth probabilities were calculated and are listed in Table 5.8. "Two alpha product distributions" were earlier reported by others (Huff & Satterfield, 1984; Claeys and Schulz, 2004), but reason for this deviation from ideal Anderson-Schulz-Flory kinetics is still under debate.

The observed chain growth probabilities do not show a strong dependency on ammonia content. The one exception is the system running under 35 vol% ammonia feed, where the chain growth probability was significantly lower compared to the other conditions. This suggests that only extreme conditions of ammonia co-feeding with very high

ammonia partial pressures impact on chain growth probability in a way that the inhibition of product desorption, which is the characteristic feature of the Fischer-Tropsch synthesis, is lessened. It is suspected that this is possibly due to effects of competitive adsorption between ammonia and carbon monoxide, the latter being known to impact strongly on chain growth (Schulz, van Steen & Claeys, 1995).

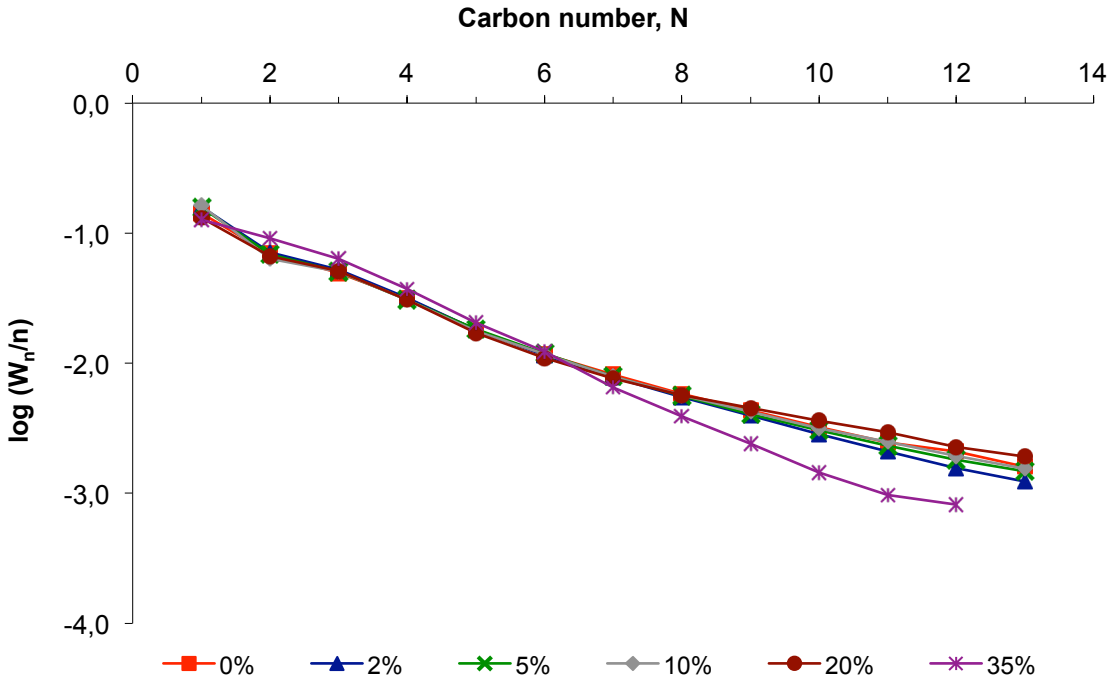

Figure 5.7: Plot of the Anderson-Schulz Flory distributions for different ammonia content in the feed for determination of the chain growth probability.

Table 5.8: Chain growth probabilities for C_3-C_7, and C_9-C_{13} carbon number ranges for linear hydrocarbons.

	Chain growth probabilities, α (%)					
vol% NH_3 in feed	**0**	**2**	**5**	**10**	**20**	**35**
α_1 (C_3-C_7)	63.1	61.8	62.7	62.7	61.7	56.8
α_2 (C_9-C_{13})	78.5	74.6	77.5	77.8	80.2	69.5

A further point to note from Figure 5.7 and the FID results from gas analysis (e.g. figure 4.7), a noted curvature in the ASF plots with increasing higher carbon numbers is observed, and this may be attributed to a change in phase in the reactor as the heavier

compounds exist in the liquid phase under reaction conditions, increasing residence time and chain growth (Jager & Espinonza, 1995). This effect may be even more pronounced for slurry phase reactors. In this work, assuming that condensation of products plays a role in this process, this effect is observed around C_{14}-C_{17}, where an unexpected increase in the amount of product relative to the preceding carbon numbers is observed.

5.3.2. Olefin content in linear hydrocarbons

Upon desorption of a terminally bonded alkyl surface species, alpha olefins and n-paraffins form via β-hydrogen abstraction or terminal hydrogen addition respectively (section 2.3.5), typically exhibiting a carbon number independent ratio of around 4:1 respectively, or 80 mol% olefins in the corresponding linear hydrocarbon fraction (Schulz & Claeys, 1999a). Under Fischer-Tropsch conditions olefins can however readsorb and undergo secondary reactions (Schulz & Claeys, 1999a; Claeys and Schulz, 2004), such as hydrogenation to the paraffin or further chain growth as shown below:

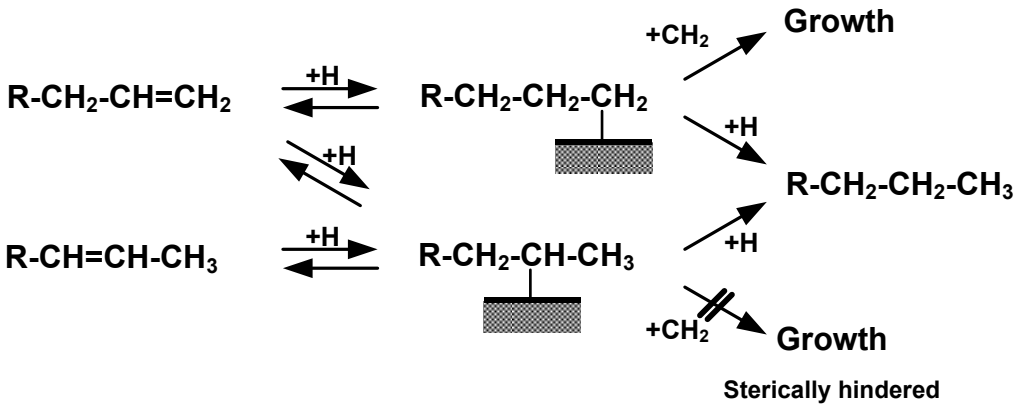

Figure 5.8: Olefin readsorption and subsequent secondary reaction.

Plotting the olefin content (olefin/olefin+paraffin) in the fraction of the linear hydrocarbon as function of carbon number can help to determine the extent of these secondary reactions. Often relatively low olefin contents in C_2 and decreasing olefin contents with increasing carbon number have been reported and attributed to preferred secondary conversion of these olefins due to higher reactivity, in case of ethene, and increased residence times due to increased solubility for higher molecular weight olefins (Schulz & Claeys, 1999a) or diffusivity (Iglesia *et al.*, 1993).

Figure 5.9 shows these molar olefin content in linear hydrocarbons for the different ammonia feed contents applied in this study (C_2-C_{13} obtained from gas/ampoule FID analysis and C_{13+} from the oil FID analysis). The overall olefin ratio in linear hydrocarbons was also calculated in the whole C_2-C_{20} range. This, along with the olefin content in the C_2, C_3 and C_5 fractions is shown in Table 5.9.

Relatively high olefin contents (>75 mol%) were obtained in the lower carbon number range, with a significant and gradual decrease with increasing carbon number observed above C_{10} under the different ammonia feed conditions applied. This almost carbon number independent behavior can be attributed to primary olefin content. It appears that at high levels of ammonia feed concentration, namely 20 and 35 vol%, a marked increase of the olefin content is observed. It may therefore be speculated that the addition of ammonia has mainly affected the primary reaction pathway and the desorption of olefins compared to that of paraffins at these conditions is even more preferred than at 'regular' Fischer-Tropsch conditions. It may also be speculated that the nitrogen-containing species which are formed by species addition to an alkyl species at the chain termination stage, would result in competition between these species and H-species for the position on the terminal carbon. However, this would not affect the β-hydrogen elimination required for olefin formation. Hence if β-hydrogen elimination and the terminal H-additions for paraffin formation occur independently, there would be a decrease in paraffinic species with the olefinic species possibly being unchanged.

It is also interesting to note that at the condition of 35 vol% ammonia in the feed, a much lower ethene content was observed. This is generally due to preferred secondary conversion of this olefin, which is more reactive (10-40 times, Schulz & Claeys, 1999b) than the larger olefins. This may mean that while ammonia increases primary olefin formation relative to paraffin formation, olefin readsorption and consecutive hydrogenation is less strongly inhibited than at normal Fischer-Tropsch conditions. This may be due to decreased effects of specific inhibition by carbon monoxide which now competes with ammonia.

Table 5.9: Molar content of olefins in linear hydrocarbons for selected carbon chain lengths at varied levels of ammonia in the feed

	olefins/ linear (olefins+paraffins) (C%)					
vol% NH_3 in feed	**0**	**2**	**5**	**10**	**20**	**35**
C_2	76.1	78.1	80.0	81.7	84.5	74.2
C_3	78.9	81.1	81.6	81.2	85.0	83.0
C_5	75.2	75.9	76.4	76.1	80.4	82.2
C_2-C_{20}	62.4	62.9	63.9	63.6	69.6	69.1

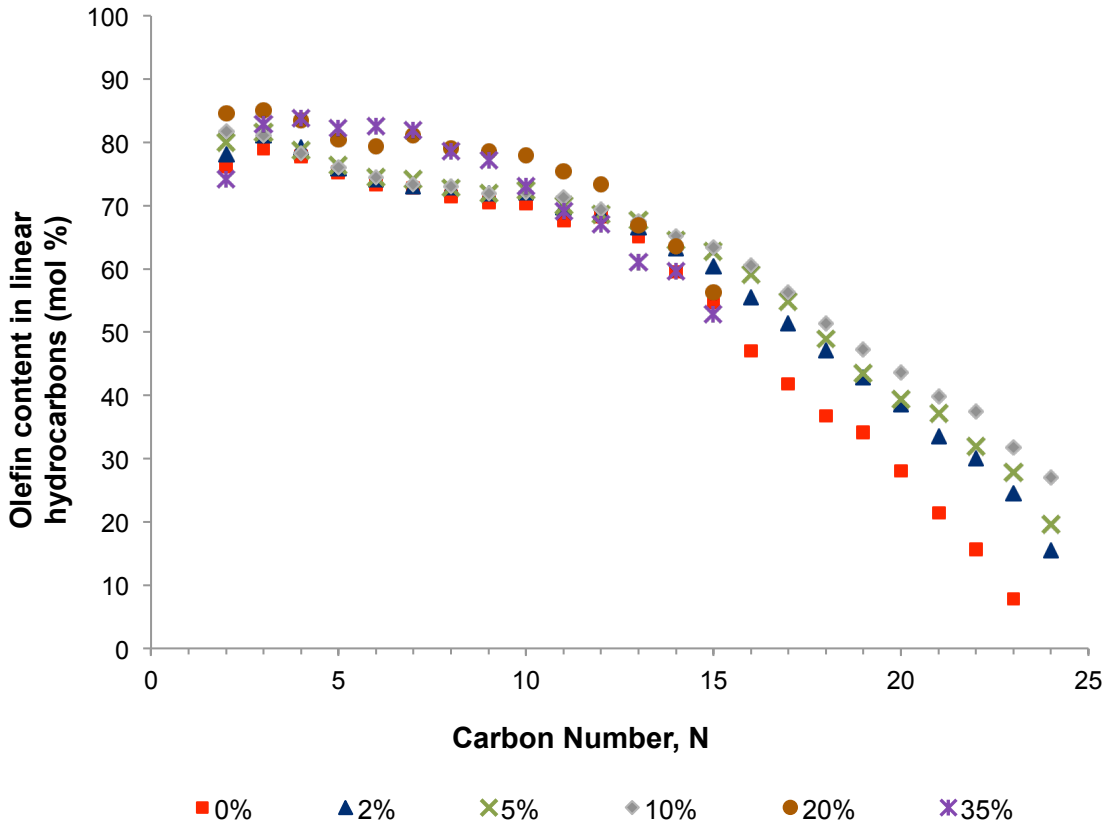

Figure 5.9: Plot of the molar olefin content in linear hydrocarbons (Ol_n/Par_n+Ol_n) as function of carbon number for different ammonia contents in the feed.

5.3.3. Alpha-olefin content in linear olefins

In addition to the secondary olefin reactions described above, primary formed α-olefins can also undergo double bond shift isomerization and form olefins with internal double bonds (see reaction scheme in previous section 5.3.2). It is believed that primarily less than 5% olefins with internal double bonds are formed under FT conditions. Plotting the molar α-olefin content in the fraction of linear olefins can give an indication of the extent of double bond isomerization. The carbon number dependency of the α-olefin content under different ammonia feed conditions is plotted for C_4-C_{10} in Figure 5.10 and listed in Table 5.10.

The α-olefin content in total olefins ranges in general between 96-98 mol% and is therefore indicative for primary selectivity and not affected by ammonia. The only exception is run with 35 vol% ammonia in the feed, which shows a decline in alpha olefins above C_6. Once again, at these high levels of ammonia this may be attributed to weakened effects of carbon monoxide adsorption, which is known to suppress secondary olefin reactions.

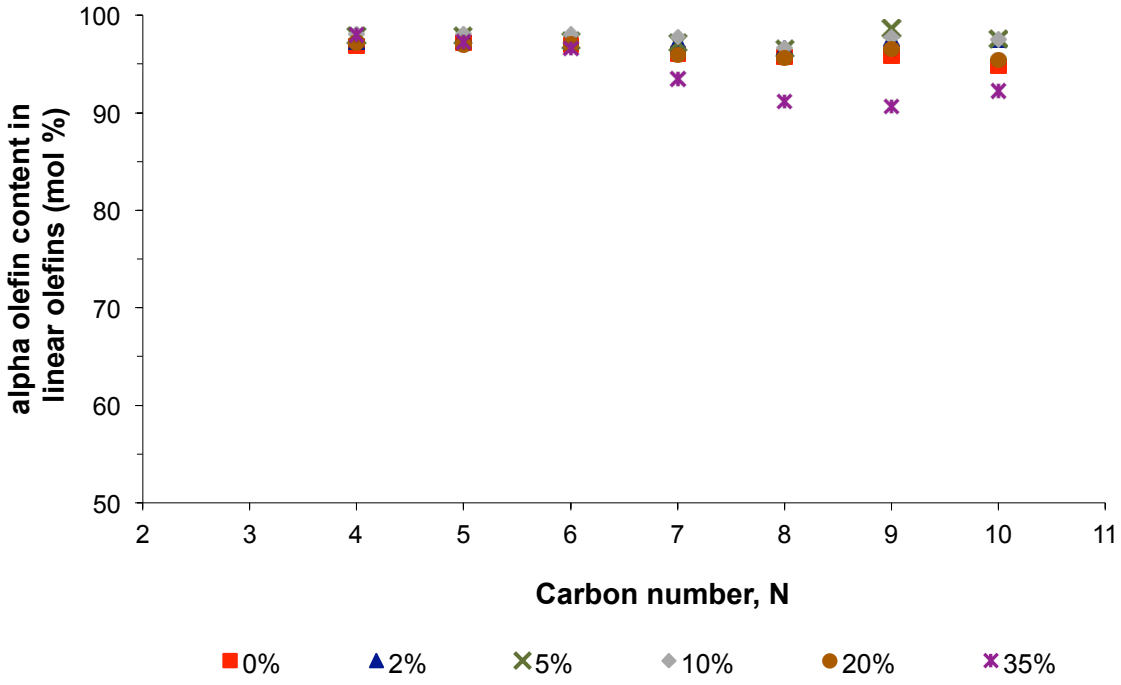

Figure 5.10: Molar α-olefin content in linear olefins fraction as function of carbon number for varied ammonia contents in the feed.

Table 5.10: Molar α-olefin content in linear olefins for selected carbon numbers at the varied ammonia contents in the feed

	α-olefin/(total n-olefins) (%)					
vol% NH_3 in feed	**0**	**2**	**5**	**10**	**20**	**35**
C_4-C_{10}	96.8	97.4	97.7	98.0	96.8	96.7
C_5	97.2	97.9	97.9	98.1	97.0	97.3
C_8	95.8	96.7	96.5	96.7	95.6	91.2

5.3.4. Degree of branching

In addition to linear compounds small quantities of branched compounds, mainly mono-methyl branched, are formed in the Fischer-Tropsch synthesis (Claeys & van Steen, 2004). Branching is thought to occur either by the secondary re-incorporation of α-olefins [1] (as shown by e.g. the co-feeding of ^{14}C labeled propene by Schulz *et al.*. (1970)) or the combination of an alkylidene and a methyl species in a primary formation step [2] (Fischer & Tropsch, 1926 and Craxford & Rideal, 1939).

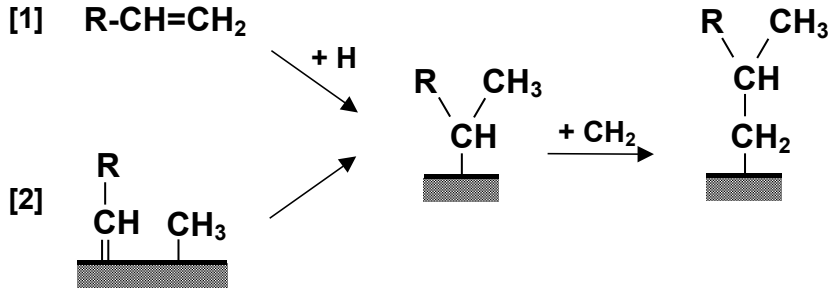

Figure 5.11: Formation of branched compounds on the catalyst surface

The ratio of branched to linear hydrocarbons was calculated for the C_5 product fraction to characterize the degree of branching. Looking at Figure 5.12, the extent of branching in the C_5 product fraction is independent of ammonia content in the feed, with ratios of around 0.21 to 0.27. The exception is the test performed under 35 vol% ammonia in the feed, where the ratio rose to 0.36. Seeing that at this condition preferred secondary

olefin conversion did take place (see previous sections) it is likely that the formation of these additional branched compounds at this condition is due to secondary olefin incorporation as depicted in mechanism [1] above.

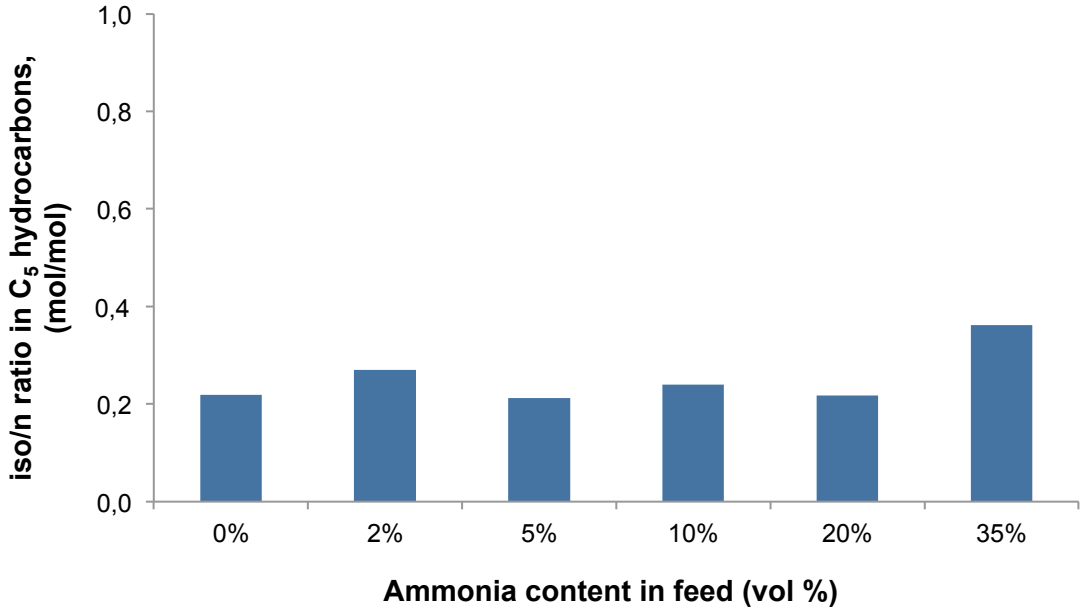

Figure 5.12: Iso- to n- ratio in C_5 hydrocarbon fraction for varied ammonia contents in the feed.

5.3.5. Oxygenates: Alcohols and aldehydes

In addition to hydrocarbons, oxygenates (mainly primary alcohols, and lower but still significant amounts of aldehydes, methyl-ketones, and organic acids) are formed in the Fischer-Tropsch synthesis. Figure 5.13 below shows a section of the total ion chromatogram obtained from the GC-MS analysis of the ammonia-free water product, and indicates the relative locations of the oxygenate peaks (alcohol, aldehyde, methyl-ketone, organic acid) in the TIC (and FID) chromatograms.

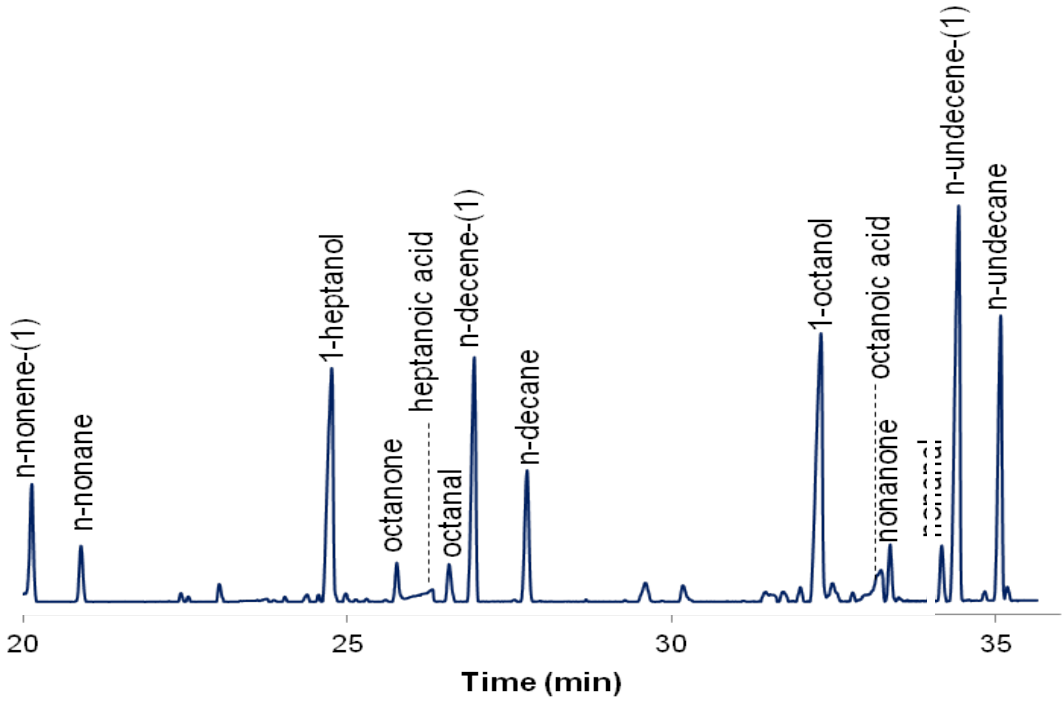

Figure 5.13: Section of TIC chromatogram obtained from analysis of water sample of the ammonia-free feed (0 vol% ammonia) to indicate location of the oxygen containing compounds (alcohols, aldehydes, methyl-ketones, acids).

Primary alcohols generally make up the bulk of the oxygenated compounds formed in the FT synthesis, with the linear aldehydes believed to be closely related to alcohol formation. Primary alcohols and aldehydes can easily interconvert into each other and in analogy to olefins, can easily readsorb and react further (Cairns, 2008). The two proposed mechanisms for oxygenate formation (via an intermediate surface hydroxyl species) proposed by Pichler and Schulz (1970) and Johnston & Joyner (1993) are shown below. Pichler and Schulz (1970) proposed that oxygenates form via the reaction of an adsorbed CO species with a surface alkyl [1], whilst Johnston & Joyner (1993) proposed that the surface hydroxyl group is formed from the reaction of a surface ethylidene species with a surface –OH group [2]. The readsorption and inter-conversion of the oxygenates as well as the secondary reaction to paraffins and olefins as described by (Cairns, 2008) is also illustrated in Figure 5.14:

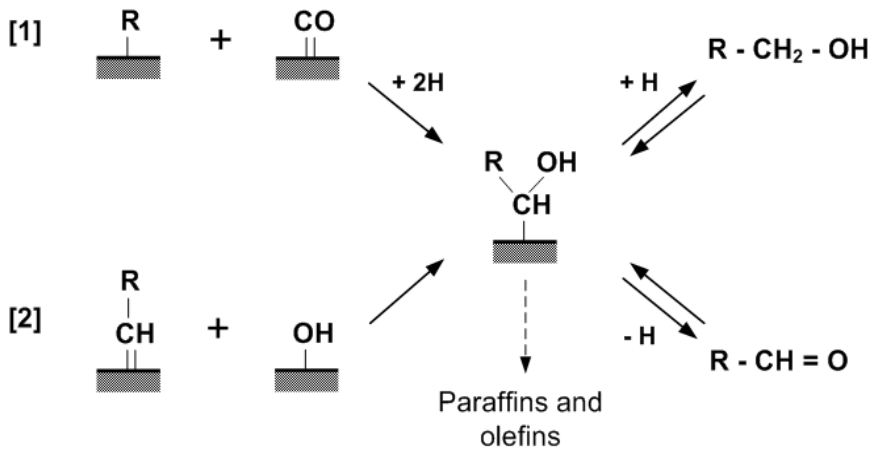

Figure 5.14: Formation of alcohols and aldehydes on the catalyst surface (adapted from Cairns, 2008)

The molar contents of oxygenates (alcohol plus aldehyde) was calculated as a fraction of the total linear product for each carbon number excluding the nitrogen-containing linear products which are discussed in the section 5.4. The results for the different ammonia feed conditions are shown in Figure 5.15. More data points are illustrated for the 0-10 vol% ammonia in the feed experiments as the gas/ampoule analyses for these were complemented by liquid phase analyses (the data for higher hydrocarbons was obtained from liquid phase analyses); whereas the 20 and 35 vol% ammonia in the feed had insufficient liquid, with the liquid inseparable from the white solid to a quality adequate for GC analysis.

The observed curves exhibit a maximum in C_2 with longer chain alcohols being subsequently less prevalent in their respective carbon number product fractions. Local maxima for oxygenate content are also observed in the C_6-C_{14} range. This trend has been described previously by others (Cairns, 2008), and the maximum at C_2 was ascribed to additional ethanol formation routes (Schulz, van Steen & Claeys, 1995). Note that no methanol could be detected in the present work.

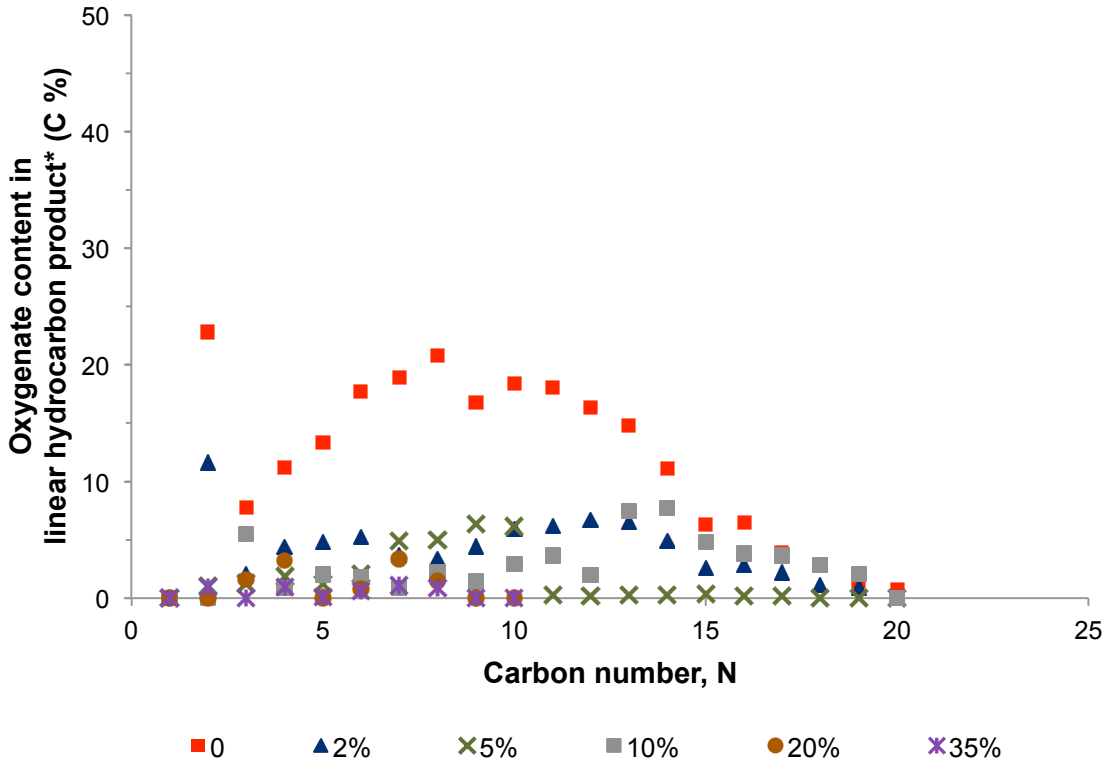

Figure 5.15: Molar content of 1-alcohol plus aldehyde in fraction of linear hydrocarbons plus oxygenates as function of carbon number for varied ammonia contents in the feed.

The molar content of oxygenates decreases strongly under ammonia addition; and at high levels of ammonia (NH_3 content in feed >10 vol%) almost no oxygenates could be identified anymore. This could be as a result of suppression of oxygenate formation via inhibition of the one or both of the above formation routes. A possible explanation is that due to an increase in available surface H-species due to ammonia dissociation on the surface leads to an increase in the reaction of surface OH and O species with H species to form water, which is expected to take part in a secondary reaction with carbon dioxide and ammonia, forming ammonium carbonate as explained in section 5.4.5.

Ultimately, with more NH_2 species available on the surface, this may then substitute OH species in the mechanism proposed by Johnston & Joyner (1993). Alternatively, the reaction step of CO insertion proposed by Pichler & Schulz (1970) may be inhibited by the addition of ammonia and the adsorbing species which form from it.

It is also possible that the oxygenates still form in a primary reaction and then undergo secondary conversion with ammonia to yield the corresponding nitrogen-containing compounds, in a reductive amination-type reaction which can occur via an alkylidene species (as shown below) of an alkyl species (Rausch *et al.*, 2008).

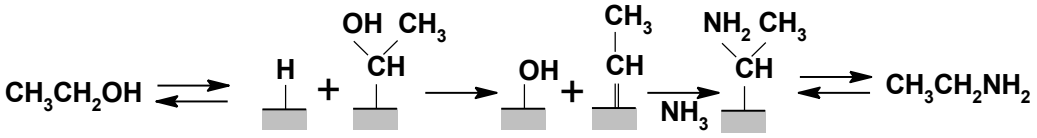

Figure 5.16: Formation of aminated compounds via reductive amination of alcohols (adapted from Rausch, 2008)

Table 5.11 shows the molar oxygenate contents (1-alcohol plus aldehyde) for the linear C_2, C_5 and C_8 fractions, as well as the molar aldehyde content within these oxygenates. Some of the data were not available due to poor FID responses. Aldehyde contents in oxygenates of 0 and 100% were more likely due to this fact, rather than absence of either aldehydes or alcohols. Consequently no clear trend regarding aldehyde:1-alcohol ratio could be observed.

Table 5.11: Molar oxygenate (alcohol + aldehyde) content in linear product; and aldehyde content in these oxygenates for selected carbon numbers at the varied ammonia contents in the feed.

	Oxygenate (alcohol + aldehyde) content in linear products (mol%) and (*aldehyde fraction in alcohol + aldehyde* (mol%))			
vol% NH_3 in feed	**0**	**2**	**5**	**10**
C_2	22.8 (*30*)	11.6 (*100*)	1.0 (*100*)	5.1 (*0*)
C_5	13.4 (*59*)	4.7 (*60*)	1.1 (*100*)	1.6 (*0*)
C_8	15.5 (*72*)	3.3 (*34*)	3.2 (*18*)	1.1 (*53*)

5.3.6. Methyl-ketones and carboxylic acids

In addition to alcohols and aldehydes, methyl-ketones and carboxylic acids are usually formed in the Fischer-Tropsch synthesis; but these products are often not analyzed or

reported by others. From extensive studies including co-feeding of different oxygenate classes during iron-based Fischer-Tropsch synthesis, Cairns (2008) proposed that methyl-ketones and acids can form from the corresponding aldehydes or 1-alcohols most likely via scavenging reactions of a surface acyl species and a methyl or an OH group respectively (Figure 5.17):

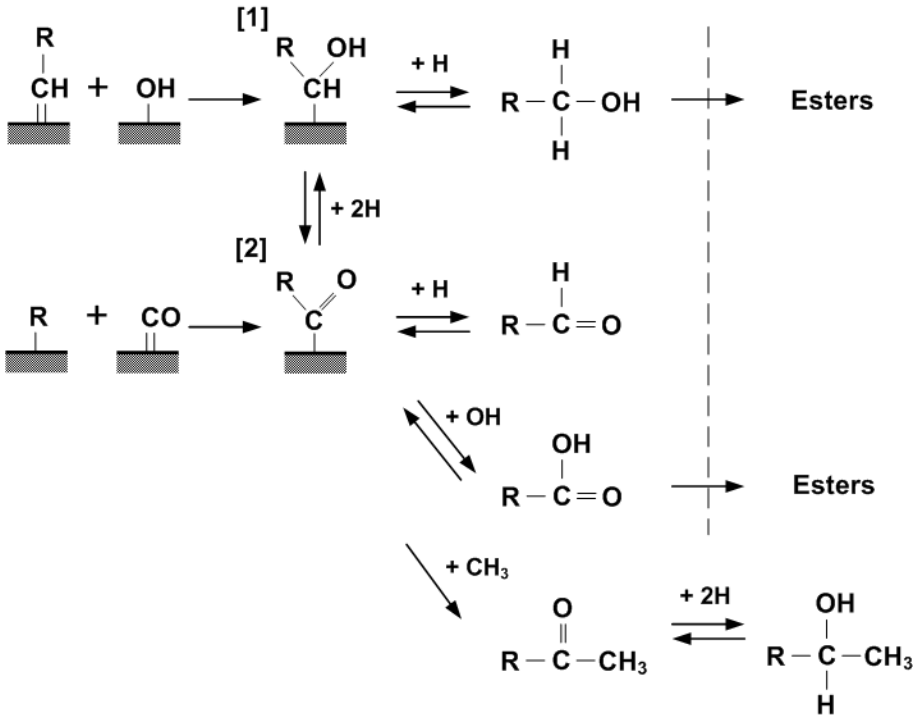

Figure 5.17: Kinetic scheme of oxygenate formation and interaction as seen from co-feeding tests (Cairns, 2009)

The methyl-ketones can easily be detected in FID analyses of the different product fractions; in addition they can be “extracted” from total ion chromatograms using the m/z ion=58. Figure 5.18 shows the chromatogram obtained when ions with m/z = 58 are extracted from the total ion chromatogram from the analysis of the water product fraction obtained in the ammonia-free experiment.

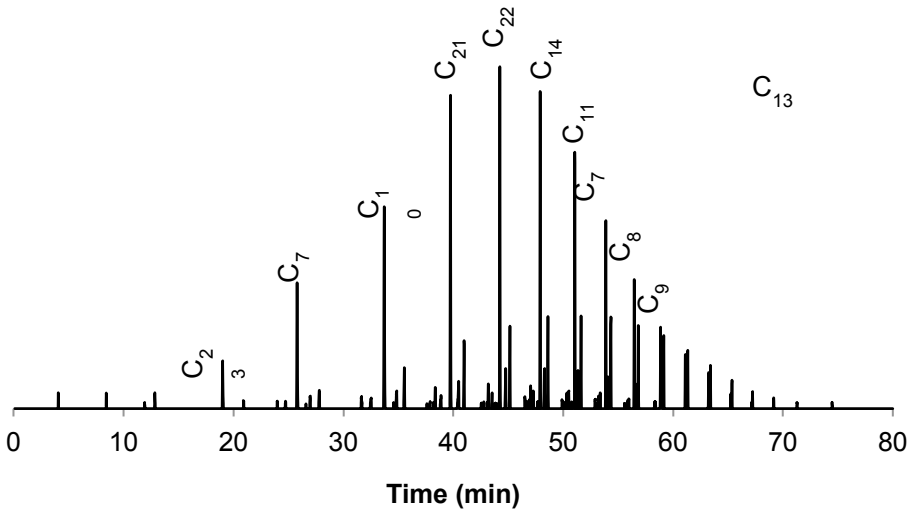

Figure 5.18: Extracted ion chromatogram (m/z=58) from analysis of water obtained from the ammonia-free feed (0 vol% ammonia)

Carboxylic acids are generally more difficult to identify in the FT-product spectrum, but extraction of the m/z=60 signal from the total ion chromatogram obtained with the MS detector shows clear evidence of the carboxylic acids. Figure 5.19 shows the extracted ion chromatogram for ions with m/z of 60 from the GC-MS analysis of the water produced under the 0 vol% ammonia in the feed. The resultant chromatogram is exclusive to organic acids. A section of the full TIC chromatogram (synonymous to the FID chromatogram) illustrates the location of acid peaks relative to other products (Figure 5.13).

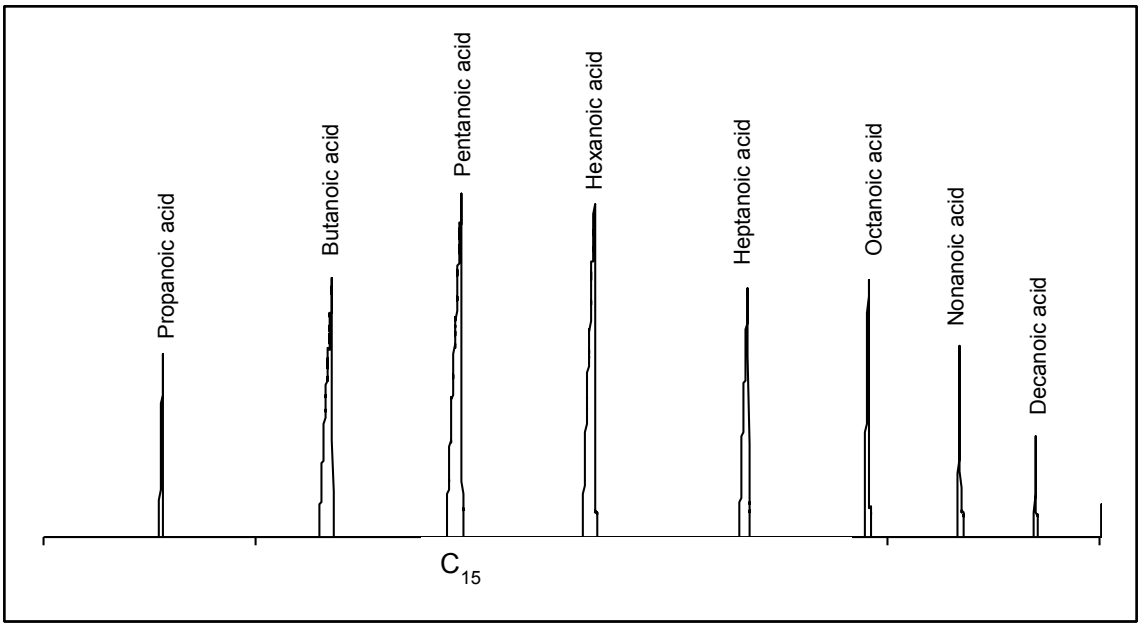

Figure 5.19: Extracted ion chromatogram (m/z=60) from analysis of water sample obtained from ammonia-free feed (0 vol% ammonia).

Figure 5.20 goes on to show the extracted ion chromatograms (m/z=60) for 0 vol%, 2 vol%, 5 vol% and 10 vol% water analyses, with the resultant peaks obtained from the ammonia-containing analysis not showing peaks that are as clear or as distinct as those obtained from ammonia-free runs. Furthermore, the MS did not identify these peaks as belonging to acids, but in general to compounds containing multi-functional groups, e.g. products containing both the acid functional groups as well as amine functional groups.

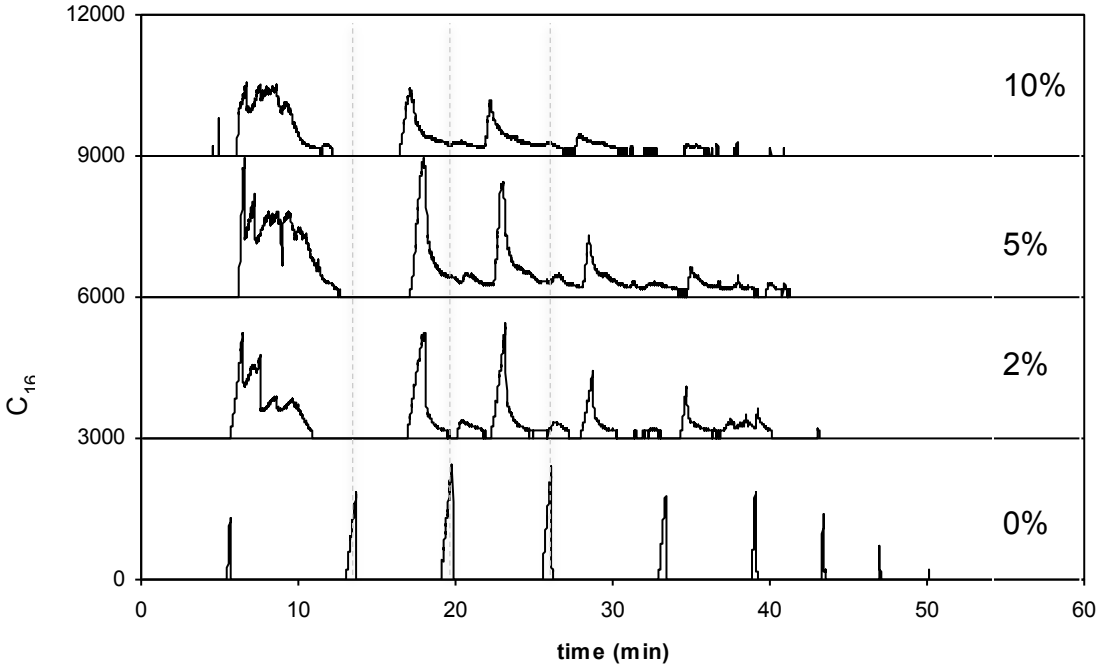

Figure 5.20: Extracted ion chromatograms (m/z=60) from analysis of water obtained from the experiments with varied ammonia feed concentration (0 to 10 vol% ammonia).

Although the FID analysis of the gas phase product was more ideal for quantification purposes, the acid peaks from the FID could only be quantified 'cleanly' up to C_8 due to peak overlap thereafter. A 'pseudo' ASF plot of the hydrocarbon (paraffin + olefin) in the liquid products has a positive slope up to about C_{12} (Figure 5.21). A positive slope indicates that not all the (hydrocarbon) product in the lower carbon numbers has been collected in the liquid trap, and hence the fractions below this cannot be used directly for quantitative analysis. This makes quantification of acids (and amines) from liquid analysis even more complex. Furthermore, the oxygenates (especially alcohols), acids and amines have much lower boiling points than the corresponding hydrocarbons (olefin/paraffins) in each carbon number, and as such the acid/amine/oxygenate capture in the liquid traps results in condensation of most of these products. This assumption is supported by the results of Figure 5.23, showing a 'normalized' molar ratio of acids (to n-pentadecene-1) obtained in the water phase (0 vol% ammonia in feed) vs carbon number, and this is highest for the C_2 fraction, decreasing thereafter. (Quantitative analysis for acids and amines was made difficult due to absence of these compounds in the 'total' sample (ampoule/gas) as explained in section 4.3.2, a finding also supported

by Cairns (2008) using the same setup). Although a method was devised to estimate the flows (section 4.3.2), it must be noted that this method was still crude, and as such there is room for refinement of the method.

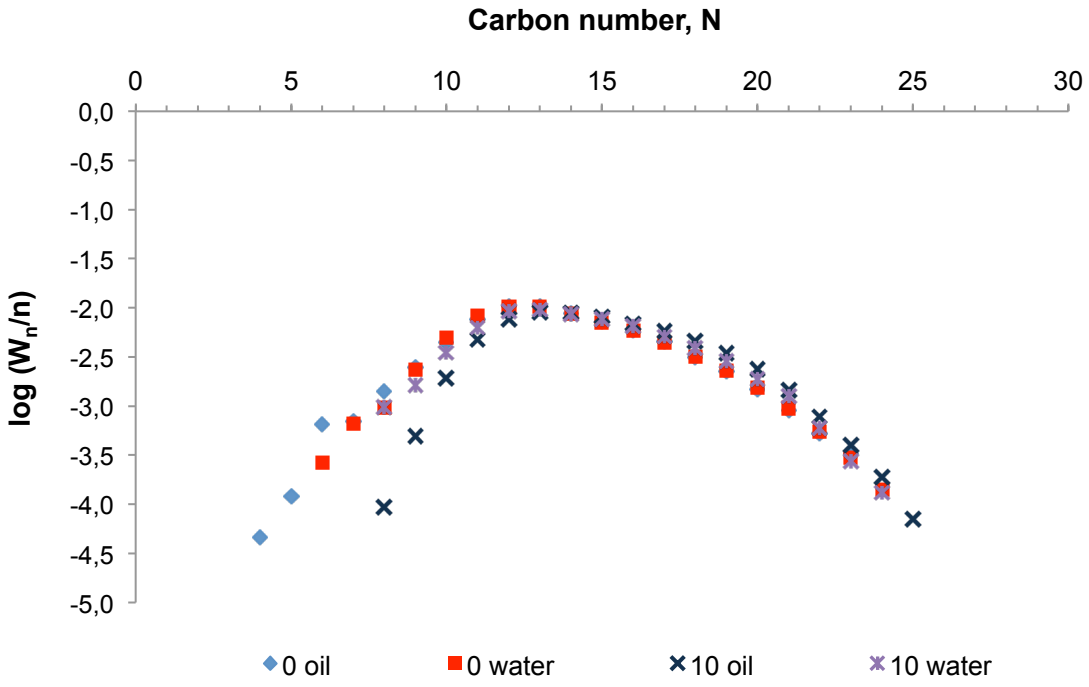

Figure 5.21: Pseudo-ASF plot obtained from analyses of the liquid obtained for 0 vol % and 10 vol % NH_3 in the feed.

Figure 5.22 shows the carboxylic acid content as a function of total linear products in each carbon number as a function of carbon number. Figure 5.23 shows the molar ratio of C_2-C_8 acids relative to the C_{15} 1-olefin for the 0 vol% ammonia (obtained by combining the ampoule and liquid analyses). From these, we clearly observe formation of carboxylic acids in the 0 vol% ammonia-in-feed run across a wide carbon number range, and the expected general decrease in molar content with increasing carbon number. Carboxylic acids disappear completely with ammonia addition to the process. Figure 5.24 shows the content of ketones for the 0 vol%, 2 vol%, 5 vol % and 10 vol% water analyses and there is no discernible trend with increasing ammonia content in the feed.

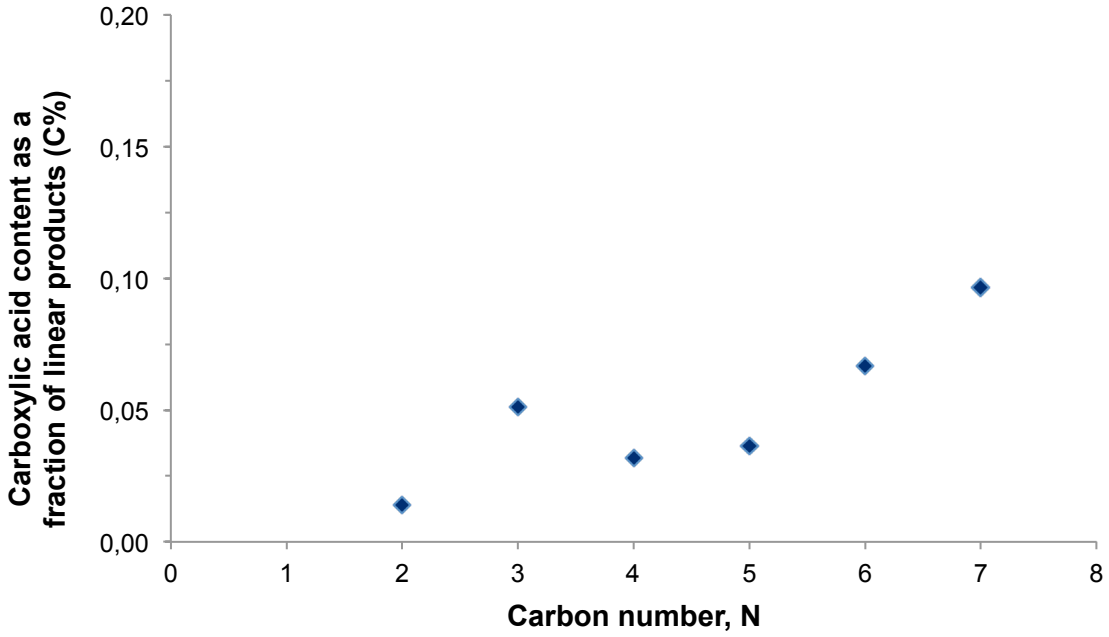

Figure 5.22: Molar content of carboxylic acids in fraction of linear hydrocarbons as function of carbon number for the experiment with 0 vol% ammonia in feed.

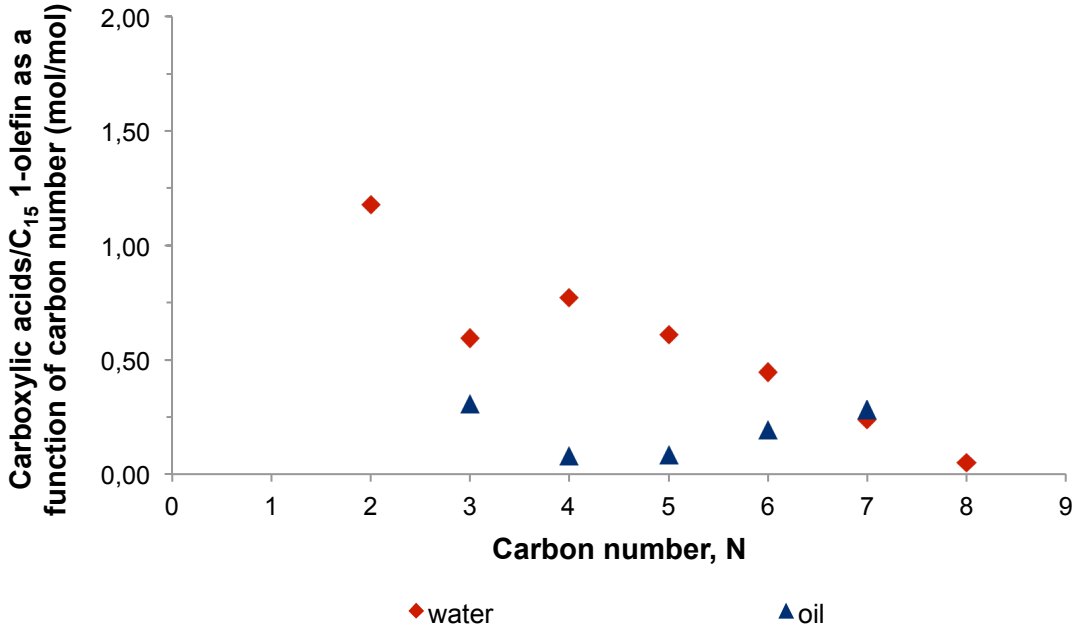

Figure 5.23: Molar ratio of carboxylic acids to pentadecene-1 (C_{15} 1-olefin) as function of carbon number for the 0 vol% NH_3 in feed (from analysis of both the water & oil products)

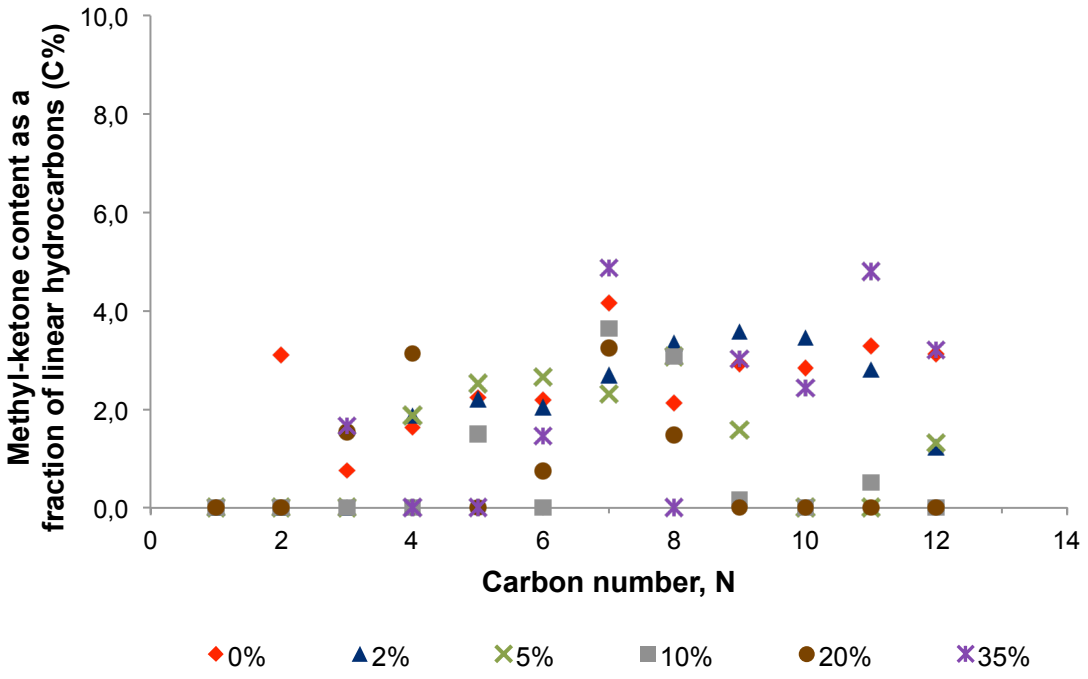

Figure 5.24: Molar content of methyl-ketones in fraction of linear products as function of carbon number for varied ammonia contents in the feed.

From the figures above the following are noted:

Methyl-ketones:

- The levels of methyl-ketone formation remains largely unaffected by the addition of ammonia as observed from figure 5.24. This suggests that methyl-ketone formation is not affected by ammonia and that methyl-ketones do not undergo secondary conversion reactions with ammonia.

Carboxylic acids:

- Whereas the analysis of the products of the experiment of the ammonia-free conditions resulted in definite, sequential peaks, the product of the experiments with ammonia-containing syngas indicated absence of carboxylic acid formation;
- From the NIST database, the peaks from the 0 vol% ammonia resulted in definite matches with aliphatic organic acids, whereas the peaks from the ammonia containing products resulted in different but possibly related products. The major

peaks containing the m/z=60 ion where identified as simultaneously oxygenated and nitrogen-containing compounds, such as amides and/or formamides as explained later in section 5.4.4;

- Acid content shows a complete suppression with ammonia addition.

It is interesting to note that while the methyl-ketone content remains largely unaffected by the addition of ammonia to the feed, the acid content decreases strongly. Assuming that the formation of both products occurs through the same precursor(s) as proposed in Figure 5.17 by Cairns (2008), one may expect a similar effect of ammonia on their formation. However only the acids are affected by ammonia addition; and unless the addition of the OH species is specifically inhibited by ammonia, it may be speculated that acids once formed are converted to other products in the presence of ammonia in secondary reactions. Such secondary reactions do not seem to occur with methyl-ketones though.

The disappearance of acids with the addition of ammonia can be explained by any of a number of theories, including spontaneous reaction of acids with ammonia to form a number of products, including amides and carboxylate salts:

Carboxylate salts: $RCOOH + NH_3 \rightarrow [RCOO]^-[NH_4]^+$ (5.10)

Amides: $RCOOH + NH_3 \rightarrow RCONH_2 + H_2O$ (5.11)

(McNaught & Wilkinson, 1997).

Tests were carried out to ascertain whether the acid disappearance was due to the homogeneous reaction of acids formed via primary synthesis with ammonia in a spontaneous, secondary reaction (uncatalyzed). Some oil collected from the ammonia-free run was charged into a batch reactor, and then heated to 220°C at atmospheric pressure. Ammonia was then bubbled through the heated acid for 4 hours. Samples were then analyzed using the GC-MS to check for disappearance of the acids and formation of new compounds. However, no disappearance of acids was detected using GC-MS analysis and it can therefore indeed be concluded that they react in a secondary reaction on the catalyst surface or alternatively, ammonia in the system may inhibit the formation of acids on the catalyst surface.

5.4. Nitrogen-containing compounds

The formation of mono-amines during ammonia addition in the Fischer-Tropsch synthesis had previously been reported by others (Brown & Maselli, 1973; Kliger *et al*. 1986; Kölbel & Trapper, 1966; Röttig, 1958) and these products were also obtained in the present study. In addition, and in contrast to previous studies, linear nitriles, amides and formamides were also detected and confirmed via the GC-MS analysis of the product. The identification of nitrogen containing compounds and their possible formation routes will be discussed in the following section. The nitrile analysis was based predominantly on ampoule analysis, with the liquid product being used to quantify the longer-chain nitriles. Amines, amides and formamides were only detected in the liquid product, and hence this was used for identification and quantification of these compounds. The weight fractions of these products normalized to the C_1-C_{20} fraction are listed in Table 5.12 - 5.15.

Table 5.12: Amine content as a percentage (C %) of the total linear C_1-C_{20} products.

	vol% NH_3 in the feed		
	2%	**5%**	**10%**
C_2-C_5	0.10	1.93	2.04
C_6-C_{12}	0.09	4.08	4.50
C_{13}-C_{20}	0.00	0.28	0.46
C_1-C_{20}	**0.18**	**6.28**	**7.00**

Table 5.13: Nitrile content as a percentage (C %) of the total C_1-C_{20} linear products.

	vol% NH_3 in feed				
	2%	**5%**	**10%**	**20%**	**35%**
C_2-C_5	0.73	0.85	0.58	n/a	1.6
C_6-C_{12}	0.65	2.46	1.94	4.0	3.3
C_{13}-C_{20}	0.11	0.12	0.09	n/a	n/a[2]
C_1-C_{20}	**1.38**	**3.43**	**2.61**	**4.0**	**4.9**

Table 5.14: Amide content as a percentage (C %) of the total C_1-C_{20} linear products.

	2% NH_3	**5% NH_3**	**10% NH_3**
C_2-C_5	0.004	0.35	1.54
C_6-C_{12}	0.008	0.08	0.19
C_{13}-C_{20}	n/a	n/a	0.01
C_1-C_{20}	**0.012**	**0.43**	**1.74**

Table 5.15: Formamide content as a percentage (C %) of the total C_1-C_{20} linear products.

	2% NH_3	**5% NH_3**	**10% NH_3**
C_2-C_5	n/a	0.02	0.06
C_6-C_{12}	0.006	0.07	0.28
C_{13}-C_{20}	n/a	0.02	0.08
C_1-C_{20}	**0.006**	**0.10**	**0.42**

[2] Higher nitriles were not observed in the 20 vol% and 35 vol% experiments due to lack of clean liquid for quantitative analysis.

Figures 5.25 – 5.27 show the extracted ion chromatograms from the analysis of the water phase obtained from the 0 vol% and 10 vol% experiments. The overall qualitative effect of ammonia addition to our FT system is observed:

- Decrease in oxygenate content (alcohol and aldehydes);
- Disappearance of acids in the product;
- Little effect on methyl ketones;
- Formation of amines and nitriles in significant quantities.

The m/z = 82 ion is not exclusive to nitriles. Figure 5.27 is included to highlight a section of the m/z = 82 ion to highlight the position of the nitriles.

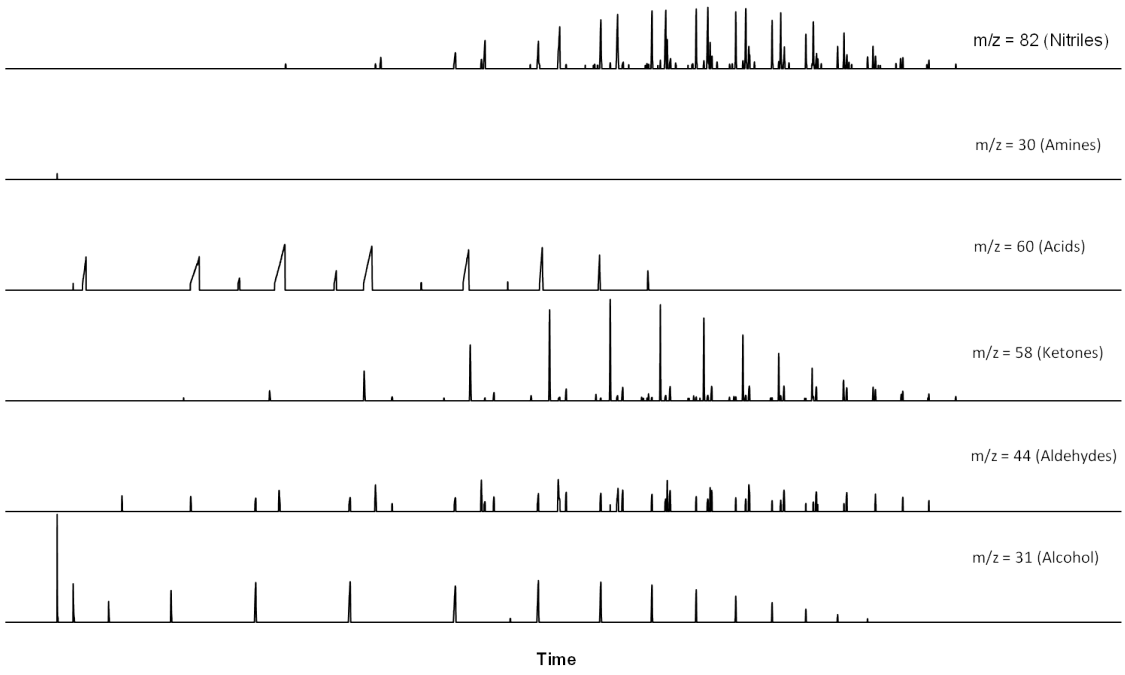

Figure 5.25 Extracted ion chromatogram obtained from analysis of the water product from the 0 vol% ammonia run

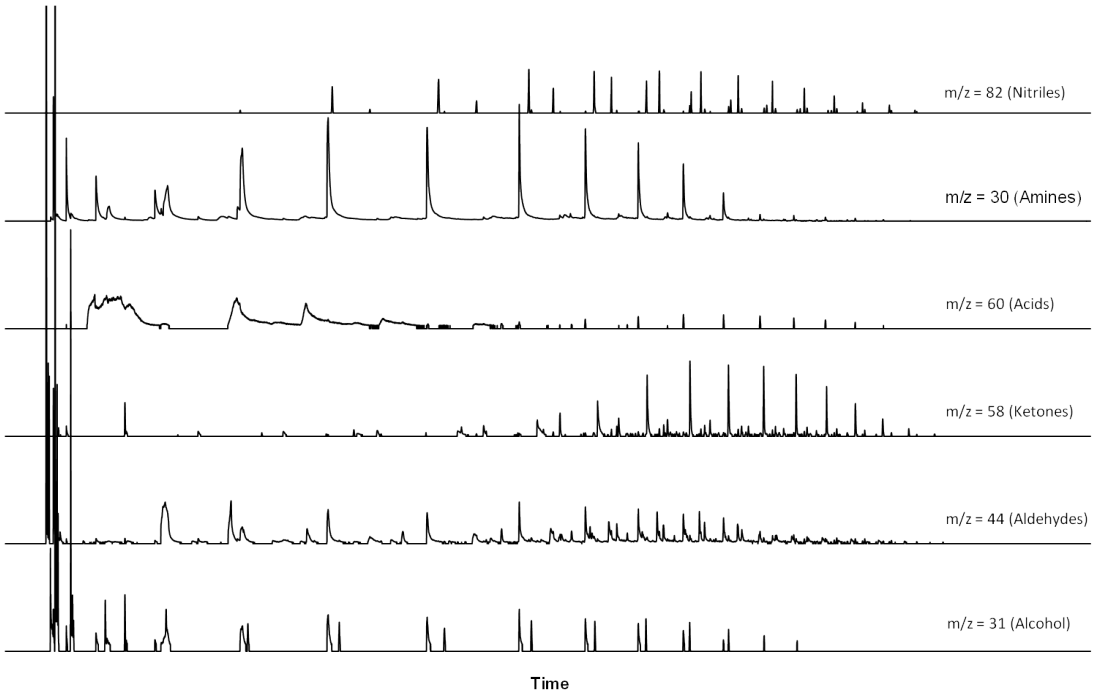

Figure 5.26 Extracted ion chromatogram obtained from analysis of the water product from the 10 vol% ammonia run

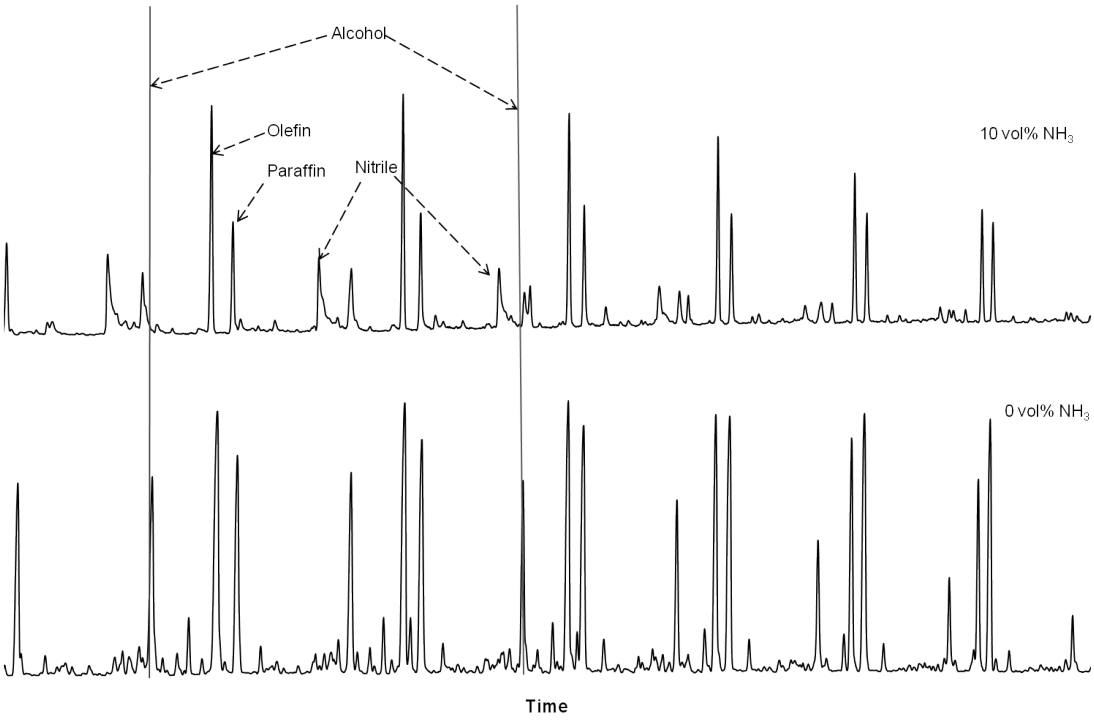

Figure 5.27 Extracted m/z = 82 ion chromatogram for the 0 vol% and 10 vol% ammonia run (water analysis)

5.4.1. Amines

Evidence of amine formation

Figure 5.28 shows the extracted ion chromatogram (m/z=30) obtained from the analysis of the analysis of the water sample obtained under 10 vol% ammonia in the feed. The figure shows a clear, wide carbon number distribution of compounds containing the m/z=30 ion, representing presence of amines as described in section 4.3.3. This peak/ion is totally absent in the standard, ammonia free, FT product spectrum. The amine formation was further confirmed via injection of an amine standard (n-octanamine).

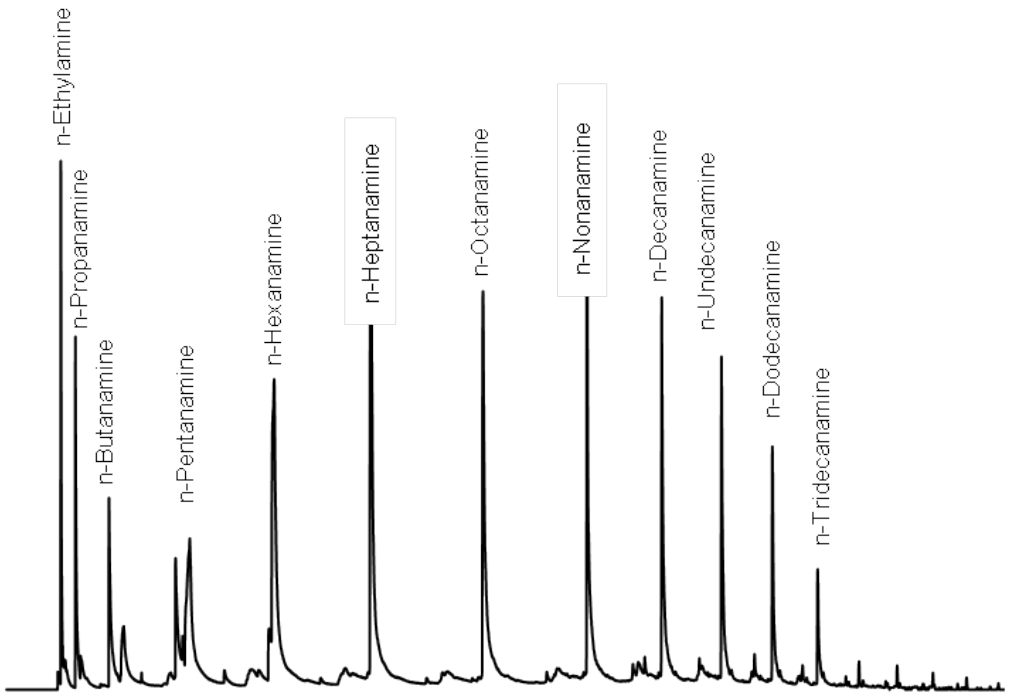

Figure 5.28: Extracted m/z=30 ion chromatogram from analysis of water sample obtained from 10 vol% ammonia-in-feed run.

The amines can also be found in the corresponding chromatograms using FID detection, and quantification using correction factors appendix D were based on these chromatograms. Figure 5.29 shows a section of the FID chromatogram obtained from analysis of the water sample from the 10 vol% ammonia-in-feed run.

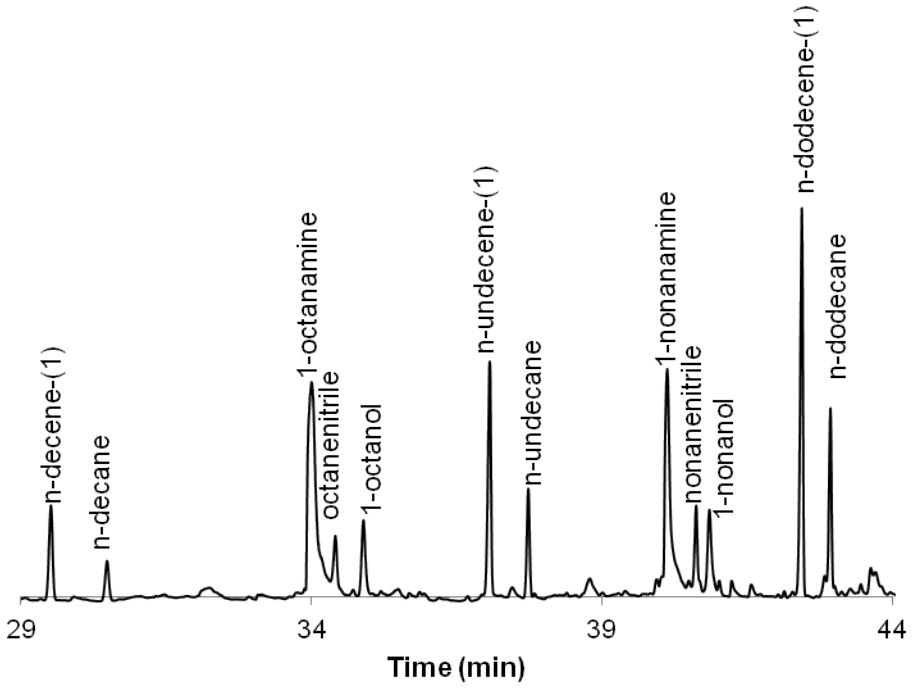

Figure 5.29: Cross section (C_{10}-C_{12}) of GC/FID chromatogram from analysis of water sample obtained from 10 vol% ammonia-in-feed run showing relative locations of amine, nitrile and hydrocarbon peaks.

The formation of amines was in agreement with previous studies conducted by Rottig (1958), Kölbel and Trapper (1966), and Brown & Maselli (1973) using similar systems.

Effect of ammonia content on amine selectivity

Figure 5.30 shows the molar amine content in each carbon number (linear products). The liquid product (water and oil) was used for quantification as described in section 4.3. It is suspected that loss of the lighter amines occurs in the cold trap due to only partial condensation of the lighter compounds taking place. Below a certain optimum carbon number (characterized by the lowest carbon number where the entire amine product condenses quantitatively), the results may therefore be slightly biased in the amine content determined. Looking at the figure, it is expected that this carbon number lies between C_6-C_8. Stated otherwise, the amine content can only be compared quantitatively above this point. This is supported by Figure 5.31a & b, which show amine

content relative to n-pentadecene-1 in the water phase, indicating an apparent higher amine content for the 2 vol% ammonia at lower carbon numbers. This is probably as a result of incomplete capture of the lower amines for the runs at higher ammonia contents in the feed. Looking at the higher carbon numbers, the amine content is definitely higher with higher ammonia content in the feed. Although there appears to be a connection between ammonia content in the feed and resultant amine content, the effect does not seem to be linear, as the relative changes in amine content are not proportional to the relative increases in ammonia content. In fact it appears that an increase of the ammonia level in the feed from 5 to 10 vol% does not lead to a further increase of the molar amine content; correspondingly the total amine content increased to constant values of approximately 7 C% (see Table 5.12).

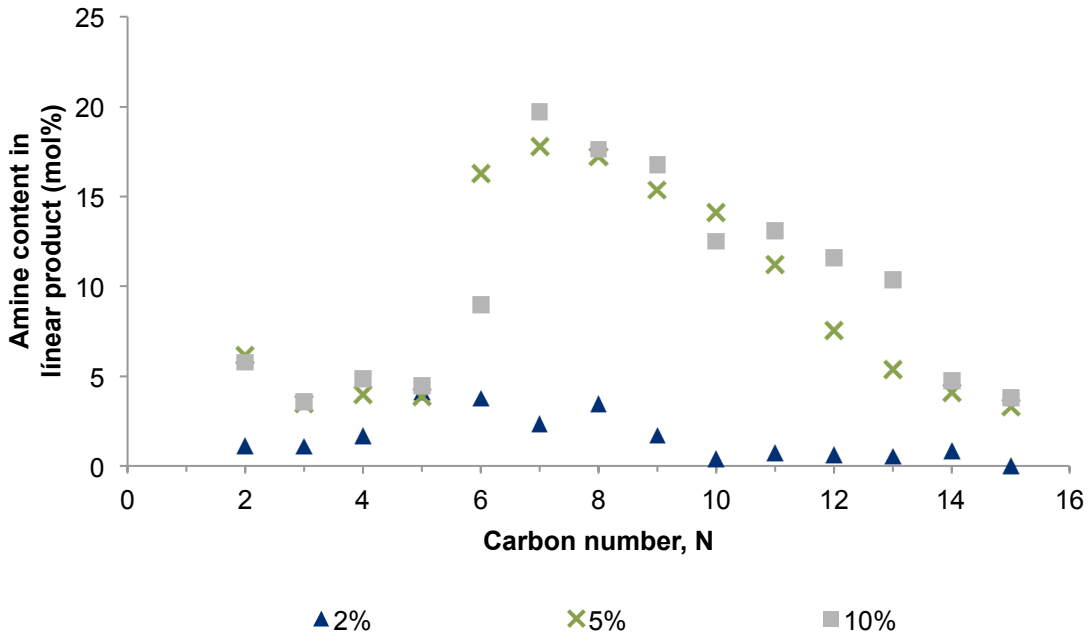

Figure 5.30: Molar amine content in each linear carbon product fraction ($Amine_n/Pr_n$) as a function of carbon number.

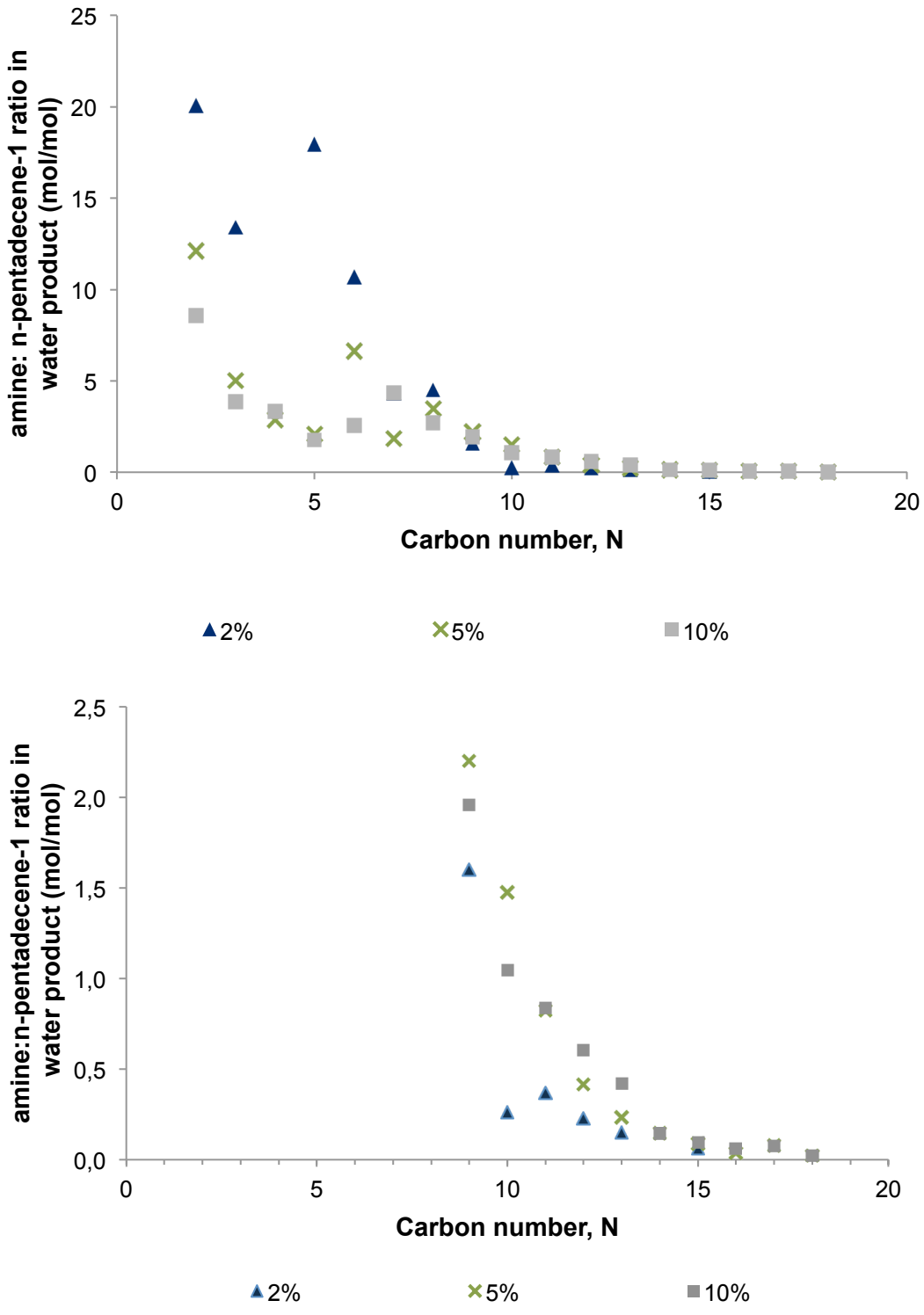

Figure 5.31 a & b: Molar ratio of amines to pentadecene-1 (C_{15} 1-olefin) as function of carbon number for the varied ammonia feed contents (from analysis of the water product)

Proposed mechanism of amine formation

Without further studies, the mechanism of reaction cannot conclusively be identified. However, based on the reactor product a number of possible mechanisms can be suggested. One of the main defining factors is the formation of principally aliphatic, primary mono-amines, which suggests addition of a nitrogen containing species, NH_x, to a terminally bonded surface chain, followed by product desorption.

Ammonia is generally expected to adsorb dissociatively on the catalyst surface (Yin *et al.* (2004) and Kowalczyk *et al.* (1997)). The proposed adsorption mechanism of ammonia onto the catalyst surface followed by subsequent hydrogen elimination is shown in Figure 5.32. All of the species are expected to exist on the catalyst surface.

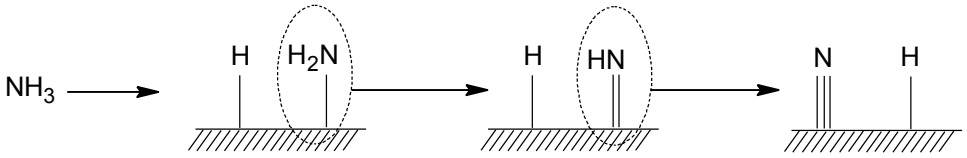

Figure 5.32: Proposed ammonia adsorption on the catalyst surface

The simplest possible mechanism proposed from this work is perhaps explained by the addition of an NH_2 surface species to an alkyl surface species at the chain termination stage. This is dependent on the formation of surface alkyl species via the alkyl or CO-insertion mechanisms (Chapter 2.3.5). Similar to the terminal H-addition for paraffin formation at the chain termination stage, NH_2 addition takes place. The chain termination is illustrated in Figure 5.33.

Figure 5.33: Mechanism of amine formation via NH_2 addition at the chain termination stage.

Assuming that the NH_2 species essentially replaces surface hydrogen, the NH_2 should theoretically be able to replace H at any position in the chain as it should be readily available on the catalyst surface. If an NH_2 group replaces an H in the monomer ($-CH_2-$),

then non-terminal amines should be detected. Also, if an NH_2 group replaces an H in the chain initiator, then coupled with the chain termination-amine addition hypothesis, we would also expect di-amines of the form shown below:

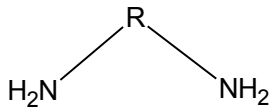

For the proposed mechanism of amine formation via chain termination to hold, the chain initiator can only be the surface CH_3 species and the monomer being the CH_2 species exclusively. If either species have an NH_2 replacing an H, then these aminated species do not take any part in chain growth, hence the absence of internal amines, or di-amines in the product. If chain initiation and growth is as described by the alkyl or CO-insertion mechanism, coupled with NH_2 addition at the chain termination stage, then terminal mono-amine formation can be the only result. The mechanism suggested above, and elimination of amine addition into the chain initiator or monomer is also in agreement with work done by previous researchers. In their work, Kliger *et al.* (1986) also suggested that amine formation occurs in a primary synthesis step via hydroamination of a surface species. Kölbel *et al.* (1966) also came to the conclusion that the mechanism for amine formation results in chain termination. It should be noted that according to this mechanism all alkyl surface species can result in nitrogen-containing compounds upon ammonia addition, however, no further increase of the content of amines was detected when increasing the ammonia levels in the feed from 5 to 10 vol%. This may suggest that something is limiting the formation of these products, and other option for their formation must therefore be considered, these may include:

- a condensation reaction between alcohol or aldehydes and ammonia, forming terminal amines and water in a secondary reaction. Amines have indeed been synthesized from alcohols (Turcotte & Hayes (2001); Rausch *et al.* (2008)). In contrast, Kliger *et al.* (1986) tested a Fischer-Tropsch system for amination of alcohols where ammonia had no effect on alcohol selectivity. However, in the system used for the present work, alcohol and aldehyde content decreased with ammonia feed content, and this could be as a consequence of the proposed secondary reaction to amines. The proposed intermediates for this reaction include a hydroxyl-group containing species (Figure 5.34) or an ethylidene

species (Figure 5.35) as described by Rausch *et al.* (2008). The mechanism involving a hydroxyl intermediate is dependent on a primary or secondary amine, resulting in amines, imines and enamines as final products. However, if ammonia instead is used in the feed, it is also possible to produce amines in the product using the same mechanism, and absence of imines and enamines from our product would suggest that secondary reaction of amines is minimal or absent from the system. Alternatively, imines and enamines are potentially thermodynamically and kinetically unfavourable. It can be noted that both these species (hydroxyl and ethylidene) are also suspected to play a role in the formation of oxygenates (see Figure 5.14). In other words amine formation may proceed through these species via a primary or a secondary reaction during Fischer-Tropsch synthesis. Thermodynamically the formation of amines from oxygenates in particular aldehydes is feasible at Fischer-Tropsch conditions as can be seen in Figure 2.5 and 2.5 in section 2.6.

- amine synthesis via hydrogenation of nitrile species in secondary reaction concurring with a known (industrial) method for amine formation from nitriles (Turcotte & Hayes, 2001).

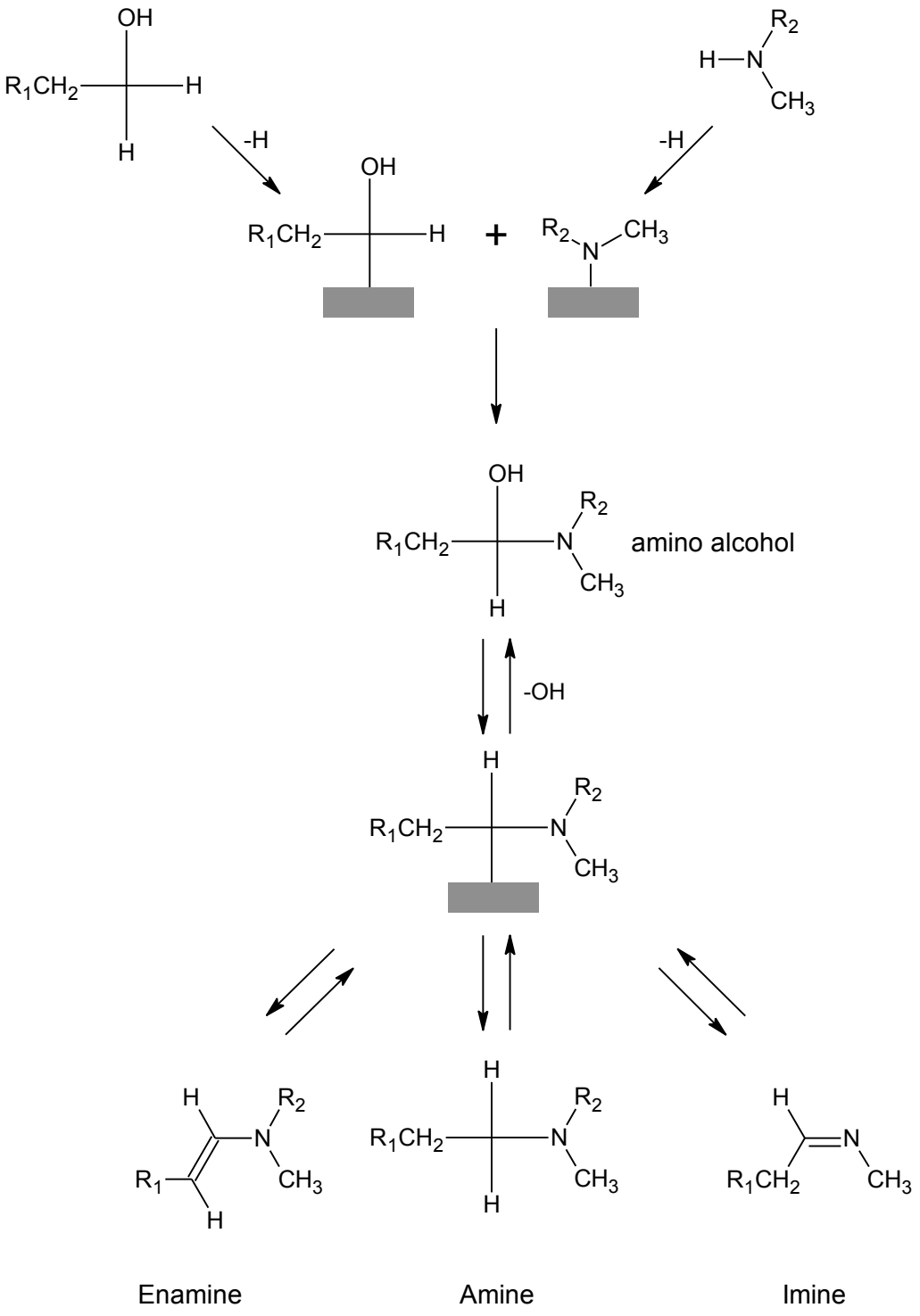

Figure 5.34: Mechanism of alcohol amination via a hydroxyl intermediate as proposed by Rausch *et al.* (2008)

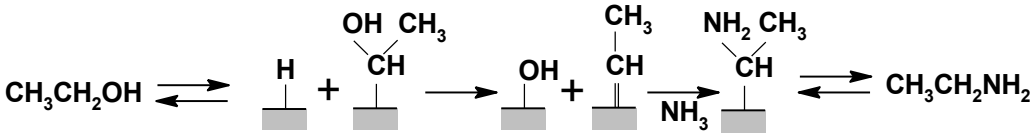

Figure 5.35: Mechanism of amine formation via an ethylidene intermediate Rausch *et al.* (2008)

5.4.2 Nitrile formation

Evidence of nitrile formation

Previous work conducted did not report on the formation of nitriles as a product of ammonia addition to the FT synthesis. In this work, nitriles were detected from GC-MS/FID analyses of all three types of sample (gas ampoules, oil and water samples) obtained during ammonia-containing syntheses. Unlike amines, the nitriles did not have an exclusive ion from the mass spectrometer. However, the ion with an m/z ratio of 82 (Figure 5.36) was prominent and the database matched the unknown peaks in the samples from the reactor product to corresponding nitriles in the NIST database of chemical compounds.

Furthermore, injection of a standard (n-octane-nitrile) coincided with the peak obtained and identified as n-octane-nitrile from the experimental samples. The nitriles can also be found in the corresponding chromatograms using FID detection (Figure 5.29), and quantification using correction factors were based on these chromatograms.

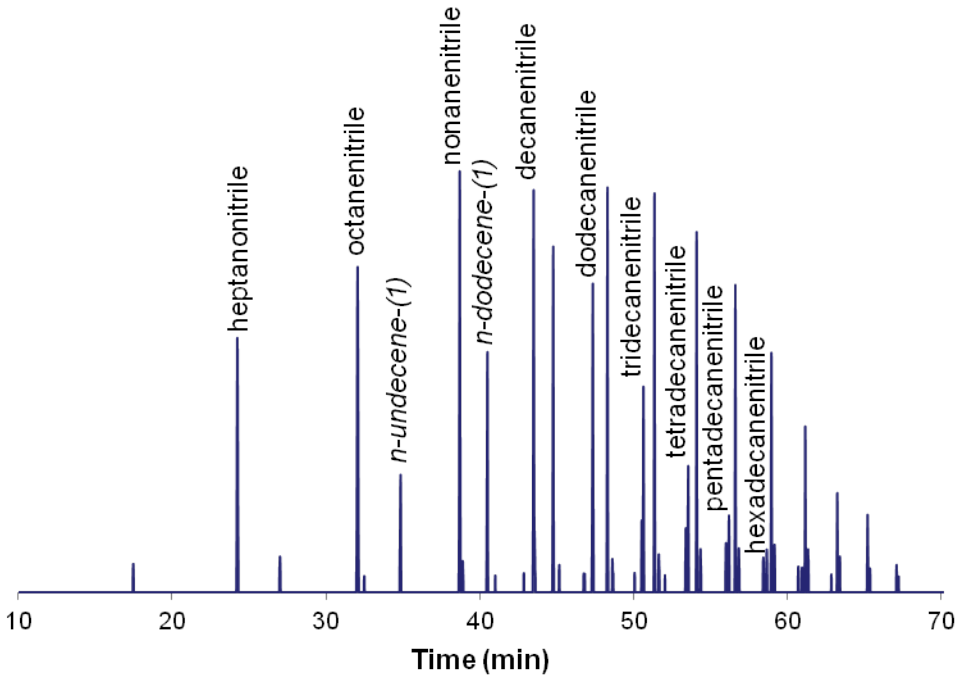

Figure 5.36 Extracted m/z=82 ion chromatogram from analysis of water sample obtained from 10 vol% ammonia-in-feed run.

Effect of ammonia content on nitrile selectivity

The amount of nitriles is lower than that of amines. Upon increasing ammonia from 2 to 35 vol% in the feed, an increase from 1.5 to at least 4.9 wt% of the nitriles in the C_1 to C_{20} fraction was obtained (note, the lower nitriles did not always give clean peaks in the FID, hence the overall content may be underestimated). Figure 5.37 shows variation of the molar nitrile content in each carbon number fraction with increasing ammonia content in the feed (note that data for conditions of 20 and 35 vol% ammonia in the feed is included here as analysis was possible from ampoules). However due to absence of data for the liquid phase, and hence unavailability of amine and acid data, these values become biased, i.e. inflated. It also appears that there is some discrimination of short chain nitriles, in particular of those with a carbon number shorter than C_5, and HCN could not be detected in any of the samples. Nonetheless, there is a clear increase in nitriles with increasing ammonia content. At lower ammonia content, the fraction of nitriles levels off with increasing carbon number, typically indicative for primary selectivity

of products in Fischer-Tropsch synthesis (Schulz and Claeys, 1999a). With the 20 and 35 vol% ammonia conditions, the amount of nitriles increases with increasing carbon number, possibly suggesting their formation via a secondary route which is normally preferred for long chain products due to their increased retention in the reactor system (Schulz and Claeys, 1999a).

Figure 5.38 and 5.36 further show the molar ratio of the nitriles in each carbon number fraction relative to n-pentadecene-1 obtained from analysis of the oil from the cold trap and gas phase respectively. Once again the observed trend is an increase towards a maximum, probably indicative of incomplete condensation. A further note, the results shown here show a modified sample of the oil from the 10 vol% ammonia run, which was spiked with octane-nitrile before injection into the GC-MS/FID. The result confirmed nitrile formation as predicted by the MS, and this was indicated by an inflated peak corresponding to the location of the octane-nitrile peak as observed by the result in the chart. Comparing the ratios of nitriles:n-pentadecene-1 in the oil phase to the gas phase, we can see indeed that there is considerable loss of lower nitriles in the liquid phase, and hence we can apply the same idea to amine, amide, formamide and acid collection in the liquid samples, with the results underestimating their respective contents in the lower carbon numbers.

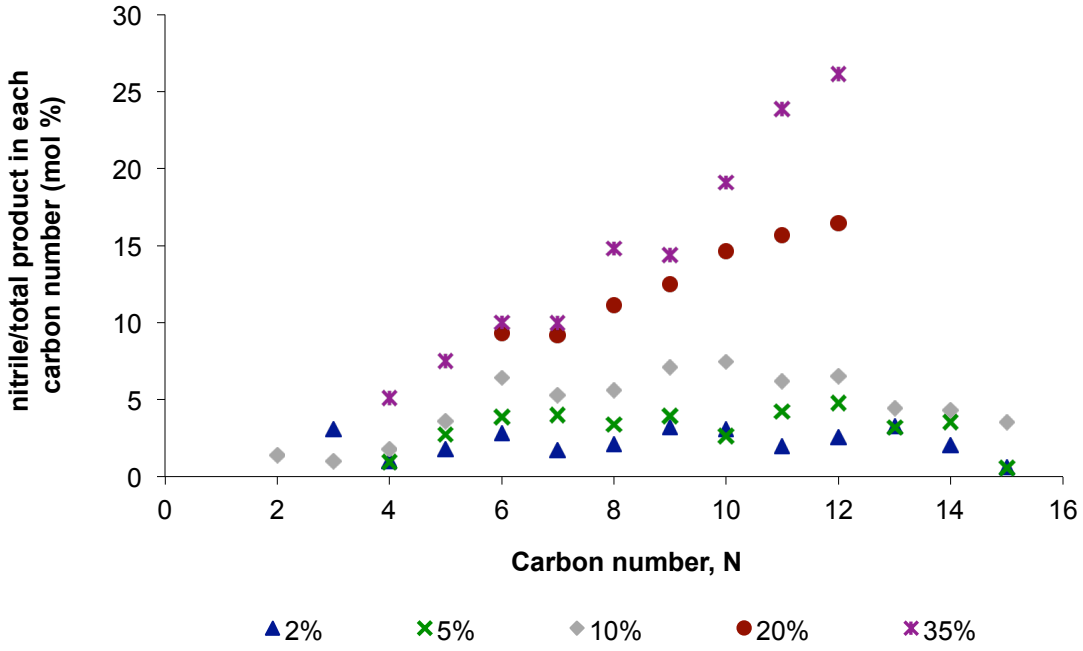

Figure 5.37: Molar nitrile content in each linear carbon product fraction (Nit_n/Pr_n) as a function of carbon number.

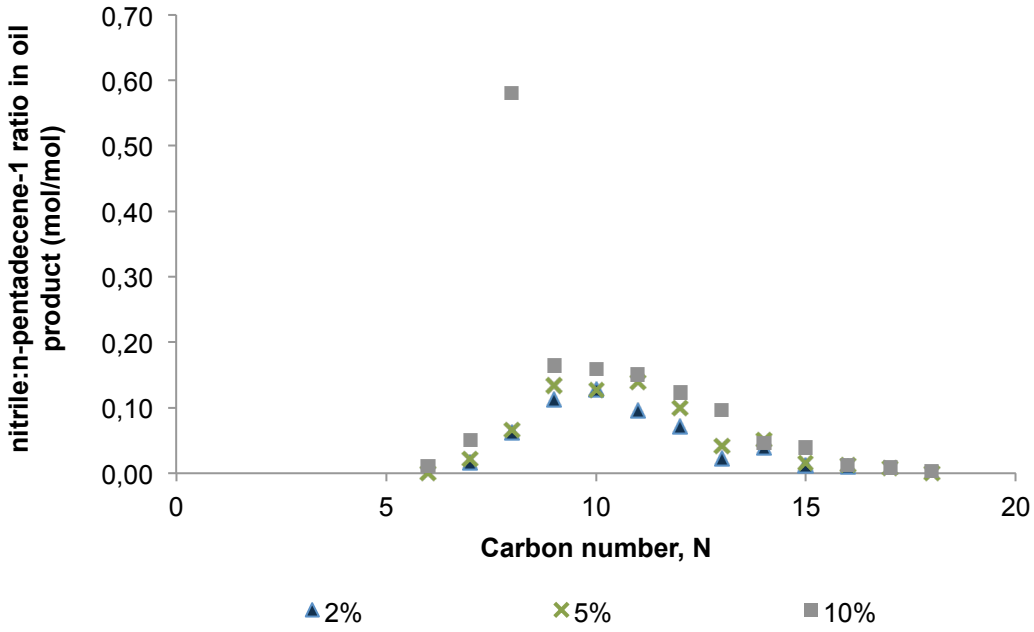

Figure 5.38: Nitrile: n-pentadecene-1 molar ratio in the oil phase as a function of carbon number.

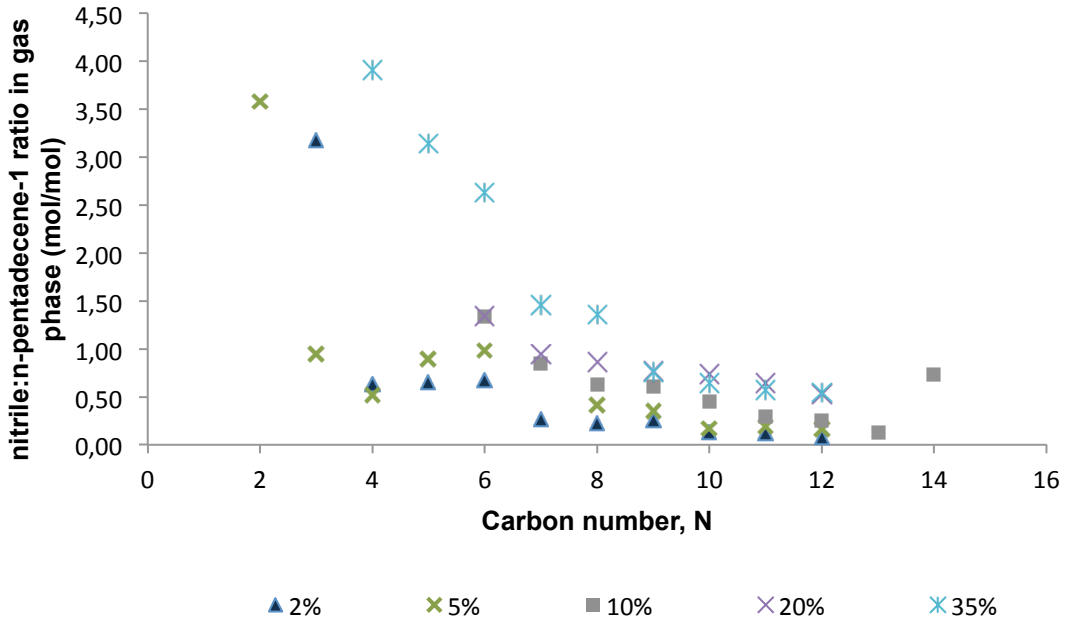

Figure 5.39: Nitrile: n-pentadecene-1 molar ratio in the gas phase as a function of carbon number.

Proposed mechanism of nitrile formation

A proposed mechanism for the synthesis of nitriles in a primary synthesis step involves the reaction of surface carbide and surface nitride to form a surface CN species. This can only then react with a surface alkyl species in a chain termination step to form the corresponding nitrile:

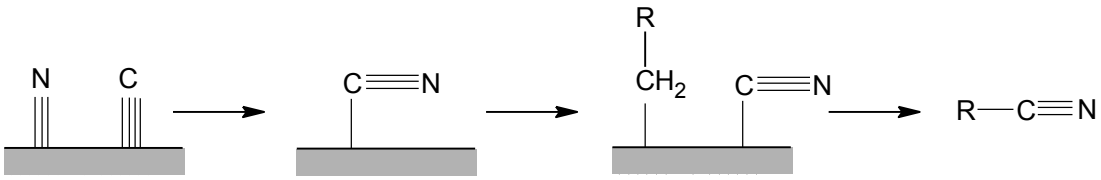

Figure 5.40: Proposed mechanism of nitrile formation

Other possible sources of nitriles include:

- Reaction of acids with ammonia (US Patents by Nicodemus & Wulff, 1939; Hull, 1956; Hagemeyer & Holmes, 1976);

- At high ammonia contents, reaction of olefins with ammonia (Dixon and Burgoyne, 1986).

It is however more likely that the formation of nitriles is related to the formation of amines and/or that these products interconvert. The formation of nitriles may proceed through the same precursor as that of the corresponding amines, e.g. via a hydroxyl group containing intermediate (see Figure 5.31, 5.32), but via addition of a nitrogen surface atom instead of an NH_2 group and accompanied by dehydration (loss of H_2O):

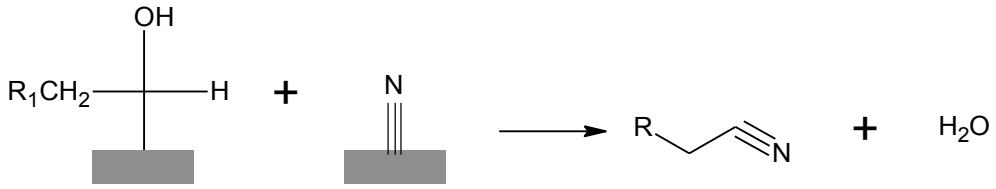

Instead of

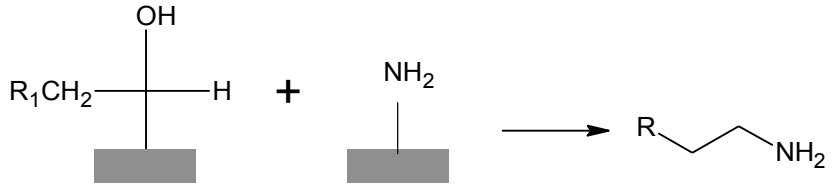

Depending on the reaction conditions and the relative availability of the NH_x species, relative amounts of nitriles versus amines may form in each carbon number, similar to the primary formation of olefins versus paraffins. Figure 5.41 shows the molar nitrile content in the nitrogen-containing product comprising of nitriles and amines as function of carbon number. The graph begins at C_9 due to loss of the lower amines.

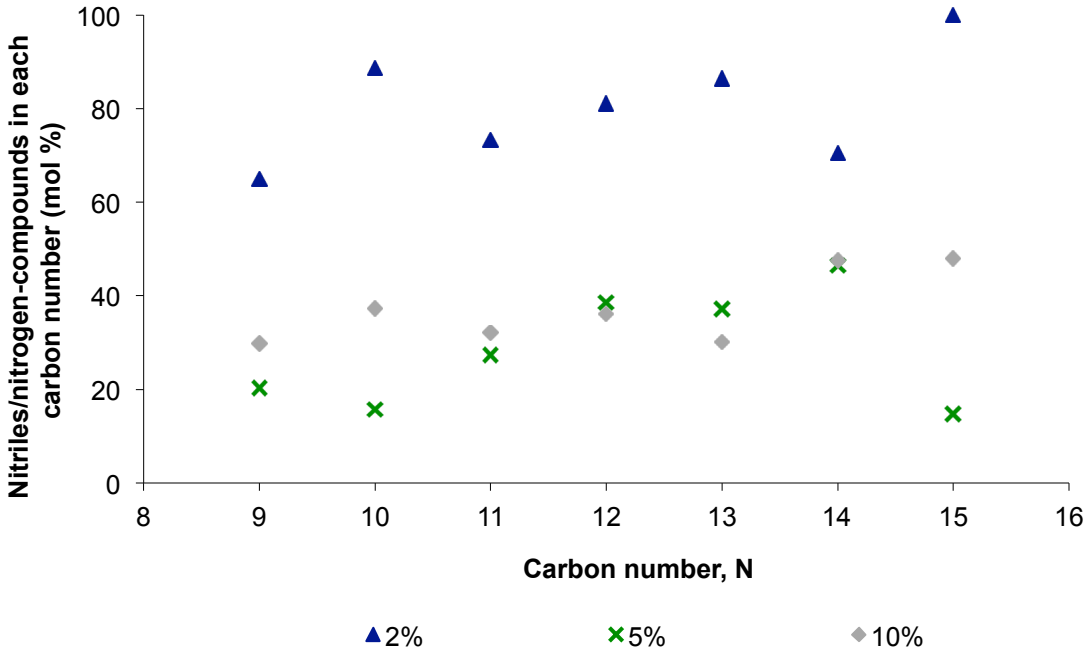

Figure 5.41: Molar nitrile content in nitrogen-containing compounds for each carbon chain fraction ($Nit_n/(Nit_n+Amine_n)$) as a function of carbon number.

From the chart, the nitrile content decreases with increasing ammonia content from around 80 to 30-40 mol%. These contents do not seem to be carbon number dependent and it is therefore likely that the observed product selectivities reflect the relative desorption rates of nitriles versus amines. Pronounced secondary conversion of reactive product in the Fischer-Tropsch synthesis can often be found at higher carbon numbers due to their longer retention in the reactor, in which case a decrease of the nitrile content may be expected, according to:

$$RCH_2CN + 2H_2 \rightarrow RCH_2CH_2NH_2 \qquad (5.12)$$

Thermodynamically amines are the more stable compounds at Fischer-Tropsch conditions (see also Figure 2.5 and 2.6 in section 2.6). At the conditions used in this study the below ratios of n-hexanamine to n-hexanenitrile would be expected (see Table 5.16, note that thermodynamic data for nitriles were only available up to carbon number 6). These can then be compared with the corresponding observed product ratios of these compounds. Listed in the table are values obtained for both C_6 and C_9, with C_9

expected to be representative for ratios in higher carbon numbers (note that no carbon number dependency was observed in Figure 5.41). Equations 5.13-5.15 show the equations used to determine theoretical equilibrium ratios:

$$K_a = \exp\left(\frac{\Delta G_R}{R \cdot T}\right) \tag{5.13}$$

where ΔG_R is the Gibbs free energy of reaction (J/mol) at the reaction temperature T (523K), and R is the ideal gas constant, 8.314 J/mol·K.

$$K_a = \frac{P_{amine}}{P_{nitrile} \cdot P_{hydrogen}^2} \tag{5.14}$$

where P_{amine} and $P_{nitrile}$ are the partial pressures of the amine and nitrile in each carbon number fraction and $P_{hydrogen}$ is the partial pressure of hydrogen in the reactor product.

$$\therefore \frac{P_{amine}}{P_{nitrile}} = K_a \cdot P_{hydrogen}^2 \tag{5.15}$$

The amine:nitrile ratio obtained in this way is then compared to the actual amine:nitrile ratio in the reactor product. It can be seen that the equilibrium is on the side of the amine, but based on the C_9 data, it is not reached at the low ammonia feed condition, indicating strict kinetic control. The equilibrium is apparently exceeded at the higher ammonia feed conditions, with the test at 5 vol% showing a considerable deviation.

Table 5.16: Equilibrium ratios of C_6 amine and nitrile for different ammonia contents in the feed compared with observed ratios in the synthesis product.

		Ammonia feed content (vol%)		
		2	5	10
Hexanenitrile + $2H_2 \leftrightarrow$ hexanamine	ΔG_R (kJ/mol)	-7.23		
Hexanamine/hexanenitrile	Eq[a]	2.30	2.20	2.12
	Obs[b]	1.40	4.18	1.39
Nonanamine/nonanenitrile	Obs[b]	0.54	3.92	2.36

[a]Eq- Expected ratio at equilibrium

[b]Obs- Observed product ratios from GC/FID analyses

It is perhaps surprising to see that higher relative nitrile contents, i.e. the hydrogen-leaner product, are obtained at conditions of low ammonia concentration, whereas molar olefin contents in the corresponding hydrocarbon fractions increased with ammonia in the feed (Figure 5.9). Lower hydrogen availability was suspected to cause higher primary olefin selectivity (see section 5.3.2). It may be speculated that the ratio of *N versus $*NH_2$ species is dependent on the ammonia partial pressure, and that at higher pressures $*NH_2$ species are predominant. As formation of an $*NH_2$ species only coincides with the formation of one surface *H compared to 3 surface *H in case of the formation of *N, indeed lower levels of hydrogen may be expected at high ammonia pressures therefore explaining the observed selectivity patterns regarding olefins and nitrogen-containing compounds.

Furthermore it should be borne in mind that both amines and nitriles can be hydrogenated to the corresponding paraffin, which is the most preferred compound thermodynamically. However no pronounced decrease of either the amine or nitrile contents- is observed with increasing carbon number (Figure 5.30 and Figure 5.37), indicating that these products are relatively stable at the test conditions used.

Assuming that the nitrogen-containing compounds are formed via precursors for oxygenate formation or through secondary oxygenate readsorption and assuming no secondary hydrogenation of oxygenates and nitrogen-containing compounds, the sum of nitrogen containing compounds plus oxygenates should match the selectivity of oxygenates in the base case experiment without ammonia in the feed. The corresponding data are listed for the conditions where all these products could be quantified, i.e. 0 to 10 vol% ammonia, (Table 5.17).

Table 5.17: Alcohol, aldehyde, amine and nitrile distribution for different ammonia contents in the feed.

wt%	vol% NH_3 in feed			
	0	2	5	10
Alcohols	6.5	1.4	1.2	1.9
Aldehydes	5.0	1.2	0.2	0.1
Amines		0.2	6.3	7.0
Nitriles		1.4	3.4	2.6
Sum	**11.5**	**4.2**	**11.1**	**11.6**

Although some loss of the nitrogen-containing compounds may have occurred in the analyses, it can be seen that, except for the conditions with 2 vol% ammonia in the feed, the sum of oxygenates and nitrogen-containing compounds is indeed very close to the oxygenates content in the base case experiment, supporting the possibility that the formation of amines and nitriles is coupled to the formation and secondary conversion of oxygenates.

Ultimately co-feeding tests with these compounds and their suspected precursors (alcohols and aldehydes) should be conducted in order to confirm their interaction and possible reaction pathways.

5.4.4. Amide and formamide formation

Amides and formamides in small quantities were also detected on the GC-MS. Based on the preliminary analysis, the length of the amides and formamides detected ranged from C_2-C_{15}. However, in the absence of necessary standards, full confirmation of the identity and formation rates of the compounds was not completed. It is proposed that the formation of these simultaneously oxygenated-"nitrogenated" groups may occur via an oxygenated precursor on the catalyst surface in the same way as the formation of acids (as proposed by Cairns (2008), Figure 5.17). However, chain termination would occur with $*NH_2$ addition as opposed to *OH addition as depicted below:

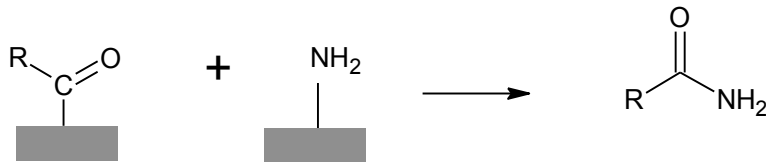

instead of:

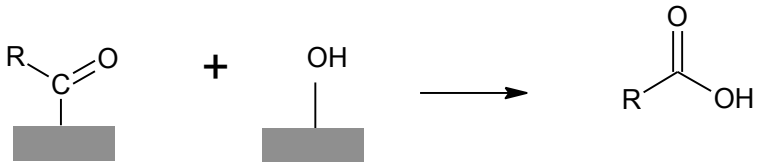

Alternatively and in analogy to proposed secondary amine and nitrile formation (see above), amides may form via a secondary reaction of primarily formed carboxylic acids.

5.4.5. Ammonium carbonate formation

Analysis of the white, solid compound formed from the ammonia addition to the process was done using Raman spectroscopy (also explained in section 5.1, and table 5.2). The resultant spectrum is shown in figure 5.39 and was found to be very similar to that of ammonium carbonate. This finding was also supported by:

- the solubility of the compound in water;
- attempted GC-MS/FID analysis was unsuccessful, and this could be easily due to thermal decomposition of the solid: which occurs readily on heating ammonium carbonate;
- attempts at establishing the melting point were inconclusive due to sublimation of the compound, consistent with the properties of ammonium carbonate.

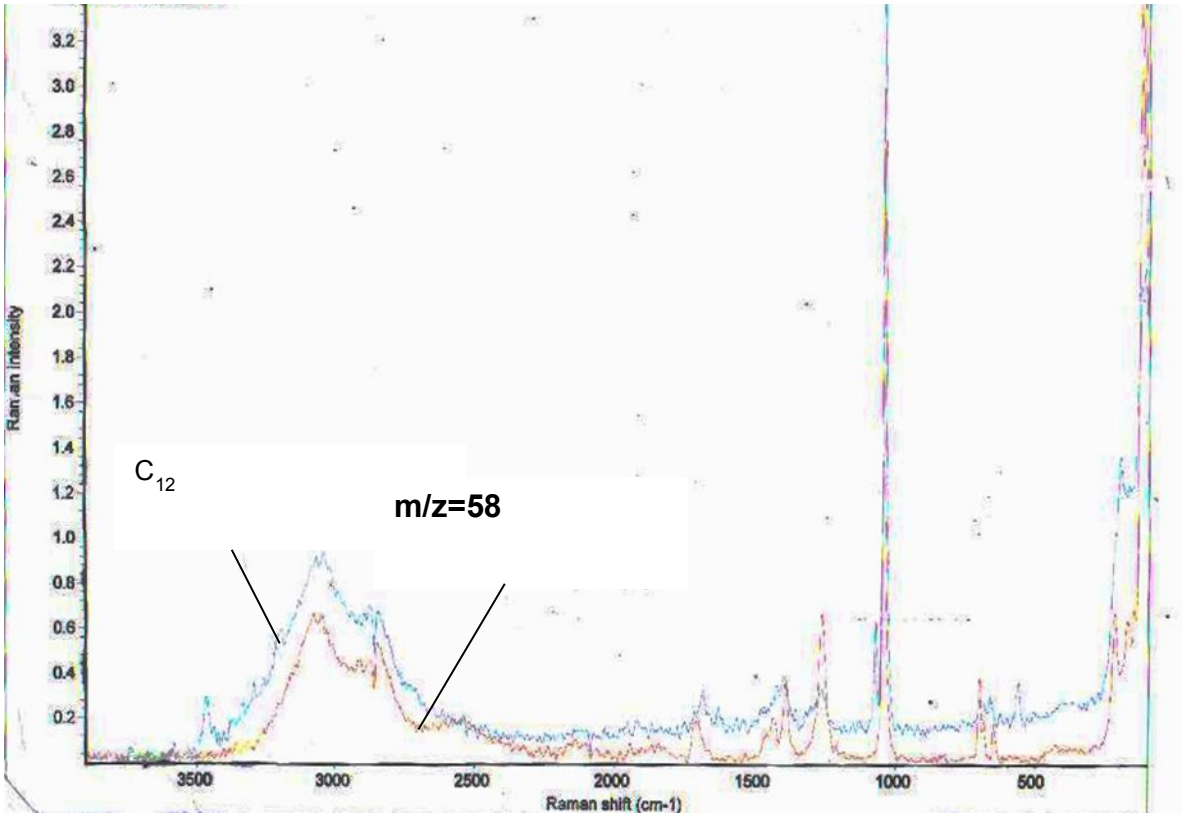

Figure 5.42: Raman spectrum of solid product obtained compared to Raman spectrum of ammonium carbonate

6. CONCLUDING REMARKS

Perhaps the most significant finding in this project was the synthesis of other nitrogen-containing species (in addition to amines) using this modified FT process. Previous workers in this field, working under similar conditions reported mainly on the formation of amines (Kölbel and Trapper, 1966, Rottig, 1958 and Knifton *et al.*, 1993). In this work, we produced amines, nitriles, amides and formamides, with ammonium carbonate as a side product.

Previous research suggests amine formation occurs via a primary route -in the chain termination step- resulting in exclusive formation of primary, terminal n-alkyl amines. Similarly, nitrile formation can possibly occur via addition of a CN-species to a surface alkyl in a chain termination step. In this work, it is hypothesized that in addition to these formation routes, there are other mechanisms in play, leading to multiple mechanisms for the formation of each of these compounds. In summary, for amine formation, we have the following:

- primary formation via addition of an $–NH_2$ species to a surface alkyl (RCH_2) in a chain termination step;
- a secondary condensation reaction between alcohols/aldehydes and ammonia with either a hydroxyl or ethylidene intermediate on the catalyst surface;
- alternatively, the amines can form primarily via the same hydroxyl or ethylidene species on the surface;
- secondary reaction of nitriles with hydrogen;

For nitrile formation, it is hypothesized that the formation routes include:

- primary formation via addition of a –CN species to a surface alkyl (RCH_2) in a chain termination step;
- a secondary reaction of alcohols/aldehydes involving either a hydroxyl or ethylidene intermediate on the catalyst surface;
- secondary reaction of acids/olefins with ammonia.

Amide and formamide formation is less clear, but is proposed to occur via the same oxygenated species (RCO) on the catalyst surface that results in acid formation as

proposed by Cairns (2008). However, -NH_2 addition would occur in place of –OH addition in the chain termination step.

To test for primary versus secondary formation routes, it is proposed that a co-feed of certain classes of compounds be added to the system. For example, operation at a fixed ammonia feed content, different classes in the C_8 length (e.g. n-octanal, n-octan-1-ol, n-octan-1-amine, n-octanenitrile, n-octanoic acid) can be added in individual tests via a saturator. Analysis of the feed and the product from each of these tests would then be used to establish the effect of each of these compounds, and any interconversion between different compound classes will give a further indication of the mechanisms at play in the system.

By testing different parameters in the system (e.g. temperature, space velocity, gas feed ratios), the system can be tailored to maximize formation of certain classes of compound. For example, nitriles, because of their reactivity, are used as feedstock/intermediates for a number of end products. Understanding the system may lead to a new route of formation of nitriles for commercial use.

In conclusion, this work set out to determine the effect of ammonia and its partial pressure on the formation of nitrogen containing compounds. In summary:

- Amines, nitriles, amides and formamides were synthesized with their selectivity increasing with ammonia content in the feed;
- There is strong evidence for formation of these compounds via primary synthesis steps, but secondary formation or reaction of these compounds cannot be disregarded.
- Acids, aldehydes and alcohols were suppressed to varying degrees with increasing ammonia concentration;
- An undesired side product in the form of ammonium carbonate was produced with increasing yields at higher ammonia partial pressures;
- Overall FT hydrocarbons were still produced, and with most of the FT indicators unchanged;
- The iron catalyst employed lost a significant amount of activity, but remained active over 500 hours online and under quite extreme ammonia conditions.

7. REFERENCES

Anderson, R.B. (1984), *The Fischer-Tropsch Synthesis,* Academic Press, Florida (USA), 203-204.

Auvil, S.R., and Penquite, C.R. (1981), *Process for preparing acetonitrile,* US Patent 4272452.

Brown, P.M., and Maselli, J.M. (1973), *Process for preparing N-alkylamines,* U.S. Patent 3726926.

Bukur, D.B., Mukesh, D., and Patel, S.A. (1990), 'Promoter effects on precipitated iron catalysts for Fischer-Tropsch synthesis', *Ind. Eng. Chem. Res.,* **29**, 194.

Cairns, P. (2009), PhD thesis: *Oxygenates in Iron Fischer-Tropsch Synthesis: is Copper a selectivity promoter?,* University of Cape Town.

Claeys, M., and Schulz, H. (2004), Effects of internal mass transfer on activity and selectivity in iron based Fischer-Tropsch synthesis, *Prer. Pap.-Am. Chem. Soc., Div. Pet. Chem.*, vol. **49**, no. 2, 195.

Claeys, M., and van Steen, E. (2004), 'Basic studies', in A Steynberg and M Dry (eds), *Studies in Surface Science and Catalysis*, **152,** 601.

Craxford, S., and Rideal, E. (1939), 'Die Fischer-Tropsch synthese von kohlonwasserstoffen und einige verwandte reaktionen', *Brennstoff Chemie*, **20**, 263.

Daubert, T. (1999), *Physical and thermodynamic data of pure chemicals: evaluated process design data,* Taylor and Francis, Philadelphia, Pennsylvania, USA.

Dixon, D.D., and Burgoyne, W.F. (1986), 'Nitriles from olefins and ammonia via one-carbon homologation', *Applied Catalysis,* **20**, 79.

Dry, M.E. (1996), 'Practical and theoretical aspects of the catalytic Fischer-Tropsch process', *Applied Catalysis A: General,* **138**, 319.

Dry, M.E. (2002), 'The Fisher-Tropsch process', *Catalysis Today,* **71**, 227.

Dry, M.E. (2004a), 'Editorial'; *Applied Catalysis A: General*, **276**, 1.

Dry, M.E. (2004b), 'FT catalysts', in A Steynberg and M Dry (eds), *Studies in Surface Science and Catalysis*, **152**, 533.

Dry, M.E. (2004c), 'Chemical concepts used for engineering purposes', in A. Steynberg and M. Dry (eds), *Studies in Surface Science and Catalysis*, **152**, 231.

Fischer, F., and Tropsch, H. (1926), 'The synthesis of petroleum at atmospheric pressures from gasification products from coal', *Brennstoff Chemie*, **7**, 97.

Fluchaire, M.L.A., and Lavorsky, S. (1942), *Process for the manufacture of nitriles,* US Patent 2273633.

Gambelli, J.W., and Auvil, S.R. (1981), *Acetonitrile process with improved catalysts,* US Patent 4272451.

Gradassi, M.J. (1998), Developments in Fischer-Tropsch Technology*, Studies in Surface Science and Catalysis,* **119**, 35.

Hagemeyer, H.J., and Holmes, J.D. (1976), *Preparation of nitriles,* U.S. Patent 3979432.

Huff, G., and Satterfield, C. (1984), Evidence for two chain growth probabilities on iron catalysts in the Fischer-Tropsch synthesis, *Journal of Catalysis,* **85**, 370.

Hull, D.C. (1956), *Preparation of aliphatic nitriles*, US Patent 2732397.

Hummel, A.A., Badani, M.V., Hummel, K.E., and Delgass, W.N. (1993), 'Acetonitrile synthesis from CO, H_2 and NH_3 over iron catalysts', *Journal of Catalysis,* **139**, 392.

Iglesia, E., Reyes, S.C., Mdon, R.J., Soled, S.L. (1993), 'Selectivity control and catalyst design in the Fischer-Tropsch synthesis: Sites, pellets and reactors', *Advances in Catalysis* **39**, 221.

Inga, J., Kennedy, P., and Leviness, S. (2005), *Fischer-Tropsch process in the presence of nitrogen contaminants,* United States Patent Application 20050154069.

Jager, B., 1998, Developments in Fischer-Tropsch Technology*, Studies in Surface Science and Catalysis,* **119**, 25.

Jager, B., and Espinoza, R. (1995), 'Advances in low-temperature Fischer-Tropsch synthesis, *Catalysis Today,* **23**, 17.

Johnston, O., and Joyner, R. (1993), Structure function relationships in Heterogeneous catalysis: The embedded surface molecule approach and its application, *Studies in Surface Science and Catalysis,* **75a**, 165.

Kaiser, R. (1969), *Chromatographie in der Gasphase,* Bibliographisches Institut, Mannheim.

Khoobiar, S., Kinnelon, N.J., and Shapiro, A.J. (1986), *Process for preparing unsaturated nitriles from alkanes,* US Patent 4609502.

Khoobiar, S., Kinnelon, N.J., and Shapiro, A.J. (1988), *Process for preparing unsaturated nitriles from alkanes,* US Patent 4754049.

Kim, K.N., and Lane, A.M. (1992), 'The selective synthesis of acetonitrile from carbon monoxide, hydrogen and ammonia over Mo/SiO_2', *Journal of Catalysis,* **vol. 137, no. 1**, 127.

Kliger, G.A.,, Glebov, L.S., Ryzhikov, V.P., Shiryaeva, V.E., Popova, T.P., and Loktev, S.M. (1986), 'Hydroamination of aliphatic alcohols under Fischer-Tropsch synthesis conditions on a fused iron catalyst', *Russian Chemical Bulletin,* **vol. 36, no. 8**, 1738.

Knifton, J.F., Lin, J.J., Storm, D.A., & Wong S.F. (1993), 'New synthesis gas chemistry', *Catalysis Today,* **18**, 355.

Kölbel H., and Trapper J. (1966), 'Aliphatic amines from carbon monoxide, steam and ammonia', *Angew. Chem. Internat. Edition,* **vol 5, no. 9,** 843.

Kölbel, H., Abdulahad, I., Kanowski, S., and Ralek, M. (1974), 'Formation of terminal secondary and tertiary alkylamines by single-step synthesis from carbon monoxide, steam and monomethylamine and dimethylamine, respectively', *Reaction Kinetics and Catalysis Letters,* **vol. 1, no. 3**, 267.

Kölbel, H., and Ralek M. (1984), 'The Kölbel-Engelhardt Synthesis' in R.B. Anderson (ed), *The Fischer-Tropsch Synthesis,* Academic Press, 287.

Kowalczyk, Z., Sentek, J., Jodzis, S., Muhler, M., and Hinrichsen, O. (1997), 'Effect of Potassium on the Kinetics of Ammonia Synthesis and Decomposition over Fused Iron Catalyst at Atmospheric Pressure', *Journal of Catalysis* **169**, 407.

Mabaso, I.E. (2005), PhD Thesis: *Nanosized iron crystallites for Fischer-Tropsch synthesis*, University of Cape Town.

McKinney, R.J., and DeVito, S.C. (1998), 'Nitriles' in *Kirk-Othmer Encyclopaedia of Chemical Technology,* 5th Edition, Retrieved June 11, 2007, http://www.mrw.interscience.wiley.com.

McNaught, A.D., and Wilkinson, A. (1997), *Compendium of Chemical Technology,* 2nd ed, Blackwell Scientific Publications, Oxford.

Miller, D.G., and Moskovits, M. (1988), 'A study of the effects of potassium addition to supported iron catalysts in the Fischer-Tropsch reaction', *Journal of Physical Chemistry,* **92**, 6081.

Nicodemus, O., and Wulff, O. (1939), P*rocess of producing nitriles,* US Patent 2177619.

O'Brien, R.J., Xu, L., Spicer, R.L., Bao, S., Milburn, D.R., and Davis, B.H. (1997), 'Activity and selectivity of precipitated iron Fischer-Tropsch catalysts', *Catalysis Today,* **36**, 325.

Olivé, G., and Olivé, C. (1979), *Process for preparing acetonitrile,* US Patent 4179462.

Pichler, H., and Schulz, H. (1970), 'Neuere erkenntnisse auf dem gebiet der synthese von kohlenwasserstoffen aus CO und H_2', *Chemie-Ing.-Techn.,* **vol. 42 no. 18,** 1162.

Ramachandran, R., Malik, V.A., MacLean, D.L., Satchell, D.P. (Jr) (1989), *Process for the production of nitriles,* U.S. Patent 4870201.

Rausch, A.K., van Steen, E., and Roßner, F. (2008), 'New aspects for heterogeneous cobalt-catalyzed hydroamination of ethanol', *Journal of Catalysis*, **vol. 253 no. 1**, 111.

Röttig, W. (1958), *Catalytic hydrogenation of carbon monoxide with addition of ammonia or methylamine*, U.S. Patent 2821537.

Schulz, H. (1999), 'Short History and present trends of Fischer-Tropsch synthesis', *Applied Catalysis A: General,* **186**, 3.

Schulz, H., and Claeys, M. (1999a), 'Reactions of α-olefins of different chain length added during Fischer-Tropsch synthesis on a cobalt catalyst in a slurry reactor', *Applied Catalysis A: General*, **186**, 71.

Schulz, H., and Claeys, M. (1999b), 'Kinetic modelling of the Fischer-Tropsch product distributions', *Applied Catalysis A: General*, **186**, 91.

Schulz, H., Rao, B.R., and Elstner, M. (1970), '^{14}C-Studien zum Reaktionmechanismus der Fischer-Tropsch-Synthese', *Erdöl und Kohle*, **22**, 651.

Schulz, H., van Steen, E., and Claeys, M. (1995), 'Specific inhibition as the kinetic principle of Fischer-Tropsch Synthesis', *Topics in Catalysis* **2**, 223.

Sewell, G.S. (1996), PhD Thesis: 'The reductive amination of ethanol using supported metal catalysts', University of Cape Town.

Steynberg, A.P. (2004), 'Introduction to Fischer-Tropsch Technology' in 2004, *Studies in Surface Science and Catalysis*, **152**, 1.

Turcotte, M.G., and Hayes, K.S. (2001), 'Lower aliphatic amines', *Kirk-Othmer* Encyclopedia of Chemical Technology, *Encyclopedia of Chemical Technology*, vol.2, John Wiley and Sons, New York, 537.

Visek, K. (2001), 'Fatty amines', *Kirk-Othmer*, *Encyclopedia of Chemical Technology*, vol.2, John Wiley and Sons, New York, 518-537. [Online]. Available: http://www.mrw.interscience.wiley.com/kirk/ [Accessed: June 24, 2007].

Vosloo, A.C. (2001), 'Fischer-Tropsch: a futuristic view', *Fuel Processing Technology,* **71**, 149.

Yin, S.F., Xu, B.Q., Zhou, X.P., and Au, C.T. (2004), 'A mini-review on ammonia decomposition catalysts for on-site generation of hydrogen for fuel cell applications', *Applied Catalysis A: General* **277**, 1.

APPENDICES

Appendix A: Ampoule breaker

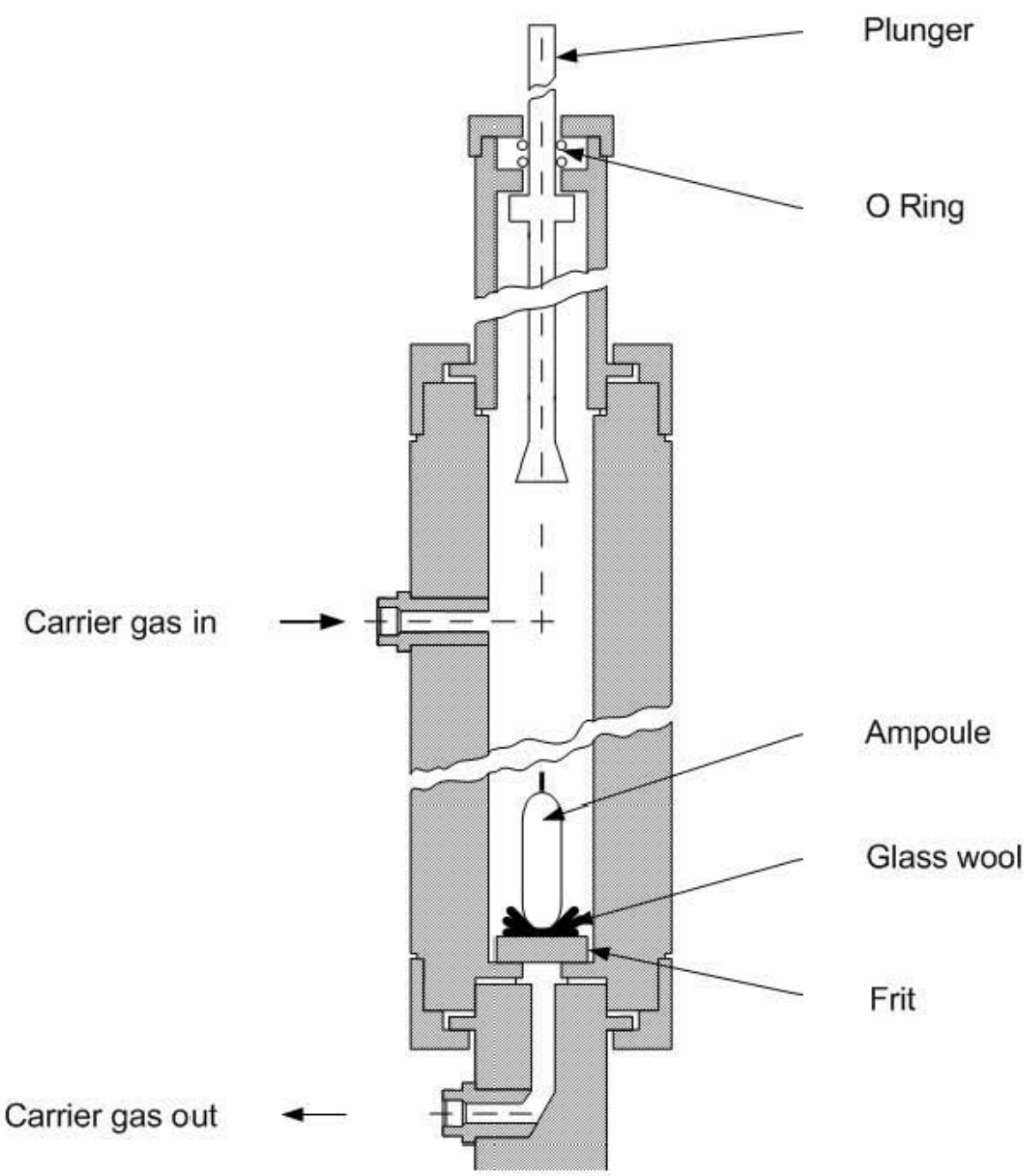

Appendix B: TCD calibration

Component	Concentration (vol%)	TCD peak area				response factor ($rf_{i,TCD}$)
		1	2	3	average	
N_2	9.7	14900	16336	14773	15336	1.0000
H_2	41.1	617580	696700	630950	648410	0.1022
CO	19.6	28006	31728	28694	29476	1.0750
CO_2	9.8	13018	14662	13133	13604	1.1564
CH_4	9.7	43020	49196	44470	45562	0.3464

$$\mathrm{rf_{i,TCD}} = \frac{\mathrm{C_i}}{\mathrm{C_{N_2}}} \times \frac{\mathrm{A_{N_2}}}{\mathrm{A_i}} \quad (4.2)$$

Appendix C: Conversion and selectivity calculations

CO conversion:

- overall CO conversion: $\left(\frac{\mathrm{F_{CO,in}} - \mathrm{F_{CO,out}}}{\mathrm{F_{CO,in}}}\right)$ % (B.1)
- CO conversion to FT product: $\left(\frac{\mathrm{F_{CO,in}} - \mathrm{F_{CO,out} - F_{CO_2,out}}}{\mathrm{F_{CO,in}}}\right)$ % (B.2)

H_2 conversion: $\left(\frac{\mathrm{F_{H_2,in}} - \mathrm{F_{H_2,out}}}{\mathrm{F_{H_2,in}}}\right)$ % (B.3)

Methane selectivity from TCD analysis: $\left(\frac{\mathrm{F_{CH_4,out-TCD}}}{\mathrm{F_{CO,in} - F_{CO,out-TCD} - F_{CO_2,out-TCD}}}\right)$ % (B.4a)

Methane selectivity from FID/TCD analysis: $\left(\frac{\mathrm{F_{CH_4,out-FID}}}{\mathrm{F_{CO,in} - F_{CO,out-TCD} - F_{CO_2,out-TCD}}}\right)$% (B.4b)

Methane selectivity from FID/TCD analysis: $\left(\frac{\mathrm{F_{CH_4,out-FID}}}{\mathrm{\sum HC_{out-FID}}}\right)$ % (B.4c)

CO_2 selectivity: $\left(\frac{\mathrm{F_{CO_2,out}}}{\mathrm{F_{CO,in} - F_{CO,out}}}\right)$ % (B.5)

Table C1: Table of hydrocarbon descriptors used

Descriptor*	molecule
n00	linear paraffin
n01	linear α-olefin
n02	linear trans-β-olefin
n07	linear aldehyde
n10	linear terminal alcohol
n17	linear 2-ketone
n22	linear cis-β-olefin
nCN	linear nitrile
nNH_2	linear amine
n-Amide	linear amide
520	2-Me-Butane
521	2-Me-But-1-ene
531	3-Me-But-1-ene
597	2-Me-But-2-ene

**n-* Indicates the length of the carbon skeleton*;* 00, 01, 02 etc indicates the type and nature of the hydrocarbon, (e.g. n00 represents paraffin of chain length n; n10 represents an alcohol of chain length n) (also check table D1).

$$\text{Linear [ol/(ol+par)]} = \left(\frac{n01+n02+n22}{n00+n01+n02+n22}\right) \quad \text{(B.6)}$$

$$\text{Double bond shift} = \left(\frac{n01+n02+n22}{n00+n01+n02+n22}\right) \quad \text{(B.7)}$$

$$\text{Branched:linear ratio (iso/n) } C_5 = \left(\frac{520+521+531+597}{500+501+502+522}\right) \quad \text{(B.8)}$$

$$\text{Alcohol content} = \left(\frac{n10}{n00+n01+n02+n07+n10+n17+n22+nCN}\right) \quad \text{(B.9)}$$

Aldehyde content = $\left(\frac{n07}{n00+n01+n02+n07+n10+n17+n22+nCN}\right)$ (B.10)

Molar flow rate of reference (cyclohexane), F_{ref} = 1.563mmol/min (B.11)

Molar flow rate of compound Z, F_z = $\frac{A_z}{A_{ref}} \times \frac{rf_z}{rf_{ref}} \times \frac{N_{ref}}{N_z} \times F_{ref}$

(B.12)

Where :

- the response factor =

$$rf_z = \frac{N_{C_z,actusl}}{N_{C_z,FID}}$$

- A_z and A_{ref} are the areas obtained from the FID of compound Z and cyclohexane respectively;
- rf_z is the FID response factor

Anderson-Schulz Flory plot for linear hydrocarbons (olefins and paraffins):

W_n = (Mass of linear hydrocarbons with n-carbon atoms)/(total organic product from n=1 to n=∞).

Appendix D: FID response factors (based on Kaiser, 1969)

Table D1: Hydrocarbon notations and FID response factors

Compound	Code	Carbon Number	FID-observed carbon number	Response Factor, rf_z
Reference (cyclohexane)	**Ref**	**6**	**6**	**1.00**
Methane	**100**	**1**	**1**	**1.00**
Methanol	110	1	0.55	1.82
Ethane	**200**	**2**	**2**	**1.00**
Ethene	201	2	2	1.00
Ethanol	210	2	1.55	1.29
Ethanal	207	2	1	2.00
Ethanamine	$2NH_2$	2	1.46	1.37
Ethanenitrile	2CN	2	2.15	0.93
Ethanamide*	2-Amide	2	1	2.00
Propane	**300**	**3**		**1.00**
Propene	301	3	3	1.00
Propanol(-1)	310	3	2.55	1.18
Propanal	307	3	2	1.50
Propanol(-2)	315	3	2.55	1.18
Propanone	317	3	2	1.50
Propanamine(-1)	$3NH_2$	3	2.46	1.22
Propanenitrile	3CN	3	3.15	0.95
*Propanamide**	*3-Amide*	*3*	*2*	*1.50*
n-Butane	**400**	**4**	**4**	**1.00**
Butene-(1)	401	4	4	1.00
tr.-Butene-(2)	402	4	4	1.00
cis-Butene-(2)	422	4	4	1.00
Butanol(-1)	410	4	3.55	1.13
Butanal	407	4	3	1.33
Butanone(2)	417	4	3	1.33
Butanamine(-1)	$4NH_2$	4	3.46	1.16
Butanenitrile	4CN	4	4.15	0.96
*Butanamide**	*4-Amide*	*4*	*3*	*1.33*
n-Pentane	**500**	**5**	**5**	**1.00**
Pentene-(1)	501	5	5	1.00
tr.-Pentene-(2)	502	5	5	1.00
cis-Pentene-(2)	522	5	5	1.00
Pentanol(-1)	510	5	4.55	1.10
Pentanal	507	5	4	1.25
Pentanone(2)	517	5	4	1.25
2-Me-Butane	520	5	5	1.00
2-Me-Butene (1)	521	5	5	1.00
3-Me-Butene (1)	531	5	5	1.00
2-Me-Butene (2)	597	5	5	1.00
Pentanamine(-1)	$5NH_2$	5	4.46	1.12
Pentanenitrile	5CN	5	5.15	0.97
*Pentanamide**	*5-Amide*	*5*	*4*	*1.25*
n-Hexane	**600**	**6**	**6**	**1.00**

Hexene-(1)	601	6	6	1.00
tr.-Hexene-(2)	602	6	6	1.00
cis-Hexene-(2)	622	6	6	1.00
Hexanol(-1)	610	6	5.55	1.08
Hexanal	607	6	5	1.20
Hexanone(2)	617	6	5	1.20
Cyclopentane	C600	6	6	1.00
Hexanamine(-1)	6NH_2	6	5.46	1.10
Hexanenitrile	6CN	6	6.15	0.98
*Hexanamide**	*6-Amide*	*6*	*5*	*1.20*
n-Heptane	**700**	**7**	**7**	**1.00**
Heptene-(1)	701	7	7	1.00
tr.-Heptene-(2)	702	7	7	1.00
cis-Heptene-(2)	722	7	7	1.00
Heptanol(-1)	710	7	6.55	1.07
Heptanal	707	7	6	1.17
Heptanone(2)	717	7	6	1.17
Heptanamine(-1)	7NH_2	7	6.46	1.08
Heptanenitrile	7CN	7	7.15	0.98
*Heptanamide**	*7-Amide*	*7*	*6*	*1.17*
n-Octane	**800**	**8**	**8**	**1.00**
Octene-(1)	801	8	8	1.00
tr. -Octene-(2)	802	8	8	1.00
cis-Octene-(2)	822	8	8	1.00
Octanol(-1)	810	8	7.55	1.06
Octanal	807	8	7	1.14
Octanone(2)	817	8	7	1.14
Octanamine(-1)	8NH_2	8	7.46	1.07
Octanenitrile	8CN	8	8.15	0.98
*Octanamide**	*8-Amide*	*8*	*7*	*1.14*
n-Nonane	**900**	**9**	**9**	**1.00**
Nonene-(1)	901	9	9	1.00
tr.-Nonene-(2)	902	9	9	1.00
cis-Nonene-(2)	922	9	9	1.00
Nonanol(-1)	910	9	8.55	1.05
Nonanal	907	9	8	1.13
Nonanone(2)	917	9	8	1.13
Nonanamine(-1)	9NH_2	9	8.46	1.06
Nonanenitrile	9CN	9	9.15	0.98
*Nonanamide**	*9-Amide*	*9*	*8*	*1.13*
n-Decane	**1000**	**10**	**10**	**1.00**
Decene-(1)	1001	10	10	1.00
tr.-Decene-(2)	1002	10	10	1.00
cis-Decene-(2)	1022	10	10	1.00
Decanol(-1)	1010	10	9.55	1.05
Decanal	1007	10	9	1.11
Decanone(2)	1017	10	9	1.11
Decanamine(-1)	10NH_2	10	9.46	1.06
Decanenitrile	10CN	10	10.15	0.99

*Decanamide**	*10-Amide*	*10*	*9*	*1.11*
n-Undecane	**1100**	**11**	**11**	**1.00**
Undecene-(1)	1101	11	11	1.00
tr.-Undecene-(2)	1102	11	11	1.00
cis-Undecene-(2)	1122	11	11	1.00
Undecanol(-1)	1110	11	10.55	1.04
Undecanal	1107	11	10	1.10
Undecanone(2)	1117	11	10	1.10
Undecanamine(-1)	$11NH_2$	11	10.46	1.05
Undecanenitrile	11CN	11	11.15	0.99
*Undecanamide**	*11-Amide*	*11*	*10*	*1.10*
n-Dodecane	**1200**	**12**	**12**	**1.00**
Dodecene-(1)	1201	12	12	1.00
tr.-Dodecene-(2)	1202	12	12	1.00
cis-Dodecene-(2)	1222	12	12	1.00
Dodecanol(-1)	1210	12	11.55	1.04
Dodecanal	1207	12	11	1.09
Dodecanone(2)	1217	12	11	1.09
Dodecanamine(-1)	$12NH_2$	12	11.46	1.05
Dodecanenitrile	12CN	12	12.15	0.99
*Dodecanamide**	*12-Amide*	*12*	*11*	*1.09*
n-Tridecane	**1300**	**13**	**13**	**1.00**
Tridecene-(1)	1301	13	13	1.00
tr.-Tridecene-(2)	1302	13	13	1.00
cis-Tridecene-(2)	1322	13	13	1.00
Tridecanol(-1)	1310	13	12.55	1.04
Tridecanal	1307	13	12	1.08
Tridecanone(2)	1317	13	12	1.08
Tridecanamine(-1)	$13NH_2$	13	12.46	1.04
Tridecanenitrile	13CN	13	13.15	0.99
*Tridecanamide**	*13-Amide*	*13*	*12*	*1.08*
n-Tetradecane	**1400**	**14**	**14**	**1.00**
Tetradecene-(1)	1401	14	14	1.00
tr.-Tetradecene-(2)	1402	14	14	1.00
cis-Tetradecene-(2)	1422	14	14	1.00
Tetradecanol(-1)	1410	14	13.55	1.03
Tetradecanal	1407	14	13	1.08
Tetradecanone(2)	1417	14	13	1.08
Tetradecanamine(-1)	$14NH_2$	14	13.46	1.04
Tetradecanenitrile	14CN	14	14.15	0.99
*Tetradecanamide**	*14-Amide*	*14*	*13*	*1.08*
n-Pentadecane	**1500**	**15**	**15**	**1.00**
Pentadecene-(1)	1501	15	15	1.00
cis-Pentadecene-(2)	1522	15	15	1.00
Pentadecanol(-1)	1510	15	14.55	1.03
Pentadecanal	1507	15	14	1.07
Pentadecanone(2)	1517	15	14	1.07
Pentadecanamine(-1)	$15NH_2$	15	14.46	1.04
Pentadecanenitrile	15C	15	15.15	0.99

*Pentadecanamide**	*15-Amide*	*15*	*14*	*1.07*

*Amide factors are estimated based on the functional groups, and that influence of the groups does not extend to more than 1 carbon. Amine and nitrile responses were obtained using C_8 compounds as tabulated below.

Appendix E: FID calibration for nitrogen-containing compounds

The response factors of the C_8 amine and nitrile were determined using n-octene(-1) as the internal standard, and hexane as a solvent.

Table E1: Calibration for amine FID response factor

Component	n_i/n_{801}	Area				C_{obs}*	rf
		A_1	A_2	A_3	Average		
801	1	3.04E+08	4.39E+08	5.14E+08	4.19E+08	8	1.00
8CN	1.031	2.98E+08	4.22E+08	4.90E+08	4.03E+08	7.46	1.07

*C_{obs} refers to the 'apparent' number of carbon atoms detected per molecule, area (A_1, A_2, A_3 and average) are the FID areas detected for the respective compound, n_i/n_{801} is the molar carbon ratio of each compound relative to n-octene(-1), and rf is the determined FID response factor.

Table E2: Calibration for nitrile FID response factor

Component	n_i/n_{801}	Area				C_{obs}	rf
		A_1	A_2	A_3	Average		
801	1	6.97E+08	6.19E+08	7.03E+08	6.73E+08	8	1.00
8CN	0.993	7.04E+08	6.52E+08	6.87E+08	6.81E+08	8.15	0.98

Appendix F: Mass balance at the different ammonia feed conditions

Table F1: Mass balance at the different ammonia feed conditions

Component	0%	2%	5%	10%	20%	35%
			(mol C/min)*			
H_2 in	2.05E-03	2.05E-03	2.05E-03	2.05E-03	2.05E-03	2.05E-03
CO in	1.02E-03	1.02E-03	1.02E-03	1.02E-03	1.02E-03	1.02E-03
NH_3 in	-	6.26E-05	1.61E-04	3.41E-04	7.67E-04	1.65E-03
H_2 out	1.30E-03	1.50E-03	1.51E-03	1.64E-03	1.74E-03	1.89E-03
CO out	3.19E-04	3.33E-04	3.86E-04	4.76E-04	5.39E-04	6.09E-04
NH_3 out[#]	-	5.64E-05	1.58E-04	3.38E-04	-	-
CO_2 out	2.40E-04	2.51E-04	2.12E-04	2.16E-04	1.53E-04	9.45E-05
CH_4 out TCD						
CH_4 out FID	2.09E-05	2.25E-05	2.60E-05	2.34E-05	1.86E-05	1.30E-05
Approx of HC's out	1.74E-04	1.56E-04	1.94E-04	1.76E-04	1.49E-04	1.10E-04
CO in	1.02E-03	1.02E-03	1.02E-03	1.02E-03	1.02E-03	1.02E-03
$CO+CO_2$ out	5.59E-04	5.84E-04	5.98E-04	6.93E-04	6.92E-04	7.03E-04
C out in product	1.74E-04	1.56E-04	1.94E-04	1.76E-04	1.49E-04	1.10E-04
ΔC, %	**28.3**	**27.6**	**22.4**	**15.0**	**17.7**	**20.4**

*mol/min for non-carbon containing components

[#]NH_3 balance based on outlet flows of nitrogen-containing compounds and ammonia feed, and does not include white solid (ammonium carbonate). Also, 20% and 30% ammonia-in feed conditions excluded due to absence of liquid for analysis of amines/amides.

Appendix G: Rates of formation and selectivities of selected components at the different ammonia feed conditions

Table G1: Flow rates for selected components in selected carbon number fractions

Carbon #	linear olefins (C mol/min)					
2	1.56E-05	1.57E-05	1.80E-05	1.50E-05	1.60E-05	1.40E-05
3	1.73E-05	1.80E-05	2.04E-05	1.77E-05	1.85E-05	1.61E-05
4	1.44E-05	1.43E-05	1.60E-05	1.39E-05	1.46E-05	1.29E-05
5	1.00E-05	9.71E-06	1.15E-05	9.64E-06	9.75E-06	8.65E-06
6	7.65E-06	7.26E-06	8.75E-06	7.57E-06	7.41E-06	6.21E-06
7	6.06E-06	5.65E-06	6.72E-06	5.88E-06	6.15E-06	3.84E-06
8	4.88E-06	4.53E-06	5.39E-06	4.79E-06	5.14E-06	2.53E-06
9	4.03E-06	3.61E-06	4.31E-06	3.95E-06	4.57E-06	1.71E-06
10	3.35E-06	2.91E-06	3.63E-06	3.29E-06	4.03E-06	1.09E-06
	linear paraffins (C mol/min)					
1	2.09E-05	2.25E-05	2.60E-05	2.34E-05	1.86E-05	1.30E-05
2	4.90E-06	4.39E-06	4.50E-06	3.36E-06	2.93E-06	4.85E-06
3	4.61E-06	4.19E-06	4.60E-06	4.11E-06	3.26E-06	3.32E-06
4	4.14E-06	3.74E-06	4.33E-06	3.87E-06	2.88E-06	2.48E-06
5	3.30E-06	3.08E-06	3.56E-06	3.03E-06	2.38E-06	1.87E-06
6	2.78E-06	2.52E-06	2.98E-06	2.59E-06	1.92E-06	1.32E-06
7	2.26E-06	2.09E-06	2.35E-06	2.13E-06	1.43E-06	8.48E-07
8	1.95E-06	1.68E-06	2.01E-06	1.77E-06	1.36E-06	6.89E-07
9	1.69E-06	1.40E-06	1.68E-06	1.54E-06	1.25E-06	5.05E-07
10	1.41E-06	1.12E-06	1.39E-06	1.27E-06	1.14E-06	4.00E-07
	linear alcohols (C mol/min)					
2	4.22E-06	0.00E+00	2.41E-07	1.07E-06		
3	1.25E-06	7.41E-08	0.00E+00	1.88E-07		
4	1.25E-06	4.03E-07	3.86E-07	3.63E-07		
5	8.36E-07	2.52E-07	1.86E-07	2.29E-07		
6	9.81E-07	2.39E-07	2.49E-07	9.00E-08		
7	5.83E-07	1.43E-07	3.20E-07	5.44E-08		
8	3.42E-07	1.41E-07	3.15E-07	4.52E-08		
9	4.52E-07	1.79E-07	3.64E-07	1.63E-07		
10	1.21E-07	2.23E-07	3.28E-07	1.69E-07		
	linear aldehydes (C mol/min)					
2	1.84E-06	0.00E+00				
3	5.93E-07	4.03E-07				
4	1.09E-06	4.25E-07				
5	1.22E-06	3.92E-07				
6	1.26E-06	3.03E-07				
7	1.13E-06	1.58E-07	1.46E-07	1.24E-07		
8	9.12E-07	7.49E-08	7.29E-08	5.07E-08		
9	2.20E-07	5.26E-08	4.44E-08	2.08E-09		

Carbon #	amines (C mol/min)				
2	2.62E-07	1.49E-06	1.21E-06		
3	2.62E-07	9.18E-07	8.19E-07		
4	3.26E-07	8.67E-07	9.38E-07		
5	5.85E-07	6.36E-07	6.26E-07		
6	4.18E-07	2.45E-06	1.09E-06		
7	1.97E-07	2.17E-06	2.15E-06		
8	2.35E-07	1.69E-06	1.53E-06		
9	9.38E-08	1.22E-06	1.24E-06		
10	1.73E-08	9.06E-07	7.39E-07		
	nitriles (C mol/min)				
2	0.00E+00	0.00E+00	2.95E-07	0.00E+00	0.00E+00
3	7.13E-07	2.82E-07	2.22E-07	0.00E+00	0.00E+00
4	1.89E-07	2.06E-07	3.50E-07	0.00E+00	8.55E-07
5	2.44E-07	4.45E-07	5.05E-07	0.00E+00	8.59E-07
6	3.00E-07	5.86E-07	7.80E-07	9.68E-07	8.63E-07
7	1.42E-07	4.87E-07	5.79E-07	7.94E-07	5.58E-07
8	1.36E-07	3.33E-07	4.89E-07	8.28E-07	5.94E-07
9	1.74E-07	3.10E-07	5.28E-07	8.29E-07	3.72E-07
10	1.37E-07	1.69E-07	4.40E-07	8.85E-07	3.51E-07

Table G2: Selectivities/ratios for selected components in selected carbon number fractions

Carbon #	linear olefins/total linear hydrocarbons (%)					
2	76.1	78.1	80.0	81.7	84.5	74.2
3	78.9	81.1	81.6	81.2	85.0	83.0
4	77.7	79.2	78.7	78.3	83.5	83.8
5	75.2	75.9	76.4	76.1	80.4	82.2
6	73.3	74.2	74.6	74.5	79.4	82.5
7	72.8	73.0	74.1	73.4	81.1	81.9
8	71.5	72.9	72.8	73.0	79.1	78.6
9	70.5	72.0	72.0	72.0	78.6	77.2
10	70.4	72.1	72.4	72.1	77.9	73.1
	Double bond shift (α-olefins in linear olefins) (%)					
2	96.9	97.3	97.8	98.1	97.2	98.0
3	97.2	97.9	97.9	98.1	97.0	97.3
4	96.9	97.5	97.3	98.0	97.0	96.6
5	96.0	97.4	97.2	97.8	95.9	93.5
6	95.8	96.7	96.5	96.7	95.6	91.2
7	95.9	97.6	98.7	97.8	96.5	90.6
8	94.8	97.5	97.6	97.5	95.4	92.2
9	96.9	97.3	97.8	98.1	97.2	98.0
10	97.2	97.9	97.9	98.1	97.0	97.3

Carbon #	linear alcohols/total linear hydrocarbons (%)				
2	15.9		1.0	5.1	
3	5.3	0.3	1.4	0.8	
4	6.0		1.8	1.9	
5	5.4	1.7	1.1	1.6	
6	7.7	2.1	1.7	0.7	
7	5.8	1.7	2.6	0.5	
8	4.2	2.0	3.2	0.5	
9	7.1	3.2	4.6	2.2	
10	2.4	5.0	1.0	2.9	
	linear aldehydes/total linear product (%)				
2	6.9	1.7			
3	2.5	2.2			
4	5.2	2.7			
5	7.9	2.7			
6	10.0	1.9			
7	11.3	1.1			
8	11.3	1.0			
9	3.4	0.7			
	amines/total linear product (%)				
2		1.1	6.1	5.8	
3		1.1	3.5	3.6	
4		1.7	4.0	4.8	
5		4.1	3.9	4.5	
6		3.8	16.3	9.0	
7		2.4	17.8	19.7	
8		3.5	17.2	17.6	
9		1.7	15.4	16.8	
10		0.4	14.1	12.5	
	nitriles/total linear product (%)				
2		0.0		1.4	
3		3.0		1.0	
4		1.0	0.95	1.8	
5		1.7	2.72	3.6	5.1
6		2.7	3.90	6.4	9.3 7.5
7		1.7	4.00	5.3	9.2 10.0
8		2.0	3.39	5.6	11.1 10.0
9		3.2	3.91	7.1	12.4 14.8
10		3.1	2.64	7.4	14.6 14.4